2013

# Functional Characterization of CRIP1a Knockout Mice

Joanna Jacob
*Virginia Commonwealth University*

# Functional Characterization of $CRIP_{1a}$ Knockout Mice

A thesis submitted in partial fulfillment of the requirements for the degree of Master of Science at Virginia Commonwealth University.

By

Joanna Caitlin "Jacy" Jacob
B.S. Virginia Polytechnic Institute and State University, 2009

Director: Dana E. Selley, Ph.D.
Associate Professor, Department of Pharmacology and Toxicology

Virginia Commonwealth University
Richmond, Virginia,
August, 2013

**Acknowledgements**

This degree would not have been a possibility, much less a reality, if it had not been for my advisor, Dr. Dana Selley, and for that, I wish to thank him. He saw potential in me that others, including myself, had not been able to see before. By taking a chance, and a leap of faith on both our parts, Dr. Selley has helped me accomplish things I thought were perhaps at one point unattainable. I have learned valuable skills not only as a scientist, but as a person, too. For that, I am grateful.

I must also thank my committee members, Dr. Laura Sim-Selley and Dr. Ching-Kang "Jason" Chen. They have been extremely helpful and encouraging throughout this process, and have provided valuable insight to my project. I want to thank them for their time and energy devoted to my and this project's success.

I would not have survived without my friends and lab mates here at VCU. Jordan, Aaron and Matt – thank you for accepting me as easily as you all did. All your advice and humor made life in the lab fun and interesting, which I will always appreciate. To Irma – truly without you this past year I would not be where I am today. Thank you for everything. To all of my friends I have made along the way in grad school – I am thankful for each and every one of you, particularly Richard and Travis. Even after all of the days, nights and weekends of studying, we somehow managed to have a pretty good time. I also want to thank Joy for always being there with a big beautiful smile and a hug when I needed one, or simply, just because.

I would also like to thank Dr. Lichtman, Dr. Divya Ramesh, Dr. Hoon Shim, Dr. Pretal Muldoon, Dr. Akbarali, Dr. Sawyer and Dr. Dewey for taking time to provide input on my project and for always providing encouragement along the way. It meant so much to have your support.

Finally, I must thank my family (Mom, Dad, Cary, Grandpa, Mary, Granddaddy George and Grandma Jinney) and of course, Devin. Your love, support, encouragement, and as always, humor, has made this all possible. You have always been there and I know you always will. I love you all.

**Table of Contents**

## List of Tables

**Table**

## List of Figures

**Figures**

## List of Abbreviations

| | |
|---|---|
| 2-AG | 2-arachidonylglycerol |
| ADase | adenosine deaminase |
| AEA | anandamide |
| BLA | basolateral amygdala |
| BSA | bovine serum albumin |
| cAMP | cyclic adensosine monophosphate |
| $CB_1$ | cannabinoid receptor type 1 |
| $CB_2$ | cannabinoid receptor type 2 |
| CBD | cannabidiol |
| CCK | cholecystokinin |
| cDNA | complimentary deoxyribonucleic acid |
| CeA | central amygdala |
| CNS | central nervous system |
| CP | CP 55,940 |
| CREB | cAMP Response Element Binding Protein |
| $CRIP_{1a}$ | Cannabinoid Receptor Interacting Protein 1a |
| $CRIP_{1b}$ | Cannabinoid Receptor Interacting Protein 1b |
| Ct | cycle threshold |
| D2 | dopamine D2 receptor |
| DAG | diacylglycerol |
| DAGL | diacylglycerol lipase |
| DEPC | diethylpyrocarbonate |
| DMSO | dimethyl sulfoxide |
| DSE | depolarization-induced suppression of excitation |
| DSI | depolarization-induced suppression of inhibition |
| DTA | diphtheria toxin A |
| DTT | dithiothreitol |
| $EC_{50}$ | half maximal (50%) effective concentration |
| $ED_{50}$ | half maximal (50%) effective dose |
| EDTA | ethylenediaminetetraaceticacid |
| EGTA | ethylene glycol tetraacetic acid |
| $E_{max}$ | maximal effect |
| EMSA | electrophoretic mobility shift assay |
| FAAH | fatty acid amide hydrolase |
| GABA | γ-aminobutyric acid |
| GAPDH | glyceraldehyde-3-phosphate dehydrogenase |
| GASP1 | G-protein receptor associated sorting protein |
| GDP | guanosine diphosphate |

| | |
|---|---|
| GIRK | inwardly rectifying potassium channels |
| GPCR | G-protein coupled receptor |
| GTP | guanosine triphosphate |
| GTPase | guanosine triphosphate hydrolase |
| GTPγS | guanosine-5-O-(γ-thio)-triphosphate |
| HA | human influenza hemagglutinin |
| HEK | human embryonic kidney |
| HEPES | 4-(2-hydroxyethyl)-1-piperazineethanesulfonic acid |
| HET | heterozygous |
| HotSHOT | hot sodium hydroxide and Tris |
| i.p. | intraperitoneal |
| KA | kainic acid |
| $K_D$ | equilibrium dissociation constant |
| KO | knockout |
| MAEA | methanandamide |
| MAGL | monoacylglycerol lipase |
| MPE | max percent effect |
| mRNA | messenger ribonucleic acid |
| NAPE | N-arachidonoyl phosphatidylethanolamine |
| NE | noladin ether |
| NEO | neomycin |
| NTC | no template control |
| PAG | periaqueductal gray area |
| PAGE | polyacrylamide gel electrophoresis |
| PBS | Phosphate buffered saline |
| PCR | polymerase chain reaction |
| PDZ | PSD-95, Disc large protein and ZO-1 |
| PTX | pertussis toxin |
| qPCR | quantitative polymerase chain reaction |
| RIM | rimonabant |
| SEM | standard error of the mean |
| SCG | superior cervical ganglion |
| SDS | sodium dodecyl sulfate |
| TBS | TRIS-buffered saline |
| TBST | Tris buffered saline with Tween-20 |
| THC | $\Delta^9$-tetrahydrocannabinol |
| TRIS | tris(hydroxymethyl)aminomethane |
| VEH | vehicle |
| WIN | WIN 55,212-2 |
| WT | wild type |

**Abstract**

FUNCTIONAL CHARACTERIZATION OF CRIP1A KNOCKOUT MICE

By Joanna Caitlin Jacob, B.S.

A thesis submitted in partial fulfillment of the requirements for the degree of Master of Science at Virginia Commonwealth University.

Virginia Commonwealth University, 2013

Major Director: Dana E. Selley, Ph.D., Department of Pharmacology and Toxicology

The $CB_1$ cannabinoid receptor is one of the most highly expressed receptors in the mammalian central nervous system (CNS). It is most densely distributed on pre-synaptic terminals in the forebrain, basal ganglia and cerebellum, where it inhibits both excitatory and inhibitory neurotransmission. Recently, two novel proteins were discovered that bind to the $CB_1$ receptor C-terminal tail, and termed cannabinoid receptor interacting protein 1a and 1b ($CRIP_{1a}$ and $CRIP_{1b}$). $CRIP_{1a}$ is expressed throughout vertebrates, whereas $CRIP_{1b}$ expression appears to be primate-specific. Studies characterizing $CRIP_{1a}$ have thus far been conducted in cellular models using over-expression (gain-of-function) approaches, and indicate that $CRIP_{1a}$ inhibits constitutive $CB_1$ receptor activity without affecting $CB_1$ receptor expression. However, very little is known about the biological function of $CRIP_{1a}$ in the intact CNS. The objective of this thesis was to characterize the first $CRIP_{1a}$ knockout mouse line for novel behavioral phenotypes and molecular changes in the CNS as a result of the loss of $CRIP_{1a}$. The absence of $CRIP_{1a}$ was confirmed using both quantitative PCR (qPCR) and Western immunoblot analysis. $CB_1$ receptor levels were found to remain unchanged in $CRIP_{1a}$ knockout (KO) mice when compared to wild

type (WT) littermate controls in the cerebellum, hippocampus and amygdala. Though high in receptor levels, the cerebellum and hippocampus did not display enhanced $CB_1$-mediated G-protein activity as determined by agonist-stimulated [35S]GTPγS binding. The amygdala, however, produced significant increases in $CB_1$-mediated G-protein activity in response to both CP55,940 and Noladin Ether. This effect was further realized when $CRIP_{1a}$ KO mice produced significant anxiolytic-like phenotypes in two models of anxiety: the light:dark box and marble burying. In addition to the anxiolytic-like phenotype, a significant antinociceptive phenotype was observed in naïve $CRIP_{1a}$ KO mice. However, after tetrad analysis with CP55,940 in male $CRIP_{1a}$ WT, heterozygous (HET) and KO mice, no significant genotype differences were revealed in antinociception, motor coordination or reduced body temperature. We also discovered that the expression of $CRIP_{1a}$ and $CB_1$ receptors is independent of one another in brain regions such as the cerebellum, prefrontal cortex and the amygdala. Our studies were the first to investigate $CRIP_{1a}$ function in live animals, and our findings suggest that $CRIP_{1a}$ could be a key player in the endocannabinoid system, serving as a promising future pharmacological target for studying and treating anxiety disorders.

# Chapter 1. Introduction

## 1.1 Cannabinoids and Cannabinoid Receptors

*Cannabis Sativa,* or Marijuana, is a plant that has been cultivated by humans for over four thousand years for a variety of uses ranging from cooking oil and fibrous material to medicinal and recreational purposes (Russo, 2007). Archeological evidence of medical marijuana use has been described in many ancient cultures including the Chinese and Egyptians, most often for relief from several types of pain, such as muscle cramps, wounds and inflammation, though numerous other uses have been documented. It is suspected that today's marijuana strains are a domesticated form, derived from the once wild plants whose origins lay in Central Asia. Marijuana is comprised of numerous compounds, including phytocannabinoids. Selective breeding has produced strains in which these phytocannabinoid ratios differ, often attributed to geographical preferences. The overall percentage of marijuana's main psychoactive constituent, $\Delta^9$-tetrahydrocannabinol (THC) is thought to have changed over the years, with modern strains containing higher levels of THC and lower amounts of cannabidiol (CBD) (King *et al*. 2005). CBD is a medically relevant, non-psychoactive cannabinoid compound, shown to exhibit neuroprotective and anxiolytic effects. In the Middle East and northern parts of Africa, THC:CBD ratios are often 1:1, however in Europe and North America, THC percentages are much higher than CBD (Leggett and Pietschmann, 2008), presumably due largely to its recreational use.

THC was first identified in its pure form in 1964 (Gaoni and Mechoulam, 1964). Initially, cannabinoids were believed to produce membrane perturbation and destabilization due to their hydrophobic properties. It wasn't until years later, in 1981, when findings reported

stereoselective differences between (+) and (-) THC isomers in behavioral tests, thus supporting a new concept in which THC acts via a receptor-mediated mechanism (Martin *et al.,* 1981). Shortly thereafter, further evidence was published supporting the likelihood of a cannabinoid receptor population, which showed various cannabinoids including THC inhibited adenylyl cyclase activity in a pertussis-toxin sensitive manner in a cultured mouse neuroblastoma (N18TG2) cell line (Howlett *et al*. 1986). The presence of cannabinoid receptors in the brain was later confirmed using a radiolabeled synthetic cannabinoid, [$^3$H]CP55,940 which bound stereoselectively, with high affinity and reached saturation (Devane *et al.* 1988). These receptors were subsequently cloned and named cannabinoid receptor type 1 ($CB_1$) (Matsuda *et al.* 1990) and cannabinoid receptor type 2 ($CB_2$) (Gérard *et al.* 1991; Munro *et al.* 1993).

Both $CB_1$ and $CB_2$ receptors are G-protein coupled receptors, and associate with $G_{i/o}$ G-protein subunits [see (Howlett *et al.* 2002) for review]. Upon cannabinoid receptor activation, cAMP production is decreased due to the inhibition of adenylyl cyclase via $G\alpha_{i/o}$ subunits (Howlett *et al*. 1985; Howlett *et al.* 1986). Simultaneously, the $G\beta\gamma$ subunits can activate inwardly rectifying potassium (GIRK) channels (Mackie *et al.* 1995; McAllister *et al.* 1999) and decrease the conductance of N- and P/Q-type voltage-gated calcium channels (Mackie and Hille, 1992; Twitchell *et al*. 1997). Collectively, these actions result in a reduction of synaptic vesicle fusion at the nerve terminal, inhibiting both excitatory and inhibitory neurotransmitter release. In addition, a well-characterized electrophysiological hallmark of $CB_1$ activation in the brain is known as depolarization-induced suppression of inhibition (DSI). First shown to be $CB_1$-mediated in the cerebellum (Vincent *et al.* 1992) and confirmed in the hippocampus (Pitler and Alger, 1992), DSI leads to hyperpolarization of a repeatedly depolarized neuron, thus suppressing successive vesicular fusion and release of γ-Aminobutyric acid (GABA). This was

later shown to be absent in $CB_1$ receptor knockout mice, strengthening the claim that DSI is $CB_1$-mediated (Ohno-Shosaku *et al*. 2001). $CB_1$ receptors also mediate depolarization-induced suppression of excitation (DSE), which differs in definition from DSI simply by the fact that it describes inhibition of the release of the excitatory neurotransmitter, glutamate, rather than GABA. Evidence for DSE is best characterized in autaptic hippocampal neurons and is reportedly mediated by 2-AG activation of $CB_1$ receptors (Straiker *et al*. 2009). Furthermore, recent studies have shown that DSE is present in other brain regions, such as the lateral amygdala, and is mediated by retrograde endocannabinoid signaling at $CB_1$ receptors (Kodirov *et al.* 2010).

**1.2 Cannabinoid Receptor Localization.**

$CB_1$ receptors are one of the most prevalent receptor types found in the brain (Herkenham *et al*. 1991), but are also peripherally located (Pertwee *et al*. 1996). $CB_2$ receptors have a limited presence in the central nervous system, where they are expressed primarily on microglial cells (Cabral and Marciano-Cabral, 2005) and neurons (Van Sickle *et al.*, 2005) but also play a supporting role in the peripheral immune system (Munro *et al*. 1993; Carlisle *et al.* 2005). Within the brain, $CB_1$ receptors are most densely expressed in the cerebellum, hippocampus, cortex, and basal ganglia (Herkenham *et al.* 1991; Sim *et al*. 1996). The hypothalamus and periaqueductal gray each exhibit modest $CB_1$ expression, whereas slightly less expression is seen in the spinal cord (Tsou *et al*. 1998). It is important to note that $CB_1$ receptor expression is very low in the pons and medulla, which are known to be involved in autonomic functions such as respiratory and cardiac regulation, and perhaps this provides one explanation as to why an absence of life-threatening effects is associated with marijuana (Herkenham *et al.*, 1991).

$\Delta^9$-THC acts as a partial agonist at $CB_1$ (Sim *et al.* 1996) and $CB_2$ receptors (Bayewitch *et al.* 1996), yet is considered the principal compound responsible for marijuana's intoxicating effects. Known functions of the brain regions exhibiting high $CB_1$ expression levels reflect the pharmacological effects (i.e. cannabimimetic effects) often described after marijuana consumption, including short-term memory loss, hypothermia, catalepsy, antinociception and reduced motor coordination (Hollister, 1986; Dewey, 1986). A behavioral tetrad model was developed to screen compounds for cannabimimetic effects in rodents, specifically catalepsy, hypothermia, reduced locomotor activity and antinociception (Little *et al.* 1988, Varvel *et al.* 2005). If the pharmacological effects of a ligand are $CB_1$ receptor-mediated, these effects are reversible or blocked by a $CB_1$ antagonist such as rimonabant (also known as SR141716A), and are absent in $CB_1$ knockout mice (Compton *et al.* 1996; Fride, 2002).

### 1.3 Cannabinoid Ligands

**1.3a. The Endocannabinoids.** The confirmed presence of two cannabinoid receptor types in multiple species (see Onaivi *et al.* 2002 for review), strongly suggested that an endogenous system is present. The search for endogenous ligands led to the discovery of N-arachidonoyl ethanolamine in 1992 (Devane *et al.* 1992). Commonly referred to as anandamide (AEA), after the Sanskrit word for "delight, bliss" *ananda,* it is synthesized from N-arachidonoyl phosphatidylethanolamine (NAPE) by multiple pathways (Wang and Ueda, 2009) and shows moderate selectivity for the $CB_1$ receptor. A second endogenous ligand, 2-arachidonylglycerol (2-AG), was reported by two independent laboratories in 1995 (Mechoulam *et al.* 1995; Sugiura *et al.* 1995). 2-AG is synthesized by cleavage of diacylglycerol (DAG) via diacylglycerol lipases (DAGL), and as been shown to bind with similar affinities to $CB_1$ and $CB_2$ receptors and

act as a full $CB_1$ agonist (Savinainen *et al*. 2001). Anandamide and 2-AG are primarily degraded by the enzymes, fatty acid amide hydrolase (FAAH) and monoacylglycerol lipase (MAGL), respectively (Cravatt *et al*. 1996; Dinh *et al.* 2002). Anandamide is broken down into arachidonic acid and ethanolamine, while 2-AG is broken down into arachidonic acid and glycerol. Both ligands are equally pertinent when defining the endocannabinoids, though it is important to note that 2-AG is present at nmol/g levels compared to pmol/g levels of anandamide. However, levels vary frequently between reports, therefore there may be anywhere from a 200 to 1000-fold difference in 2-AG concentrations compared to anandamide (for review, see Buczynski and Parsons, 2010). A third, yet putative, endocannabinoid known as 2-arachidonyl glyceryl ether, or Noladin Ether, was reported to bind with high affinity and produce sedation, hypothermia and mild nociception in mice (Hanuš *et al.* 2001). Though capable of mediating these cannabimimetic effects, its relative efficacy to 2-AG is weak (Sugiura *et al*. 1999).

**1.3b. Exogenous cannabinoid ligands.** Marijuana contains hundreds of constituents belonging to various classes of compounds including terpenoids, flavonoids, hydrocarbons and steroids (ElSohly and Slade, 2005). It was recently estimated that there are over 85 cannabinoids naturally found in marijuana (El-Alfy *et al*. 2010). In addition to THC and cannabidiol, tetrahydrocannabivarin, cannabigerol and cannabichromene are all phytocannabinoids commonly found in many strains of marijuana. Cannabichromene and cannabigerol are both non-psychoactive compounds, yet cannabichromene has been shown to be dose-dependently effective at reducing inflammation in the lipopolysaccharide-induced paw edema model (DeLong *et al*.

2010). Tetrahydrocannabivarin has been shown to antagonize the effects of THC at the $CB_1$ receptor and attenuate its psychoactive effects (Thomas *et al*. 2005).

Throughout the years, numerous synthetic cannabinoids have been developed. Both pharmaceutical companies and independent laboratories have synthesized cannabinoid analogs in an attempt to further study the various effects of these compounds and potentially circumvent the untoward effects of THC. Analogs that are structurally similar to THC are considered "classical". One example is HU-210, which has been shown to be at least 100 times more potent at the $CB_1$ receptor than THC and has a longer half-life (Felder *et al*. 1995). "Non-classical" synthetic cannabinoids range from somewhat dissimilar in structure to disparate in structure to THC, though they are still quite potent and efficacious at one or both of the cannabinoid receptors. Pfizer produced a bicyclic analog, CP55,940, which is a high-efficacy ligand at both $CB_1$ and $CB_2$ receptors, with potencies 100-fold greater than THC in behavioral assays (Wiley *et al.* 1995) and $CB_1$ receptor binding experiments (Gatley *et al*. 1997). WIN 55,212-2 (WIN) is a non-classical cannabinoid belonging to the aminoalkylindole group and is structurally dissimilar to THC. It also binds potently to $CB_1$ and $CB_2$ receptors in addition to eliciting robust behavioral effects (Kuster *et al.* 1993, Pacher *et al*. 2006).

Synthetic cannabinoids are currently being synthesized and introduced as constituents in abused herbal blends. Recently, many of these compounds have elicited widespread clinical concern relating to higher addiction liabilities, increased psychosis and even adverse cardiac events (Zimmermann *et al.* 2009, Müller *et al*. 2010, Mir *et al.* 2011). As a method to circumvent legal obstacles, these designer compounds, which are capable of mimicking THC's effects, are sprayed onto herbal substances and packaged as herbal incense, such as "spice" or "K2". Atwood *et al.* (2010) studied a common constituent of spice, JWH-018, which is now

federally regulated by the U.S. government as a schedule I drug. After applying the compound to cultured autaptic hippocampal neurons, significant inhibition of excitatory synaptic currents were observed along with rapid induction of $CB_1$ receptor internalization. JWH-018 was also found to be significantly more potent than WIN at $CB_1$ receptors but exhibited similar efficacy. These lines of evidence could explain, in part, the ability of potent synthetic cannabinoids to elicit strong episodes of psychosis and anxiogenic effects in some users.

**1.4 Cannabinoid Receptor Signaling Through G-Protein Activation.**

$CB_1$ and $CB_2$ receptors are structurally consistent with other G-protein coupled receptors (GPCRs) and consist of seven transmembrane domains, an intracellular C-terminus and an extracellular N-terminus (Matsuda *et al*. 1990, Munro *et al.* 1993). The two cannabinoid receptors share an estimated 44% homology overall (Montero *et al.* 2005), with significant variability in the intracellular C-terminus (see Figure 1). It has been well documented that G-proteins interact with the C-terminus of the $CB_1$ receptor (Nie and Lewis, 2001) and the third intracellular loop, located between transmembrane domains 6 and 7 (Mukhopadhyay and Howlett, 2001).

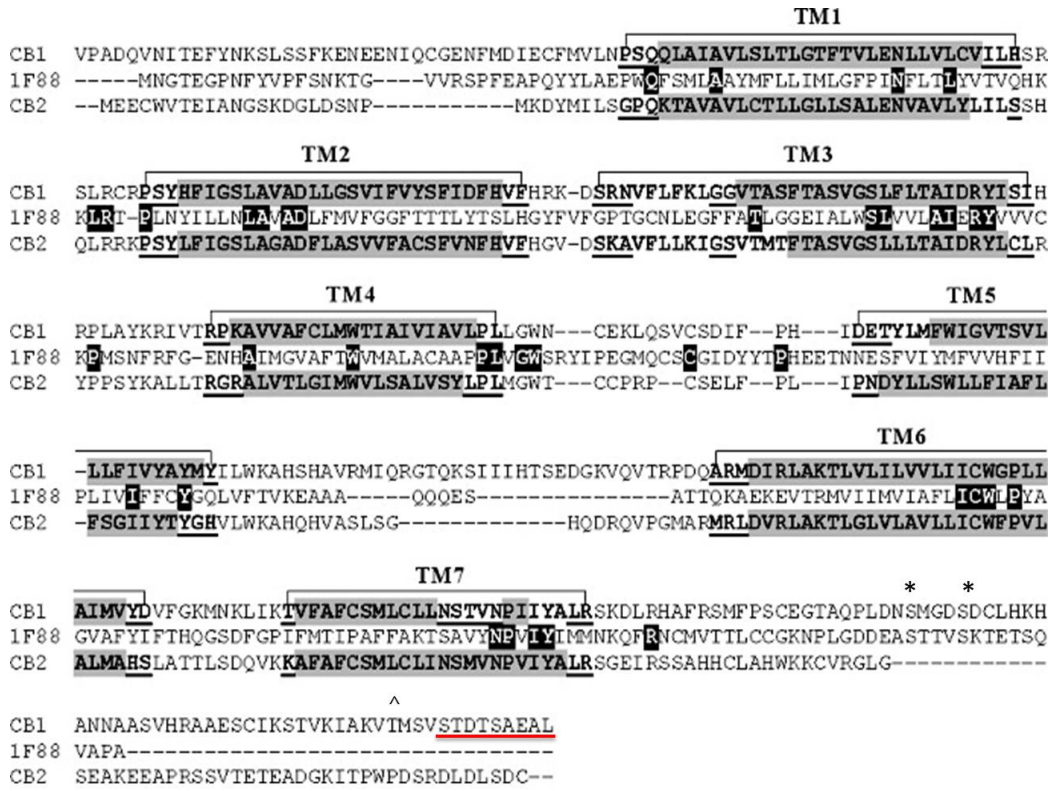


**Figure 1.** Alignment of the cannabinoid receptors and bovine rhodopsin (1F88) amino acid sequences. The identical residues shared among all three receptors are highlighted in black. α helix and β sheet predictions within the transmembrane regions were carried out by the modeling software, Psipred. The proposed α helix structures are marked in gray, while the proposed β sheet structures are underlined. Phosphorylation sites necessary for desensitization and internalization are represented by (*) and (^), respectively. Underlined in red is the $CRIP_{1a}$ binding site. Figure is adapted from Tuccinardi *et al.* (2006), Jin *et al.* (1999), Hsieh *et al.* (1999) and Niehaus *et al*. (2007).

Once an agonist binds to the receptor, a conformational change occurs, stabilizing the receptor in an active state (Sprang, 1997; Lefkowitz *et al*. 1993). Receptor activation triggers a signaling cascade, beginning with the stimulation of bound heterotrimeric G-proteins (Figure 2). An exchange of GDP for GTP occurs at the Gα subunit, allowing the Gα and Gβγ subunits to dissociate both from the receptor and from one another. This dissociation allows both G-protein subunits to implement downstream signaling events. The cycle is eventually terminated due to the Gα subunit's intrinsic GTPase activity. GTP is dephosphorylated back to GDP, which

returns the Gα subunit to its resting state, allowing it to reassociate with both the Gβγ subunit and a GPCR (Rockhold, 2002).

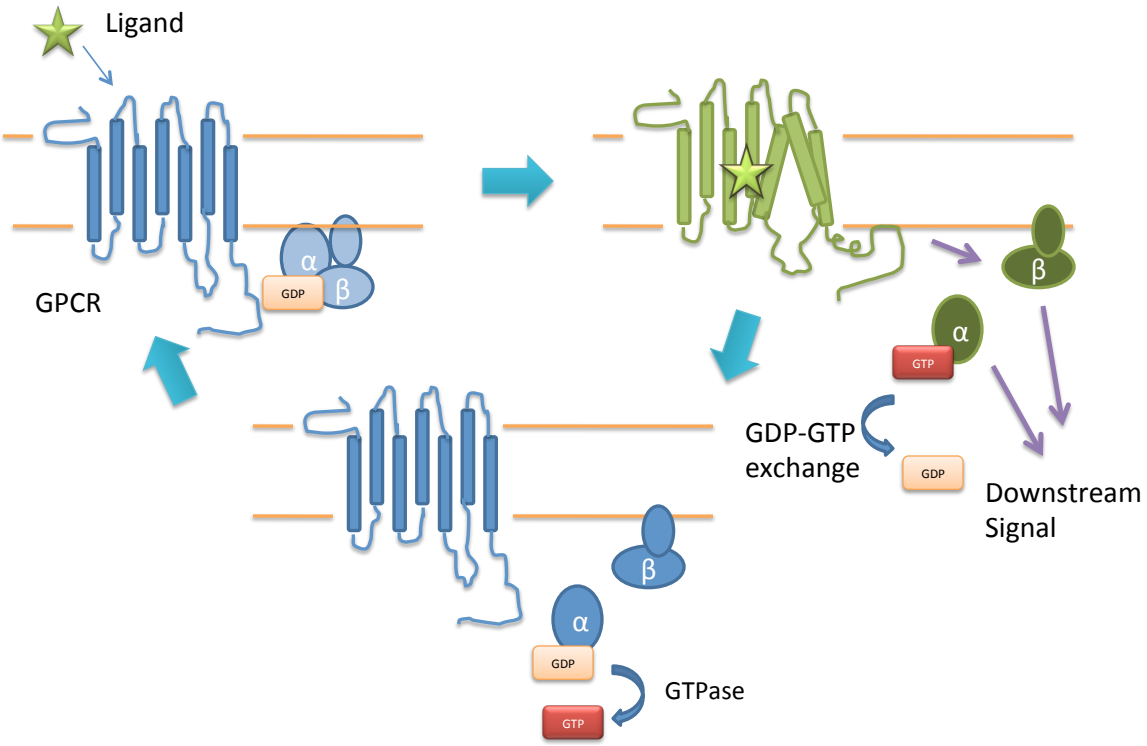


**Figure 2.** G-protein-coupled receptor (GPCR)-mediated G-protein activation. In the inactive state, G-proteins exist in the form of an αβγ heterotrimer, with the Gα subunit bound to GDP. Upon receptor activation, either by the binding of agonist or constitutively, the receptor changes to an active conformation (green), thereby activating G-proteins by promoting the exchange of GDP for GTP. The Gα-GTP and Gβγ dimer functionally dissociate from one another and the receptor and are free to modulate downstream effectors. The cycle concludes when the GTPase activity of the Gα subunit hydrolyses GTP to GDP, allowing the Gα subunit to return to its resting confirmation and reassociate with Gβγ. Figure is adapted from Smith *et al*. (2010).

GPCRs are known to act catalytically (Gilman, 1987), and are capable of signal amplification. This is possible due to the rate at which a GPCR can activate G-proteins, which is faster than the rate at which the initially activated G-protein can turn itself off. G-protein

activation can be measured utilizing the [$^{35}$S]GTPγS binding assay, in which a hydrolysis-resistant form of GTP is used. A radioactive sulfur, [$^{35}$S], replaces an oxygen molecule on the γ phosphate, which impedes GTP from being dephosphorylated to GDP. During incubation with ligands of interest and an excess of GDP, the radiolabeled GTPγS molecule readily binds to activated Gα subunits and accumulates. This complex now serves as a measure of G-protein activation in response to ligand. Ligand efficacies are often determined using this method, including numerous cannabinoid compounds that have been characterized as full, partial or inverse agonists at the $CB_1$ receptor.

A ligand's efficacy and potency can be measured utilizing a concentration effect curve, which provides an $E_{max}$ and $EC_{50}$ value, respectively. Many natural and synthetic cannabinoids have been analyzed for their respective efficacies on $CB_1$-mediated G-protein activation, as G-protein activation is an early event in $CB_1$ receptor-mediated signal transduction. CP55,940 and WIN are examples of high efficacy cannabinoids at the $CB_1$ receptor (Griffin *et al.* 1998), while THC and a more stable anandamide analog, methanandamide, are examples of partial agonists, with THC exhibiting low efficacy (Sim *et al.* 1996, Breivogel *et al.* 1998). Anandamide has also been shown to bind to $CB_1$ receptors in the cerebellum and produce moderate efficacy relative to WIN in agonist-stimulated [$^{35}$S]GTPγS binding assays (Kearn *et al*. 1999; Breivogel *et al*. 1998). The $CB_1$ receptor antagonist, SR141716A, also known as rimonabant, was reported to have inverse agonist properties (Bouaboula *et al.* 1997; Landsman *et al.* 1997), further inhibiting the agonist-independent "basal" G-protein activity. Inverse agonists, by definition, bind to the same site as agonists, but produce opposite effects (Figure 3). This concept is explained in further detail below, in Section 1.5.

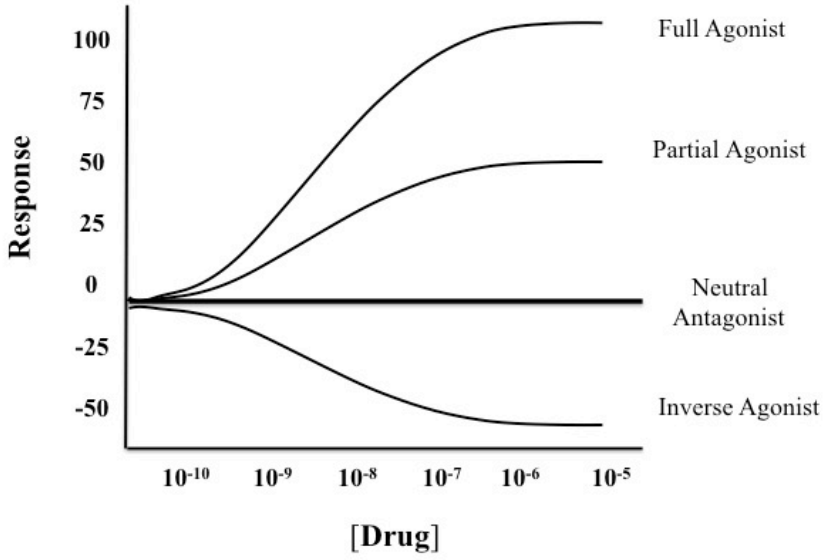


**Figure 3.** Hypothetical concentration-effect curves diagraming ligand efficacy. The curve with the greatest maximal effect represents a full agonist. The second curve represents a partial agonist, where its maximal effect lies between 0% and 100% response. A neutral antagonist binds to the receptor, but produces no response; therefore a straight line represents this state rather than a curve. Neutral antagonists may also graphically appear to have a similar response as when no agonist is present. Inverse agonists bind to the receptor and produce an opposite effect, in that they can suppress a given measure below the baseline level. It is thought that inverse agonists unmask the level of response specifically mediated by a receptor's constitutive, or basal activity. In all examples, once maximal response is reached, increases in ligand concentration produce no further change in response.

### 1.5 Constitutive G-Protein Coupled Receptor Activity

Inverse agonists are important tools in assessing the phenomenon known as constitutive activity, which is commonly reported in GPCRs. Constitutive activity is defined by the ability of a receptor to spontaneously shift from an inactive state, R, to an active state, R*, in the absence of an agonist (Figure 4). Currently, inverse agonists are thought to maintain the receptor in a closed conformation, leading to their ability to measurably reduce G-protein activity below tonic, or "basal" levels (Braestrup *et al*. 1983, de Ligt *et al.* 2000). Constitutive activity was first

observed in GPCRs by Costa and Hertz (1989), when inverse agonist properties were discovered in delta opioid receptors. Rinaldi *et al.* (1994) first observed inverse agonist effects in $CB_1$ receptors after the development of SR141716A. One criticism of these results, however, is that ligands such as SR141716A could be mediating endogenous "tone", rather than affecting the receptor state itself. In an attempt to further demonstrate this finding, studies were performed on various populations of GPCRs shown to be capable of spontaneous receptor activation by using cell lines or cultured neuronal populations that do not contain the related endogenous ligands. One such study specifically evaluated superior cervical ganglion (SCG) neurons injected with $CB_1$ cRNA and found that the $CB_1$ antagonist, SR141716A (or rimonabant), exhibited inverse agonist activity by reversing tonic inhibition of N-type voltage-gated $Ca^{2+}$ channels, thus increasing their activity and suggesting that $CB_1$ receptors display some level of constitutive activity (Pan *et al*. 1998). $CB_1$ receptor transfected cell lines provide a highly uniform and simplified model to compare inverse agonist and neutral antagonist actions. Conclusions drawn from those studies can therefore be directly related to the $CB_1$ receptor, since it is artificially expressed at higher levels compared to other GPCRs within these cell lines. [$^{35}$S]GTPγS binding has long been used as a method of identifying inverse agonist properties. Cell lines transfected with mouse or human $CB_1$ receptors have both exhibited measurable levels of constitutive activity as a result of SR141716A application in [$^{35}$S]GTPγS binding (Bouaboula *et al*. 1995; Landsman *et al.* 1997; MacLennan *et al.* 1998) suggesting it is a conserved function of the receptor and not an artifact of the species or model studied. However, similar studies performed in rat brain have not clearly detected constitutively active $CB_1$ receptors in cerebellar membranes, as the actions of SR141716A were shown to either be non-$CB_1$ receptor-specific or

the constitutive activity in these membranes was not able to be detected by the constraints of the [$^{35}$S]GTPγS binding assay (Sim-Selley *et al.* 2001).

A number of proteins have been found to interact with GPCRs, often mediating some level of control over G-protein signaling, including basal activity. β-arrestin and G-protein receptor associated sorting protein (GASP1) are known to bind to numerous GPCRs, including $CB_1$, and regulate internalization, downregulation and ultimately degradation (Martini *et al*. 2010, Bohn, 2009; Smith *et al.* 2010). The site of these protein-protein interactions is almost exclusively at the C-terminus, which is often not well conserved across GPCRs and subject to post-translational modifications. High sequence variability among the C-terminal tails of GPCRs allows for selectivity. It has been shown in metabotropic glutamate receptors that selective regulatory proteins competitively bind at the C-terminus and modulate constitutive activity (Ango *et al*. 2001). Thus, it is possible that many GPCRs known to exhibit constitutive activity might also interact with a regulatory protein that manages their tonic activity.

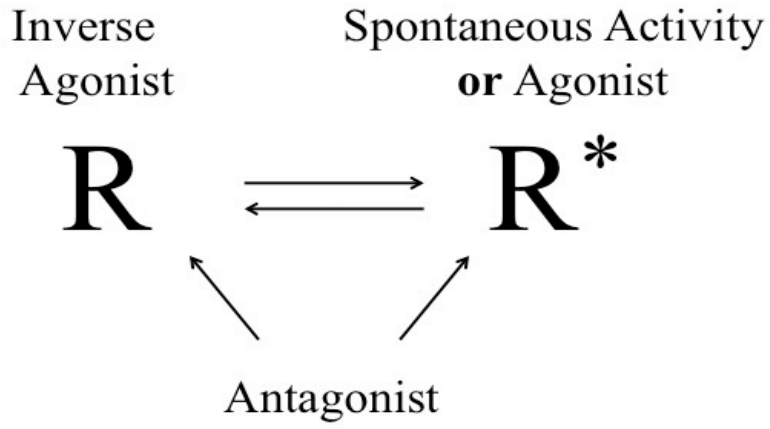


**Figure 4**. Receptor conformation state depends on stability induced by its environment. Previous receptor theories described two states: a closed, inactive receptor in the absence of ligand or presence of an antagonist, and an open active receptor when agonist is present. Inverse agonists are now thought to stabilize the receptor in an inactive conformation better than antagonists, and agonists are no longer thought to be required for the receptor to be in an activate state. However, agonists stabilize the active state.

**1.6 Cannabinoid Receptor Interacting Protein 1a.**

As discussed above, $CB_1$ receptors exhibit significant constitutive activity (Pan *et al.* 1998), and in 2001, Nie and Lewis found that truncation of the distal C-terminal tail led to increases in tonic inhibition of calcium channel currents. This evidence led to the speculation and search for a protein capable of regulating $CB_1$ receptor constitutive activity that possibly binds to the distal portion of the C-terminus. Yeast two-hybrid screening of a human cDNA library using the last 55 amino acids (aa 418 – 472) of the $CB_1$ C-terminal tail as bait revealed the successful retrieval of a new protein sequence (Niehaus *et al.* 2007). The gene encoding this protein sequence was found on human chromosome 2, and contains two alternative splice sites that produce the Cannabinoid Receptor Interacting Protein 1a ($CRIP_{1a}$) and the Cannabinoid Receptor Interacting Protein 1b ($CRIP_{1b}$), respectively. $CRIP_{1a}$ is comprised of 164 amino acids encoded by exons 1, 2 and 3a, while $CRIP_{1b}$ is slightly smaller at 128 amino acids encoded from exons 1, 2 and 3b. In mice, the gene for $CRIP_{1a}$, *Cnrip1*, is on chromosome 11 and does not appear to contain exon 3b. $CRIP_{1b}$ has not been well studied, and its function is largely unknown, in part because it is thought to be only expressed in primates. $CRIP_{1a}$ on the other hand, is expressed throughout vertebrates and has been shown to have a primary role in inhibiting $CB_1$ receptor constitutive activity by binding to the last 9 amino acids of its C-terminus (Niehaus *et al.* 2007). One study also shows a possible role in mediating $CB_1$ antagonist-induced neuroprotection from glutamate excitotoxicity (Stauffer *et al*. 2011). To date, $CRIP_{1a}$ has not been shown to interact with other GPCRs, including $CB_2$ receptors. Homology searches *in silico* showed that the 9 amino acid binding sequence required for association of $CRIP_{1a}$ with the $CB_1$ receptor was not present on the C-terminus of any other GPCR. $CRIP_{1a}$ does however contain a PSD-95, Disc large protein and

ZO-1 (PDZ) ligand domain on its own C-terminus, signifying that it could interact with other, PDZ domain-containing proteins, but not in the same manner that it interacts with $CB_1$ receptors.

$CB_1$ receptor expression is unaffected by $CRIP_{1a}$ as indicated by [$^3$H]SR141716A saturation binding in stably co-transfected HEK-293 cells (Niehaus *et al.*2007). Yet, inconsistent results have been found regarding agonist-stimulated $CB_1$ receptor activation. Niehaus *et al.* (2007) also showed that $CB_1$-microinjected SCG neurons with and without co-expression of $CRIP_{1a}$ did not display differences in $Ca^{2+}$ current inhibition after WIN 55,212-2 activation of $CB_1$ receptors. Our laboratory, however, has shown that $CRIP_{1a}$ inhibited agonist stimulated G-protein activity in N18TG2 (Figure 5) and $CB_1$-HEK-293 cells (not shown) stably over-expressing $CRIP_{1a}$ and furthermore, attenuated the inverse agonist effects of rimonabant (unpublished data, Figure 5). Potential changes in $CB_1$ receptor levels were again measured by [$^3$H]SR141716A saturation binding, however, no differences in $B_{max}$ or $K_D$ values were found in either cell line with and without stable ove-rexpression of $CRIP_{1a}$.

$CRIP_{1a}$ and $CB_1$ receptors have been shown to co-localize in superior cervical ganglion neruons (SCG) microinjected with cDNA encoding $CRIP_{1a}$ and human influenza hemagglutinin (HA) tagged $CB_1$ receptors (Niehaus *et al.* 2007). The major finding in that study suggested that $CB_1$ receptors and $CRIP_{1a}$ do indeed interact, and more importantly, the site of interaction occurred at the plasma membrane, where GPCRs are known to exert their signaling effects. Co-localization has also been reported between the two in cone photoreceptor cells (Hu *et al.* 2010). One interesting finding from that study showed $CRIP_{1a}$ was limited to presynaptic terminals, but that it reliably aligned with postsynaptic DAGL$\alpha$ in a one to one ratio. $CRIP_{1a}$ was also found to co-localize with $CB_1$ receptors on the outer plexiform layer within the synapse, thereby reinforcing a likely role of $CRIP_{1a}$ in $CB_1$-mediated signaling.

$CRIP_{1a}$ has also been investigated within the human brain for its potential association with epilepsy (Ludányi *et al.* 2008). Hippocampal tissue was obtained post-mortem from individuals who suffered from therapy-resistant temporal lobe epilepsy, as well as from those with no known neurological disorders to serve as controls. RNA was extracted from control subjects' hippocampal tissue and epileptic subjects' sclerotic and non-sclerotic hippocampal tissue. $CB_1$, $CRIP_{1a}$ and $CRIP_{1b}$ mRNA levels were then quantified relative to two housekeeping genes, β-actin and glyceraldehyde-3-phosphate dehydrogenase (GAPDH), using qPCR. $CB_1$ and $CRIP_{1a}$ mRNA levels were significantly reduced in sclerotic hippocampal tissue of epileptic patients compared to controls, while no changes were observed in $CRIP_{1b}$. This study was the first to show $CRIP_{1a}$ mRNA levels were altered in tandem with $CB_1$ receptor mRNA in response to a neurological disease.

Another study also focused on $CB_1$ receptors and $CRIP_{1a}$ within the hippocampus in a rat model of epilepsy by inducing seizures with the excitotoxin, kainic acid (KA). This time, results indicated that after KA administration, $CB_1$ and $CRIP_{1a}$ mRNA expression was increased compared to controls. Though these results differ from the human study described above, the KA model in rats and therapy-resistant temporal lobe epilepsy in humans do not exhibit the same pathology, thus potentially eliciting different alterations to the endocannabinoid system. The parallel expression patterns between $CRIP_{1a}$ and $CB_1$ receptors are consistent with the previous study, however.

$CRIP_{1a}$ has additionally been linked to glutamate excitotoxicity by engaging in a novel "switching" mechanism as shown by Stauffer *et al.* (2011). In this study, primary cortical neurons with and without over-expression of $CRIP_{1a}$ were treated with the cannabinoid agonist, WIN, or the antagonist, SR141716A, and challenged with excess glutamate. Over-expression of

$CRIP_{1a}$ was found to block the cannabinoid receptor-mediated neuroprotective role of WIN. However, when these neurons were treated with SR141716A, the neuroprotective mechanisms were restored. Furthermore, those neurons over-expressing $CRIP_{1a}$ yielded a similar level of protection against excitotoxicity (roughly 30% less cell death) when compared to neurons treated with WIN but not over-expressing $CRIP_{1a}$. These results suggest that $CRIP_{1a}$ might have additional capabilities in modulating $CB_1$ signaling, beyond that of negative regulation.

New evidence has begun to illustrate potential roles of $CRIP_{1a}$ in other receptor systems. A viral knockdown approach was used in rat dorsal striatum to show that when $CB_1$ receptors are significantly reduced, dopamine $D_2$ ($D_2$) receptors follow suit, thus suggesting cooperative regulation of the expression of these receptors within the striatum. $CRIP_{1a}$ expression was subsequently found to increase as a result, suggesting a possible role in modulating $D_2$ receptors or acting as a modulator of the $D_2$:$CB_1$ receptor interaction (Blume *et al*. 2013). In addition, this study also examined virally mediated over-expression of $CRIP_{1a}$ within the striatum. Interestingly, a trend was observed in which WIN-stimulated G-protein activation was reduced, which agrees with our own laboratory's data in cell lines over-expressing $CRIP_{1a}$, which showed significant reduction in WIN-stimulated G-protein activation (see Figure 5). Together, these results continue to suggest that $CRIP_{1a}$ negatively regulates $CB_1$ receptors.

Previous studies have primarily involved over-expression of $CRIP_{1a}$, which can be laden with pitfalls resulting from over-expressing or ectopically introducing a protein into a system. A critical complementary strategy is to use "loss-of-function" approaches to reduce or eliminate gene expression in tissues where it is normally expressed. We chose the gene knockout approach in mice because it provides a complete loss of gene expression and allows us to study the

consequences of this deletion both *in vitro* and *in vivo*. Thus, this approach can provide information about the function of $CRIP_{1a}$ in the intact animal.

This thesis outlines the first studies and findings of $CRIP_{1a}$ function in the whole animal. Both behavioral assessments and *in vitro* studies were performed on the first $CRIP_{1a}$ knockout (KO) mouse line, which was developed at VCU by our laboratory in collaboration with Dr. Ching-Kang Chen's laboratory in the Department of Biochemistry and Molecular Biology. My hypothesis is two fold: that $CRIP_{1a}$ KO mice might exhibit cannabimimetic phenotypes due to increased $CB_1$ receptor activity (either constitutive or endocannabinoid-mediated) and/or that these mice will display an enhanced response to cannabinoid agonists compared to littermate wild-type (WT) mice. Behavior will be assessed first in a naïve state with particular attention to responses that are known to be mediated by $CB_1$ cannabinoid receptors. These responses include measures of antinociception, evaluated by the warm water tail withdrawal assay and the hot plate assay, measures of locomotor activity and motor coordination, and finally, measures of anxiety-like behaviors. Mice will subsequently be administered cannabinoid agonists to determine whether $CRIP_{1a}$ KO mice exhibit altered sensitivity to agonist when this regulatory protein is absent. The brains of $CRIP_{1a}$ WT and KO mice will be dissected into specific regions and investigated for differences in $CB_1$ receptor levels, ligand affinities and basal and agonist-stimulated G-protein activity. $CRIP_{1a}$ expression levels will further be assessed in $CB_1$ receptor WT and KO mice treated chronically with either vehicle or THC. As a whole, I expect to unveil specific novel findings related to $CRIP_{1a}$ function in the CNS *in vitro* and for the first time, *in vivo,* by investigating behavioral and physiological responses in the whole animal. These studies will provide a greater understanding of the potential roles of $CRIP_{1a}$ in mediating or modulating $CB_1$ receptor signaling and function.

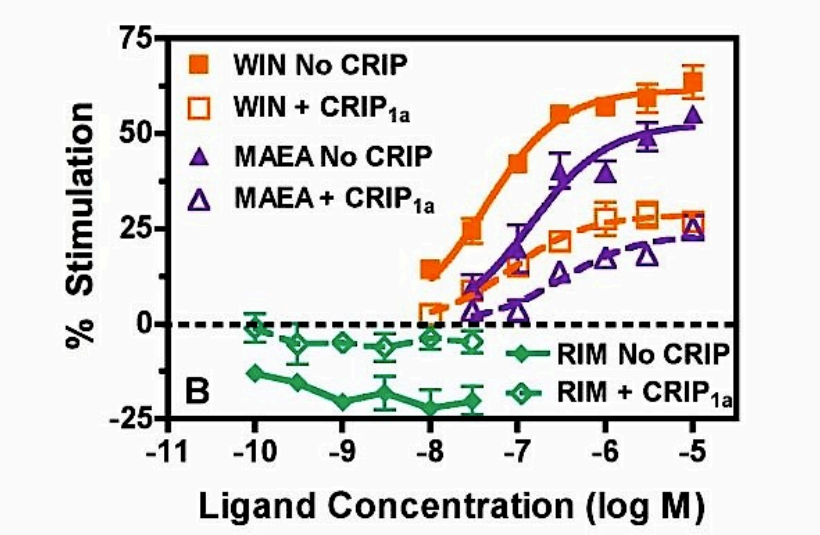


**Figure 5.** Agonist-stimulated [$^{35}$S]GTPγS binding in N18TG2 cell lines with and without overexpression of $CRIP_{1a}$. WIN55,212-2 (WIN) and methanandamide (MAEA) stimulation above basal, and rimonabant (RIM) suppression below basal levels were significantly attenuated by $CRIP_{1a}$ overexpression. Data are expressed as mean ± SEM (n =4 experiments performed on separate days).

## Chapter 2. Materials and Methods

### 2.1 Materials.

[$^{3}$H]CP55,940 (88.3 Ci/mmol) and CP55,940 (-) was obtained from the National Institute on Drug Abuse drug supply program (NIDA, Rockville, MD). [$^{35}$S]GTPγS (1250 Ci/mmol) was purchased from Perkin Elmer Life Sciences (Boston, MA). Econo-Safe scintillation fluid was purchased from Research Products International Corporation (Mount Prospect, IL). Bovine serum albumin (BSA), GTPγS, GDP and WIN 55,212-2 (dissolved in ethanol) were purchased from Sigma-Aldrich Chemical Company (St. Louis, MO). Whatman GF/B filters were purchased from VWR (Bridgeport, NJ). Methanandamide (ethanol) was purchased from Cayman Chemical (Ann Arbor, MI). Noladin Ether (ethanol), CP55,940 (ethanol) and SR-141716A (ethanol) were provided by the Drug Supply Program of the National Institute on Drug Abuse (NIDA, Rockville, MD). Protease Inhibitor Cocktail was purchased from Promega Co. (Madison, WI). $CRIP_{1a}$ antisera 077.4 was provided by Dr. Maurice Elphick (Queen Mary University of London). α-Tubulin antisera DM1A was purchased from Abcam (Cambridge, MA). Licor Odyssey infrared dye-conjugated secondary antibodies were purchased from Li-Cor Biosciences (Lincoln, NE). The High Capacity cDNA Reverse Transcription kit was purchased from Applied Biosystems (Grand Island, NY). The QuantiFast SYBR Green RT-PCR Kit was purchased from Qiagen (Germantown, MD). MyTaq™ Red PCR Master Mix was purchased from Bioline (Taunton, MA). Trizol® was purchased from Invitrogen Life Technologies (Carlsbad, CA). All other chemicals, including salts, buffers, chelating agents, detergents and acrylamide were reagent grade and purchased from Sigma-Aldrich Chemical Company (St. Louis, MO) or Fisher Scientific (Waltham, MA).

## 2.2 Generation of the *Cnrip1* Knockout Mouse Line.

A targeting vector for the *Cnrip1* locus was developed that replaces all of exon 1 and 2, including 214 base pairs upstream of exon 1 and 590 base pairs downstream of exon 2 with a neomycin (NEO) cassette (Figure 6). The homology arms were amplified by PCR using the BAC clone RP23-348N2 (CHORI BACPAC Resources, Oakland, CA) as template. The left homology arm was amplified by PCR primers CNRIP1-LAXhoF: ACCGctcgagGATCCACAGGAATTGTGCT and CNRIP1-LABgl2R: CTAagatctAAACGGGGTAGGAAACTGCT yielding a 1.6kb product. The right homology arm was amplified by PCR primers CNRIP1-RANotF: ATAAGAATgcggccgcCATGGATGCAGAGCCTATT and CNRIP-RANotR: ATAAGAATgcggccgcTTGGCATCATCAGAACCAAA yielding a 4.0kb product. The left homology arm PCR product and DNDF-7 vector was digested with *Xho*I and *Bgl*II and ligated. Afterwards, the right homology arm and the DNDF-7-LA (which contains the left homology arm) was digested with *Not*I and ligated to form the final targeting vector construct. The targeting vector was linearized with *Bsi*WI and purified by phenol/chloroform extraction prior to electroporation. By replacing some of the upstream sequence, the transcriptional start site and a portion of the promoter are no longer present after homologous recombination, therefore essentially eliminating the possibility that exon 3, which remains intact, could be transcribed into mRNA. Two diphtheria toxin A (DTA) cassettes were included in the targeting vector to serve as negative selection controls. The targeting vector was created by our collaborators, Drs. Hoon Shim and Ching-Kang (Jason) Chen, in the Department of Biochemistry and Molecular Biology, VCU School of Medicine.

The targeting vector was sent to inGenious Targeting Laboratory, Inc. (Ronkonkoma, NY) for the development of chimeric mice on a 50% C57Bl6 and 50% 129sv mixed-strain background. The chimeric mice were sent to VCU and bred to produce heterozygous offspring, which were screened for germline transmission by standard PCR methods using specific primers (Figure 7). The mice carrying a copy of the NEO allele were then bred to each other to form the founder population for the $CRIP_{1a}$ mouse line. Heterozygous breeding pairs were maintained from that point onward.

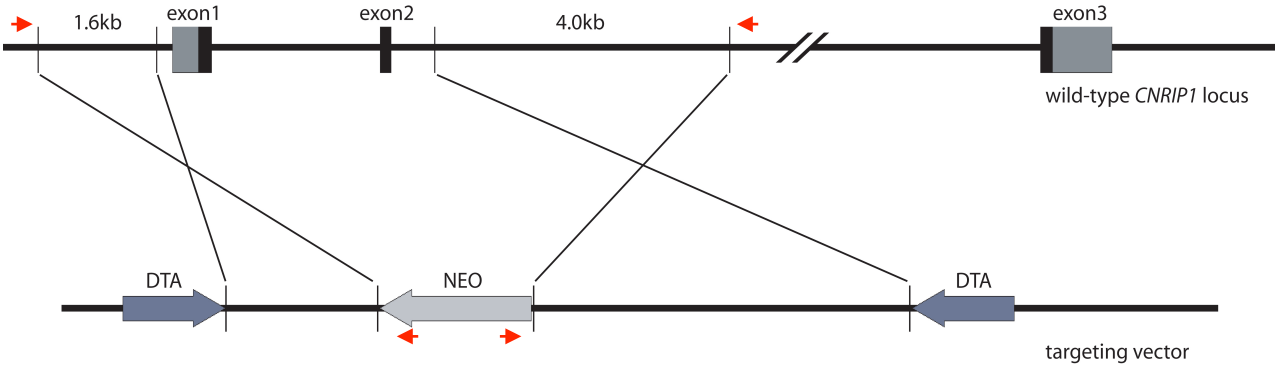


**Figure 6.** Maps of wild-type *Cnrip1* locus and the targeting vector. The *Cnrip1* coding sequence is represented in black and non-coding sequences in exon1 and exon3 are represented in gray. Arrows represent PCR primer locations. The targeting vector replaces all of exon1 and exon2, along with 214 bp upstream of exon1 and 590 bp downstream of exon2 with a NEO cassette. The targeting vector contains the NEO cassette for positive selection and 2 DTA cassettes for negative selection.

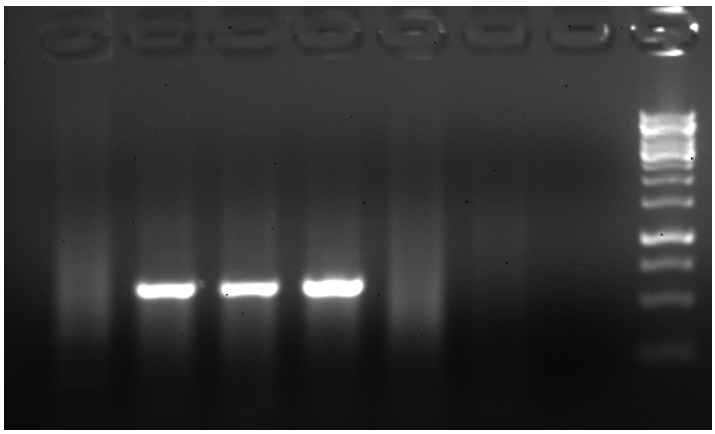

**Figure 7.** Germline transmission of *Cnrip1* KO allele achieved in 3 mice. Lanes 1 and 6 represent mice that are wild type for the *Cnrip1* locus. Lanes 2, 3 and 4 represent mice carrying the NEO allele, indicating these mice are the first heterozygous germline carriers of the *Cnrip1* locus. Lane 7 is a blank (negative) control, followed by a ladder for confirmation of product fragment size.

**2.3 PCR Genotyping of *Cnrip1* Mutant Mice.** The resulting litters were weaned at 21 days of age and a small tissue sample from each weanling was collected for genotyping. DNA was extracted and isolated via the HotSHOT method (Truett *et al.* 2000). The primer pair for the wild type (WT) allele is 3' GACCACTCACAAATGCCA-GA 5' (forward) and 3' GCACTCTAGGTTAATAGGCTCTGC 5' (reverse). The primer pair for the knockout (KO) allele, which probes for the NEO cassette, is 3' GAGACGT-GCTACTTCCATTTGTC 5' (forward) and 3' GCACTCTAGGTTAATAGGCTCTGC 5' (reverse). The reverse primer sequence is the same for both alleles. All experiments were performed using mice maintained on the mixed background described earlier.

**2.4 Measuring Body Weight and Core Body Temperature.**

**Subjects.** Subjects included littermate male and female $CRIP_{1a}$ WT, heterozygous (HET) and KO maintained on a mixed (50/50) 129sv/C57Bl6/J background. The mice were housed according to sex in groups of up to 5 per cage and maintained in a temperature-controlled environment (20-22ºC) in an American Association for the Accreditation of Laboratory Approved Animal Care-approved vivarium. Food and water were available *ad libitum*. The mice were kept in a 12-hour light/dark cycle with lights on at 06:00.

**Body Weight.** All mice were weighed weekly from weaning (3 weeks) until 12 weeks of age using a WeighMax™ gram scale. Mice were again assessed four weeks later, at 16 weeks of age.

**Core Body Temperature.** Adult mice (12-16 weeks) were assessed for core body temperature, measured using a 2.0 cm rectal thermocouple probe. Temperatures were obtained from a telethermometer. Mice were returned to their home cages after testing was completed.

**Data Analysis.** Body weights were analyzed via two-way ANOVA followed by Bonferroni post hoc test. Core body temperature was analyzed by student's t-test. Significance was reached when $p < 0.05$ for both measures.

## 2.5 Behavioral Phenotyping: Baseline Tests of Nociception, Spontaneous Motor Activity, Motor Coordination, and Anxiety in Drug-Naïve Mice.

**Subjects.** Subjects included littermate male and female $CRIP_{1a}$ WT and KO maintained on a mixed (50/50) 129sv/C57Bl6/J background. The mice (20-30g) were housed as described above (Section 2.4). All experiments were performed during the hours of the light cycle.

**Nociception.** Thermal nociception was evaluated using two assays. The first was a warm water tail withdrawal procedure that measured the time in seconds for a mouse to remove its tail from a warm water bath set to 48º, 52º or 56ºC. Mice were lightly restrained using a padded body bag covering all but the tail. Once settled, the distal portion of the tail was inserted into a warm water bath and a timer immediately started. The timer was stopped when the mouse fully removed its tail from the water, typically observed as a flicking motion. A cut-off time of 10 seconds was used to avoid any possible tissue damage to the tail. Mice were placed back into their home cage until further testing was performed at higher temperatures.

The second test used a hot plate to measure the amount of time in seconds for a mouse to lift, lick or shake one of its hind paws from the warm surface set to 52º or 56ºC. Mice were gently

placed onto the hot plate and barricaded by a clear acrylic cylinder measuring 7.5 cm in diameter. A mirrored back panel increased visibility appreciably, providing nearly a 360º view of the mouse. Once all four paws were planted on the plate surface, the timer was started. A 20 second cut-off time was applied to avoid soft-tissue damage to the paws. The trial ended when the mouse elicited any of the lifting, licking or appendage shaking behaviors indicating a response to the nociceptive stimulus. The cylinder barricade was removed and the mouse was lifted from the plate and placed back into its home cage.

**Locomotor activity.** Spontaneous motor activity was assessed using ANY-maze™ video tracking software (Stoelting Co., Wood Dale, IL) in tandem with Fire-i™ digital cameras (Unibrain, San Ramon, CA) mounted from the ceiling of sound-attenuating cabinets. A rectangular barrier made of clear plastic was set on a white tray (30 cm L x 15 cm W), forming the open-field test parameters. Mice were evaluated individually and were placed in the center of the tray to begin the test. The cameras began recording immediately after the cabinet door was latched closed and movements of each mouse were tracked for 30 minutes. Any motion, including forward movement, turns, immobility and bouts of freezing were documented within the 30-minute time period. Mice were tested in the absence of drug and had no previous exposure to this particular chamber set-up due to reports of environmental habituation (File, 2001).

**Motor coordination.** Motor coordination was evaluated using an IITC RotaRod apparatus (IITC Life Science, Inc., Woodland Hills, CA) fitted with 1¼ inch diameter drums. Mice were trained at 10 rpm two separate times for up to 120 seconds each. Any animals that clung to the drum and spun with it rather than walking on top were considered to have made a "passive

rotation", which ended the training session as if they had fallen. Any mouse that jumped from the drum was scored by the distance and rpm at which it jumped. After two training sessions, mice were then tested at 16 rpm for a maximum of 120 seconds. Again, passive rotations and jumps ended the test, with their performance based on the last rpm and distance recorded prior to jumping or rotating. Data were collected for both training and testing trials, however only the scores for maximum rpm and distance at 16 rpm were analyzed.

**Anxiety-like behavior.** Anxiety-like behaviors were assessed using two assays: the light:dark box and marble burying. All mice examined were naïve to the assay environments and had not been pretreated with any drug. The light:dark box chamber (Stoelting Co., Wood Dale, IL) was placed inside a sound-attenuating cabinet complete with ceiling-mounted Fire-i™ digital cameras. The video tracking software, ANY-maze™, was used to record the animal's movements. The light compartment measured 20.5 cm x 40 cm and was surrounded by clear plastic panels and an open ceiling. The dark compartment was smaller, measuring 10 cm x 40 cm, and was enclosed by black panels on the top and sides. Infrared camera technology was used to view the mice while in the dark compartment. A small throughway measuring 7 cm x 7 cm allowed the mice to freely move between chambers. Mice were initially placed in the bottom right-hand corner of the light compartment, lit by a 60W bulb above. The cabinet door was latched closed and the five-minute tracking period was initiated, recording the movements within and between the light and dark chambers. After five minutes, the mice were returned to their home cage. Due to habituation, the same mouse was never tested twice.

To evaluate the mice in the marble burying assay, a cage measuring 12.5 x 8 inches (100 $in^2$) was filled with minced wood chips reaching a depth of 3 inches. Bedding was not compacted to encourage mobility of marbles. Twenty clear marbles (14 mm circumference) were placed in a 4

x 5 pattern, evenly spaced throughout. The mice were each given twenty minutes to explore the surroundings and the opportunity to bury marbles. A clear plastic panel was placed on top to prevent mice from jumping or climbing out of the cage. After twenty minutes had elapsed, mice were carefully removed and placed back in their home cage. Marbles were then assessed for buried status. Any marble whose surface was more than 50% covered by bedding was considered buried. The number of marbles remaining unburied was counted and then subtracted from 20 to obtain the actual number of marbles buried.

**2.6 Data analysis: Baseline Tests of Nociception, Spontaneous Motor Activity, Motor Coordination, and Anxiety in Drug-Naïve Mice.**

**Nociception.** Latencies for warm-water tail withdrawal and hot plate were analyzed by student's two-tailed t-test with significance reached at $p < 0.05$.

**Locomotor Activity.** When collapsed by test segment, time mobile, time immobile and time freezing were analyzed using student's two-tailed t-test with significance reached when $p < 0.05$. When analyzed separately as three separate test segments, two-way ANOVA followed by Bonferroni post hoc test was used. Significance was reached when $p < 0.05$.

**Motor Coordination.** RotaRod performance was analyzed by student's two-tailed t-test for both latency to fall and distance travelled. Significance was reached when $p < 0.05$.

**Anxiety-like behavior.** Light:dark box and marble burying scores were analyzed using student's two-tailed t-test, with significance reached when $p < 0.05$.

**2.7 Behavioral Phenotyping: Tetrad Assessment of Nociception, Catalepsy, Body Temperature and Motor Coordination After CP55,940 Administration.**

**Subjects.** Subjects were adult littermate $CRIP_{1a}$ WT, HET and KO male mice, 25-35g in body weight. Mice were housed and fed as described in Section 2.4.

**Modified "Tetrad" Test with Cumulative Drug Dosing.** Mice were evaluated for a series of behaviors and physiological responses known to occur with cannabinoid agonists, compiled into a modified "tetrad" assessment. Traditionally, spontaneous locomotor activity is included in this set of experiments (Little *et al.* 1998), however, due to our implementation of a cumulative dosing protocol (see below) and evidence suggesting habituation of mice after repeated exposures to the locomotor evaluation chambers, we chose to examine motor coordination using an accelerating RotaRod protocol instead (for review, see Deacon, 2013). The remaining three portions of the tetrad assay were still examined, which include rectal temperature, catalepsy and warm water tail withdrawal. Antinociception was also evaluated in the hot plate assay.

Mice were acclimated to shoebox cages where the average ambient temperature was 24 ± 2°C and 35% humidity for at least 1 hour prior to testing. CP55,940 was dissolved in dimethyl sulfoxide (DMSO) and added to emulphor and saline for a final vehicle ratio of 1:1:18; DMSO:emulphor:saline. CP55,940 was administered to mice using a cumulative, within-session dosing protocol. The CP55,940 concentrations were as follows: 0.001 mg/ml (0.01 mg/kg), 0.003 mg/ml (0.03 mg/kg), 0.007 mg/ml, (0.07 mg/kg), 0.02 mg/ml (0.2 mg/kg), and 0.07 mg/ml (0.7 mg/kg), which result in cumulative doses of 0.01, 0.03, 0.1, 0.3, and 1 mg/kg, respectively. Baseline values for catalepsy, tail withdrawal latency, hot plate latency, rotarod performance and rectal temperature were assessed for each mouse in that order prior to any injections (least

invasive to most invasive). Intraperitoneal (i.p.) injections were administered in a volume of 1 ml/100 g bodyweight 30 minutes prior to testing the effects of each dose, with 10 minutes lapsing between the end of the previous test session and the next round of injections.

To evaluate catalepsy, the front paws of each mouse were placed on a bar measuring 0.75 cm in diameter and set to a height of 4.5 cm from the bench surface. If the mouse remained in place, a timer was started. Any movement(s) beyond normal respiration stopped the timer. Up to 3 attempts could be made to reposition the mouse if it moved at any point within a 60 second time period. All periods of immobility were totaled for the catalepsy score, with 60 seconds being the maximum. Nociception was assessed using the warm water tail withdrawal assay and the hot plate assay. Both tests were performed at 52ºC as previously described (see section 2.5). Motor coordination was assessed at each time point by placing the mice on a stationary RotaRod drum, facing outward. The drum was set to begin moving at 6 rpm and accelerate to a maximum of 25 rpm over a span of 60 seconds. The rpm and time in seconds at which the mouse fell off the drum, or completed a passive rotation (spun with the drum), was scored as the maximum performance for that trial. Core body temperature was measured using a 2.0 cm rectal thermocouple probe, and temperatures were obtained from a telethermometer. Mice were returned to their home cages after testing was completed.

**Data Analysis.** CP55,940 dose-effect curves were analyzed by two-way ANOVA with $p < 0.05$ determining significance. Data for catalepsy and both measures of nociception were transformed to %MPE and analyzed by two-way ANOVA, with $p < 0.05$ determining significance. %MPE was calculated using the following equation: [(test latency – control latency) ÷ (max latency – control latency)] x 100. Maximum latencies were determined by specific cut-off times associated with each test. The cut-off for catalepsy was 60 seconds, the cut-off for hot plate was

20 seconds and the cut-off for warm water tail withdrawal was 10 seconds. Any subject that reached the cut-off time was immediately removed from the test apparatus and assigned the maximum time score allowed.

**2.8 Dissections.** Brains were removed from the skull and forebrain regions of interest were dissected. The hippocampus and amygdala were then dissected from the remaining brain for the current studies. The cortex was removed from the superior surface of the brain to expose the hippocampus. Cuts were made at the anterior and posterior aspects of the hippocampus to produce a thick coronal section. The piriform cortex was removed, and the amygdala was dissected from the ventral lateral aspect of the section using the optic tract and bifurcation of the corpus callosum as landmarks. This dissection included most amygdalar subnuclei, except those at the most posterior extent of the complex. The hippocampus was then removed from the remaining section using the corpus callosum as an interior border. This dissection included most of the hippocampal complex. The whole cerebellum was collected by separating from the brainstem. The spinal cord was collected by using the decapitation cut as the anterior border and making a second cut at the level of the hip bone as a posterior border. The spinal cord was then extracted by inserting a $ddH_2O$ filled 40 ml syringe fitted with a 200 µl pipette tip into the spinal column at the posterior end and expelling under pressure. This procedure expels the whole intact spinal cord, although the initial cervical portion of the spinal cord is likely lost during decapitation and the most posterior sacral segments might not be included. The use of the decapitation point and hip bone as anterior and posterior landmarks, respectively, provides a consistent sample for analysis. Tissue was immediately frozen on dry ice and stored at -80°C until use.

**2.9 Membrane Preparation (for Binding Assays).** Mice were euthanized by rapid decapitation with a sharp guillotine. Brain regions were dissected on ice as described in Methods 2.8 and immediately frozen and stored at -80°C. Once thawed, the tissue was homogenized in 50 mM Tris-HCl, 3 mM $MgCl_2$, 0.2 mM ethylene glycol tetraacetic acid (EGTA), 100 mM NaCl pH 7.4 (assay buffer) using a Polytron homogenizer for 10 seconds. If homogenates were used in receptor saturation binding experiments, the assay buffer was comprised of the previous recipe minus 100 mM NaCl. Homogenates were centrifuged at 50,000 x g at 4°C for 10 minutes and resuspended in assay buffer. Membrane protein levels were assessed via the Bradford method, using 1 mg/ml BSA as the standard (Bradford, 1976).

**2.10 Whole Homogenate Preparation (for Immunoblotting).** Mice were euthanized as above and brain regions were dissected on ice as described in Methods 2.8, and immediately frozen and stored at -80°C. Once thawed, the tissue was homogenized via sonication in cell lysis cocktail buffer (electrophoretic mobility shift assay (EMSA) buffer (20 mM HEPES at pH 7.8, 0.4 M NaCl, 5 mM $MgCl_2$, 0.5 mM ethylenediaminetetraacetic acid (EDTA), 0.1 mM EGTA, 1% NP-40, 20% glycerol) plus 1% protease inhibitor and 0.1% dithiothreitol (DTT). Samples were centrifuged at 15,000 x g for 10 minutes at 4ºC. The supernatant was saved and the pellet was discarded. Protein concentrations were determined using the Bradford method, with 1 mg/ml BSA as the standard (Bradford, 1976).

**2.11 [$^3$H]CP55,940 Binding.** Membranes (10-30 μg protein) were incubated for 90 minutes at 30°C in assay buffer (with no NaCl) plus 0.5% (w/v) BSA containing ascending concentrations of [$^3$H]CP55,940 ranging from 0.1 nM to 5 nM, with and without 5 μM unlabeled CP55,940 to

measure nonspecific and total binding values, respectively. Total reaction volume was 0.5 ml. At the end of 90 minutes, the reaction was terminated by rapid vacuum filtration through GF/B glass fiber filters that were presoaked in cold Tris-HCl buffer (pH 7.4) containing 0.5% (w/v) BSA. Bound radioactivity was determined using liquid scintillation spectrophotometry at 45% efficiency for [$^{3}$H].

**2.12 [$^{35}$S]GTPγS Binding.** Membranes (5-10 μg protein) were incubated for 15 minutes at 30ºC in the presence of 2 μl/ml adenosine deaminase (ADase) immediately prior to assay. This step inactivates endogenous adenosine, which can be tightly bound to G-protein-coupled adenosine receptors thereby elevating basal [$^{35}$S]GTPγS binding (Moore *et al*., 2000). ADase pretreated membranes were then added to assay buffer containing various drugs, 30 μM GDP, 0.1% BSA and 0.1 nM [$^{35}$S]GTPγS in a total volume equaling 0.5 ml, which was then incubated for 2 hours at 30ºC. Basal [$^{35}$S]GTPγS binding was evaluated in the absence of agonist and non-specific binding was measured using 10 μM unlabeled GTPγS. The assay was terminated by rapid vacuum filtration through GF/B glass fiber filters. Bound radioactivity was determined by liquid scintillation spectrophotometry at 95% efficiency for [$^{35}$S].

**2.13 Immunoblotting.** Tissue homogenates of varying concentrations (25–100 μg) were added to sample buffer (1 M TRIS, 20% SDS, 1 M DTT, 60% w/v sucrose, bromophenol blue) and denatured by boiling for 5 minutes. The protein samples were loaded onto a 15% polyacrylamide gel and separated via electrophoresis conducted at 120 volts for 90 minutes. Protein was then electrophoretically transferred to a nitrocellulose membrane at 70 volts for 1 hour. Blots were blocked using 5% (w/v) nonfat dry milk in 0.1 M TRIS-buffered saline (TBS) for 1 hour at room temperature. They were then incubated overnight at 4°C in blocking buffer

plus 0.1% Tween 20 containing primary antibody: anti-$CRIP_{1a}$ antisera 077.4 (rabbit) 1:1000, and a loading control, anti-αTubulin [DM1A] (mouse) 1:15,000. Blots were rinsed 3 x10 minutes in 0.1M TBS + 0.1% Tween 20 (TBST). The blots were incubated at room temperature for 45 minutes with the secondary antibodies: Licor goat anti-rabbit 800 CW IR dye, 1:15,000 and Licor goat anti-mouse 680 CW IR dye, 1:15,000. Blots were rinsed 1x10 minutes in TBST, 1x10 minutes in 0.1M TBS, and stored in phosphate-buffered saline (PBS) prior to visualization with the Licor Odyssey® System.

**2.14 RNA Extraction and Quantitative PCR.** Cerebellum homogenates were sonicated in 0.5 ml Trizol®. Chloroform was added and the samples were shaken before centrifugation at 12,000 x g for 15 minutes at 4ºC. The supernatant was removed and isopropanol (200 µl) was added before incubating the samples for 10 minutes at room temperature. The samples were then subjected to centrifugation at 12,000 x g for 30 minutes at 4ºC. The pellets were then washed with 70% ethanol, prepared using diethylpyrocarbonate (DEPC) water. The samples were centrifuged again for 10 minutes at 7,500 x g. The supernatant was discarded and the pellets allowed to air dry before adding 20 µl molecular biology grade water. The pellets were heated for 5 minutes at 65ºC and then measured for total RNA concentration and quality, assessed according to RNA/DNA ratio, by ultraviolet spectrophotometry. RNA (5 µg) was then converted into cDNA using a High Capacity cDNA Reverse Transcription Kit (Applied Biosystems Inc., Foster City, CA). cDNA (10 ng) was then added to 0.2 ml wells containing a master mix from the 2x QuantiFast® SYBR® Green PCR kit and specific primers at a final concentration of 0.4 µM and water added to a final volume of 25 µl. Additional wells with no cDNA added served as no template controls (NTC) for each primer set. Samples were placed in

a BioRad real-time thermocycler programed to a 2-step cycling protocol, followed by a melt curve step at the end of the reaction. Cycle threshold (Ct) values were initially normalized to ΔCt values by subtracting sample Ct values from β-actin Ct values. Data were further converted to ΔΔCt values and final mRNA quantification was calculated using the following equation: 2^(-ΔΔCt) x 100 = % mRNA expression.

**2.15 Chronic THC treatment of $CB_1$ WT and KO mice.** $CB_1$ WT and KO mice (male littermates, 20-24g) were injected with vehicle (1:1:18 ethanol:emulphor:saline) or 10 mg/kg THC twice daily for 13.5 days. Mice were sacrificed 24 hours after the last injection. Brains were extracted and dissected on ice. The cerebellum, prefrontal cortex, and amygdala were homogenized in a cell lysis cocktail (as described in Section 2.10) and prepared for immunoblotting.

**2.16 Data Analysis.** Unless otherwise indicated, binding data are reported as mean values ± standard error of the mean (SEM) of at least four independent experiments that were each performed in either duplicate ([$^3$H]CP55,940 binding) or triplicate ([$^{35}$S]GTPγS binding). Data were analyzed using Graph Pad Prism v5.0c software. $B_{max}$, $K_D$, $E_{max}$ and $EC_{50}$ values were all determined by non-linear regression analysis. The equation used to fit the data is as follows: $y = (B_{max})(L)/(K_D + L)$ where y equals the amount of [$^3$H]CP55,940 or [$^{35}$S]GTPγS bound at each ligand concentration, L. $E_{max}$ and $EC_{50}$ were calculated after log transformation of concentration-effect curves, such that logL was substituted for L in the equation shown above. $B_{max}$ represents the amount of [$^3$H]CP55,940 bound at saturating concentrations of receptor ligand, while $E_{max}$ is equal to the % stimulation observed at maximally effective concentrations of receptor ligand in agonist-stimulated [$^{35}$S]GTPγS binding. $K_D$ and $EC_{50}$ values represent the

concentrations of receptor ligand that produce half maximal binding of [$^{3}$H]CP55,940 or modulation of [$^{35}$S]GTPγS binding, respectively. Basal binding was determined in the absence of ligand. Net-stimulated [$^{35}$S]GTPγS binding is defined as agonist-stimulated binding minus basal binding. Percentage of stimulation is defined by the following equation: % stimulation = (net-stimulated binding/basal binding) x 100. Concentration-effect curves were compared for statistical significance using two-way ANOVA, with ligand concentration and genotype as the main factors. Curve-fit values, including $B_{max}$, $K_D$, $E_{max}$ and $EC_{50}$ values, were compared between genotypes using the two-tailed Student's t-test.

Integrated intensities were measured on all Western blots using the Odyssey Licor Software 2.1 and analyzed either by the two-tailed Student's t-test or two-way ANOVA followed by the Bonferroni post hoc test.

## Chapter 3. Results

### 3.1 Confirmation of $CRIP_{1a}$ Knockout Mouse Line.

Targeted NEO cassette replacement of *Cnrip1* exons 1 and 2 successfully yielded a $CRIP_{1a}$ knockout mouse. The first $CRIP_{1a}$ knockout mouse was initially verified by PCR genotyping (Figure 8). To confirm that $CRIP_{1a}$ protein was absent in mice with the *Cnrip1* KO genotype, Western immunoblots were performed on cerebellar homogenates of WT and $CRIP_{1a}$ KO mice (Figure 9). As expected, results showed clear expression of $CRIP_{1a}$ immunoreactivity in WT mice, as indicated by a prominent band at 18 kD, the predicted molecular mass of $CRIP_{1a}$. In contrast, no $CRIP_{1a}$ was detectable in the cerebellar preparations from KO mice, even at 100 μg of protein. Similar results were seen in hippocampal homogenates from $CRIP_{1a}$ WT and KO mice, such that $CRIP_{1a}$ immunoreactivity was detected in WT but not KO mice (data not shown).

To determine whether $CRIP_{1a}$ is present throughout the central nervous system (brain and spinal cord), immunoblots were also performed on whole spinal cord homogenates. $CRIP_{1a}$ protein has been shown to be present in whole brain homogenates, as well as peripheral tissues such as heart and lung (Niehaus *et al*. 2007), but no published results have shown the presence of $CRIP_{1a}$ in the spinal cord to date. Results obtained were two-fold: there was a strong positive result showing expression of $CRIP_{1a}$ in the spinal cord of WT mice and a clear absence of the $CRIP_{1a}$ immunoreactivity in KO mice. These results also further confirmed antibody specificity, as indicated by the absence of $CRIP_{1a}$ immunoreactivity in KO mice, as well as providing evidence for CNS knockout of $CRIP_{1a}$ protein in this mutant mouse line (Figure 10).

The presence of two copies of the *Cnrip1* KO allele and the absence of $CRIP_{1a}$ immunoreactivity in the brain and spinal cord suggests that $CRIP_{1a}$ protein is absent in the KO genotype due to a lack of transcription of functional $CRIP_{1a}$ mRNA. To test this hypothesis,

quantitative PCR (qPCR) was performed. Two different primer sets were developed to assess various regions of the *Cnrip1* locus (Table 1). Results from both primer sets indicated that in the cerebellum, the $CRIP_{1a}$ KO mouse is producing a maximum of 0.4% *Cnrip1* mRNA compared to the $CRIP_{1a}$ WT control. These results confirm the essential absence of $CRIP_{1a}$ mRNA in $CRIP_{1a}$ KO mouse brain.

**Table 1**. **qPCR primer sequences for *Cnrip1* and the housekeeping gene, *β-Actin*.**

| Sequence | Gene | Product Length |
|---|---|---|
| 3' GCCCTGTTTTCTTCAAGGTG 5' (F) | *Cnrip1* | 212 bp |
| 3' TGTGTCATAGATGCCGGTGT 5' (R) | | |
| 3' CTGACGGGGAGAGAGTTGTC 5' (F) | *Cnrip1 Exon3* | 169 bp |
| 3' CAATGGTCTCGCTTGTGGTA 5' (R) | | |
| 3' TGTTACCAACTGGGACGA 5' (F) | *β-Actin* | 619 bp |
| 3' GGGGTGTTGAAGGTCTCAAA 5' (R) | | |

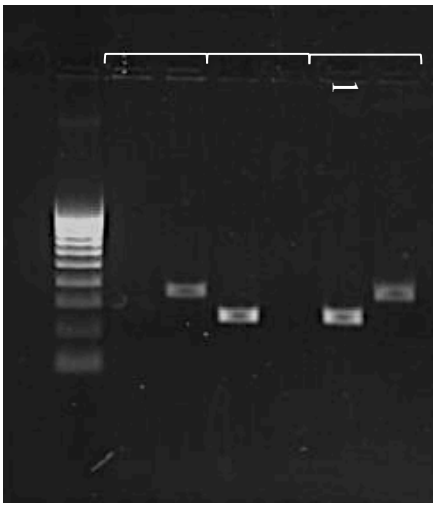

**Figure 8.** Heterozygous breeding pairs produce WT (2), HET (3) and KO offspring (1). The knockout allele fragment is 334 bp and the wild type allele fragment is 248 bp, as shown relative to a 1kb ladder (L).

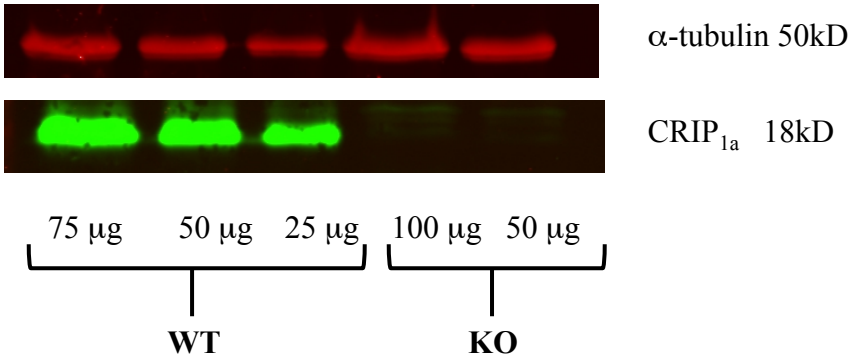


**Figure 9.** $CRIP_{1a}$ WT and KO cerebellar homogenates probed with $CRIP_{1a}$ antiserum. *Cnrip1* KO mice do not express $CRIP_{1a}$, as shown compared to WT mice and relative to the loading control, α-tubulin.

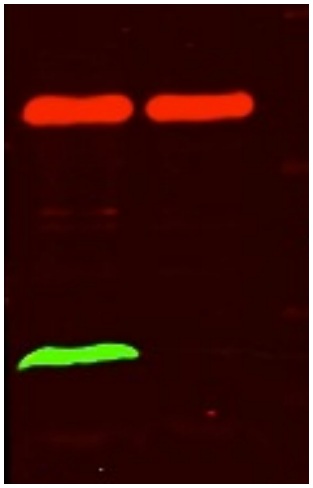

**Figure 10.** $CRIP_{1a}$ is present in the spinal cord. $CRIP_{1a}$ WT and KO spinal cord homogenates (50 µg) probed with $CRIP_{1a}$ antiserum. *Cnrip1* KO mice do not express $CRIP_{1a}$, as shown compared to WT mice and relative to the loading control, α-tubulin.

### 3.2 Loss of $CRIP_{1a}$ Does Not Affect Viability, Fertility, Weight Gain or Core Body Temperature.

The initial (and arguably most important) result when creating a knockout mouse line is determining if removal of the gene proves lethal. $CRIP_{1a}$ KO mice were born healthy along with WT and HET siblings in the first litter produced by HET x HET pairing. No overt morphological differences were observed at any point in $CRIP_{1a}$ KO mice during postnatal development or adulthood. At first, $CRIP_{1a}$ HET mice were overrepresented relative to both WT and KO mice, however over time, genotypic ratios approached the Mendelian expectation of 1:2:1, WT:HET:KO, with our mouse line currently yielding a 1:2.2:1 ratio. Interestingly, the KO genotype is preferentially observed in male mice, with the overall ratio of male to female KO mice equaling 2 to 1 in litters obtained so far.

The endocannabinoid system is an important player in male and female reproduction and endocrine function. Many studies have revealed a role of $CB_1$ receptors and endocannabinoids in sertoli cell proliferation, spermatozoa motility and the acrosomal reaction, which is essential for proper fertilization of an oocyte (Maccarrone *et al.* 2003; Rossato *et al.* 2005; Rossi *et al.* 2007). Aberrant $CB_1$ receptor signaling has been shown to negatively affect oviduct transport of an embryo, leading to ectopic pregnancies, as well as to impede the implantation event of a blastula into the uterus (Wang *et al.* 2004; Paria *et al*. 2001). Furthermore, arachidonic acid, a major metabolite of the endocannabinoids, is a precursor to prostaglandins and ultimately progesterone synthesis, which each play an important role in the estrous cycle (Wlodawer *et al.* 1976; Milvae and Hansel, 1983; Korzekwa *et al.* 2010). Given the vast involvement that the endocannabinoid system has been shown to have in reproduction, it was important to determine if the loss of $CRIP_{1a}$ would affect male or female fertility. To test this question, a KO x KO

breeding pair was established. After producing healthy pups and typical-sized litters, no impacts on fertility were detected in $CRIP_{1a}$ KO mice.

Body weight is known to be maintained in part by the endocannabinoid system, and can be affected by exogenous administration of both $CB_1$ agonists and inverse agonists (Gomez *et al.* 2002; Williams *et al*. 1998; Colombo *et al.* 1998). As a new knockout line, it was important to establish any differences related to body weight and weight gain over time in $CRIP_{1a}$ KO mice compared to WT littermates, especially given the potential for increased $CB_1$ receptor activity in relevant regions of the CNS and gastrointestinal system. Male and female $CRIP_{1a}$ WT, HET and KO mice steadily gained weight from the age of 3 weeks until 12 weeks indicating normal healthy development (Figure 11). Body weights were not different between genotypes after two-way ANOVA ($p > 0.05$).

Cannabinoid agonists often produce hypothermic effects (Crawley *et al.* 1993; Little *et al.* 1988), therefore it was necessary to determine whether core body temperature was affected in $CRIP_{1a}$ KO mice. Male and female $CRIP_{1a}$ WT and KO mice were assessed for core body temperature in a naïve state. Average body temperatures were nearly identical between the two genotypes, and therefore not significantly different after student's t-test ($p > 0.05$) (Figure 12).

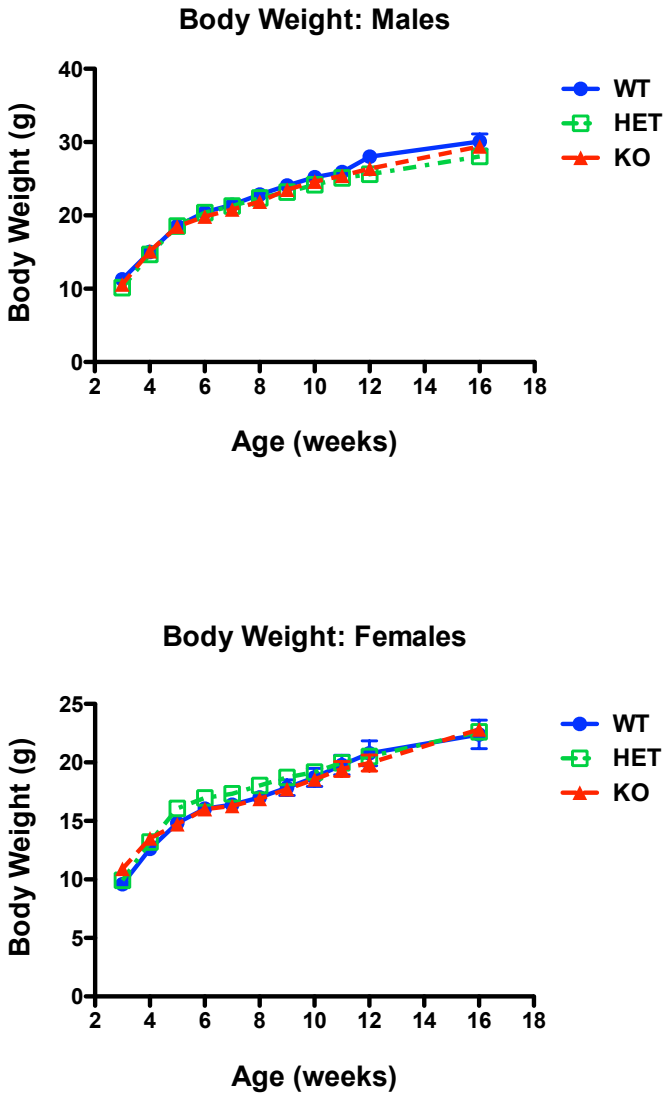


**Figure 11.** $CRIP_{1a}$ WT, HET and KO mice do not differ in body weight. Male and female mice were weighed weekly to measure growth and development. The top panel displays male weight gain while the bottom panel displays female weight gain. Data represent mean weight ± SEM, n = minimum 13 mice per genotype per sex. Two-way ANOVA determined body weight was not different between genotypes ($p > 0.05$).

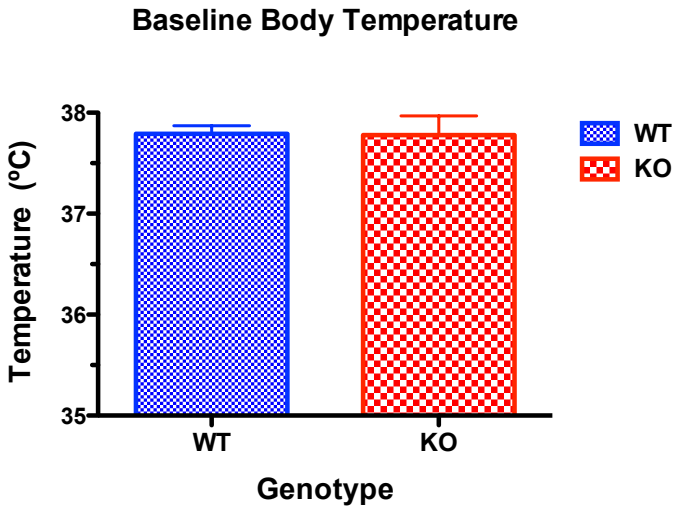


**Figure 12.** Body temperature is not different in $CRIP_{1a}$ KO compared to WT mice. Data represent mean temperatures ± SEM (collapsed by sex, n = 8 per genotype). Student's two-tailed t-test revealed no differences between genotypes ($p > 0.05$).

### 3.3 $CB_1$ Receptor Expression is Unaltered in the Cerebellum, Hippocampus, and Amygdala of $CRIP_{1a}$ KO Compared to WT Mice.

Previous studies in our laboratory have shown that $CB_1$ receptor levels do not change in multiple cell lines after stable transfection/over-expression of $CRIP_{1a}$, so we predict that genetic deletion of $CRIP_{1a}$ will not alter $CB_1$ receptor expression levels in the CNS. Nonetheless, because the global, lifelong absence of $CRIP_{1a}$ could produce adaptive changes in $CB_1$ receptor expression, it was important to determine $CB_1$ receptor levels in relevant CNS regions. Therefore, [$^3$H]CP55,940 saturation binding analysis was conducted in three brain regions known to express $CB_1$ receptors and $CRIP_{1a}$, the cerebellum, hippocampus and amygdala. Results indicated there was no difference in $CB_1$ receptor levels between genotypes in these regions, as indicated by ligand $B_{max,}$ values in $CRIP_{1a}$ KO mice compared to WT littermate controls (Table 2). In addition, ligand $K_D$ values were also unaffected by loss of $CRIP_{1a}$, as there were no significant differences between genotypes for any of the regions examined. Data were analyzed using the two-tailed t-test with significance reached at $p < 0.05$.

**Table 2. $B_{max}$ and $K_D$ Values from [$^3$H]CP55,940 Saturation Binding Analysis in Cerebellum, Hippocampus and Amygdala of $CRIP_{1a}$ WT and KO mice.**

| | $B_{max}$ (fmol/mg) | | $K_D$ (nM) | |
|---|---|---|---|---|
| | **$CRIP_{1a}$ WT** | **$CRIP_{1a}$ KO** | **$CRIP_{1a}$ WT** | **$CRIP_{1a}$ KO** |
| **Cerebellum** | 242 ± 45 | 262 ± 20 | 0.76 ± 0.09 | 0.64 ± 0.17 |
| **Hippocampus** | 217 ± 27 | 281 ± 26 | 0.53 ± 0.06 | 0.68 ± 0.11 |
| **Amygdala** | 206 ± 26 | 206 ± 22 | 0.73 ± 0.18 | 0.71 ± 0.17 |

Saturation analysis of [$^3$H]CP55,940 binding in $CRIP_{1a}$ WT and KO cerebellum, hippocampus and amygdala (data collapsed by sex, n = 8 per genotype). Data are mean values ± SEM. No significant differences in $B_{max}$ or $K_D$ values were reached between genotypes (two-tailed t-test, $p > 0.05$).

### 3.4 Agonist-Stimulated [$^{35}$S]GTPγS Binding Reveals No Differences in $CB_1$ Receptor-Mediated G-Protein Activity in the Cerebellum, Hippocampus and Spinal Cord of $CRIP_{1a}$ KO Compared to WT Mice.

$CRIP_{1a}$ is known to bind to the C-terminus of $CB_1$ receptors and inhibit their constitutive activity (see Introduction 1.6). Previously, our laboratory demonstrated that $CRIP_{1a}$ could also inhibit agonist-stimulated G-protein activity when stably over-expressed in $CB_1$ receptor-expressing cell lines, which differs from published reports that showed no effect on agonist-induced $Ca^{2+}$ inhibition in co-transfected SCG neurons (Niehaus *et al.* 2007). Without $CRIP_{1a}$ present, I hypothesized that $CB_1$ receptors in the CNS would be more constitutively active and possibly exhibit increases in agonist-stimulated G-protein activity. The first region evaluated was the cerebellum, due to its dense $CB_1$ receptor expression as well as data suggesting widespread co-localization of $CRIP_{1a}$ and $CB_1$ receptors on granule cell terminals in the molecular layer of the cerebellum (K. Sayers and D.E. Selley, unpublished results). Additionally, $CB_1$ receptors within the cerebellum are thought to mediate *in vivo* effects such as reduced motor coordination after application of exogenous cannabinoids and contribute to reduced excitatory synaptic transmission onto Purkinje cells (DeSanty and Dar, 2001; Lévénès *et al.* 1998). To determine the level of G-protein activation in $CRIP_{1a}$ WT and KO mice, agonist-stimulated [$^{35}$S]GTPγS binding was performed using the synthetic cannabinoid ligand CP55,940 and the putative endocannabinoid noladin ether (NE) as agonists (Figure 13). All [$^{35}$S]GTPγS binding studies were performed by Aaron Tomarchio, a Laboratory Research Specialist in the laboratory of our collaborator, Dr. Laura Sim-Selley. Two-way ANOVA analysis of the concentration effect curves revealed a significant main effect of genotype ($p < 0.05$) with CP55,940 and a trend towards significance with NE ($p = 0.0889$), such that $CB_1$ receptor-

stimulated [$^{35}$S]GTPγS binding was slightly lower in $CRIP_{1a}$ KO compared to WT mice. However, no significant differences in $E_{max}$ or $EC_{50}$ values between genotypes were found with either agonist (Table 3a), whereby data were analyzed using the two-tailed t-test with significance reached at $p < 0.05$. Basal G-protein activity was unaffected by the absence of $CRIP_{1a}$ (Table 3b). A single concentration (10 nM) of the $CB_1$ inverse agonist, SR141716A, which was previously found to produce maximal inhibition of basal [$^{35}$S]GTPγS binding in $CB_1$ receptor-expressing cell lines, was also tested to detect any potential genotype differences in constitutive activity of the $CB_1$ receptors in the cerebellum. Previous data showed that over-expression of $CRIP_{1a}$ in stably transfected cell lines attenuated inverse agonist activity, however no difference was seen in the effects of 10 nM SR141716A in $CRIP_{1a}$ KO mice compared to WT littermate controls (Table 3b). However, it should be noted that only modest effects on [$^{35}$S]GTPγS binding were seen with SR147116A in the cerebellum (11-17% inhibition).

Given that no enhancement of $CB_1$ receptor-mediated G-protein activity was found in the cerebellum of $CRIP_{1a}$ KO mice, we next examined the hippocampus, another region dense in $CB_1$ receptor expression and which is thought to be involved in the short-term memory impairments elicited by cannabinoids (Hampson *et al.* 2000). We also found that $CRIP_{1a}$ immunoreactivity was detected in the hippocampus of WT but not $CRIP_{1a}$ KO mice. Moreover, unpublished data from a collaboration between our laboratory and Dr. Alex Straiker (University of Indiana) found that transfection of $CRIP_{1a}$ into autaptic hippocampal neuronal preparations decreased 2-AG-mediated DSE as well as the inhibition of excitatory post-synaptic currents elicited by exogenous application of 2-AG, consistent with our hypothesis that $CRIP_{1a}$ attenuates $CB_1$ receptor signaling.

The same [$^{35}$S]GTPγS binding conditions described previously for the cerebellum were used to evaluate the hippocampus of $CRIP_{1a}$ WT and KO mice (Figure 14). Two-way ANOVA of the concentration-effect curves showed no significant main effect of genotype in this region with either CP55,940 or NE. Furthermore, concentration-effect curves for CP55,940 and NE showed no differences in $E_{max}$ or $EC_{50}$ values between genotypes (Table 4a). Similar to the cerebellum, basal [$^{35}$S]GTPγS binding was not affected by the absence of $CRIP_{1a}$, nor was the effect of a maximally-effective concentration of SR141716A (Table 4b). Again, it should be noted that only very modest inhibition of [$^{35}$S]GTPγS binding was observed with 10 nM SR141716A (1-9%) in this region.

The spinal cord is known to express a moderate level of $CB_1$ receptors and play a role in mediating antinociceptive effects of cannabinoids (Herkenham *et al*. 1991, Lichtman and Martin, 1991). Moreover, we recently demonstrated that $CRIP_{1a}$ is also expressed in the spinal cord, as noted above (see Section 3.1). Using identical [$^{35}$S]GTPγS binding conditions to those stated above, two-way ANOVA of the CP55,940 or NE concentration-effect curves showed no significant differences in the spinal cord between $CRIP_{1a}$ WT and KO mice (Figure 15). $E_{max}$ and $EC_{50}$ values were found to not be different between genotypes with either agonist after analysis by student's t-test (Table 5a). Basal levels of [$^{35}$S]GTPγS binding in the spinal cord were also not different between genotypes (Table 5b). Results for the single concentration of 10 nM SR141716A were also not significantly different between genotypes after analysis by two-tailed t-test ($p > 0$ .05), although SR141716A essentially had no effect on [$^{35}$S]GTPγS binding in the spinal cord (0-3% inhibition) (Table 5b).

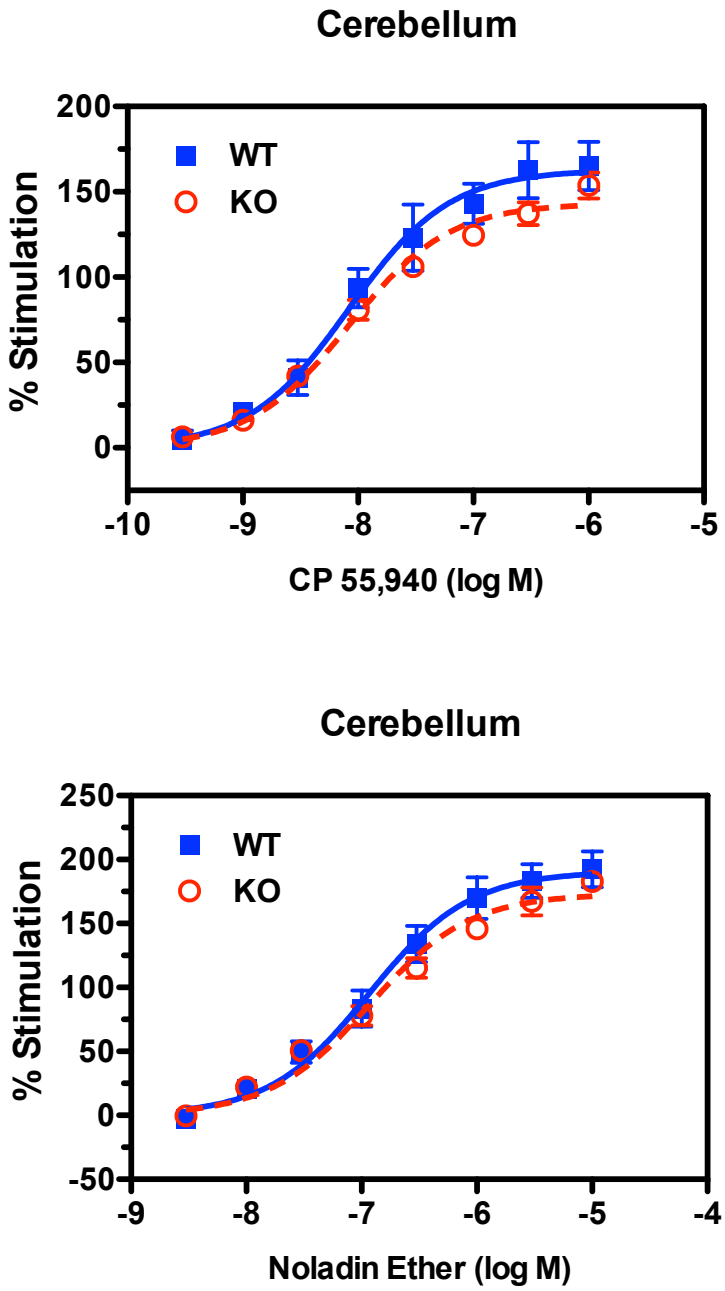


**Figure 13.** Agonist-stimulated [$^{35}$S]GTPγS binding in $CRIP_{1a}$ WT and KO cerebellum. The top panel represents concentration-effect curves for CP55,940, while the bottom represents concentration-effect curves for noladin ether (NE). Data are expressed as mean % stimulation ± SEM (collapsed by sex, n = 8 per genotype). Two-way ANOVA revealed a significant main effect of concentration with CP55,940 ($p < 0.0001$, $F = 78.36$, $df = 7$) and NE ($p < 0.0001$, $F = 109.0$, $df = 7$) and a significant main effect of genotype with CP55,940 ($p < 0.05$, $F = 5.08$, $df = 1$), but only a trend toward significance with NE ($p = 0.0889$, $F = 2.985$, $df = 1$). No significant interactions were observed with CP55,940 or NE.

**Table 3a. $E_{max}$ and $EC_{50}$ Values Derived From Agonist-Stimulated [$^{35}$S]GTPγS Binding in the Cerebellum.**

| | $E_{max}$ (% Stimulation) | | $EC_{50}$ (nM) | |
|---|---|---|---|---|
| | **$CRIP_{1a}$ WT** | **$CRIP_{1a}$ KO** | **$CRIP_{1a}$ WT** | **$CRIP_{1a}$ KO** |
| **CP55,940** | 164 ± 13 | 143 ± 8 | 9.7 ± 2.3 | 8.7 ± 1.1 |
| **NE** | 191 ± 16 | 174 ± 10 | 124 ± 16 | 123 ± 16 |

Agonist-stimulated [$^{35}$S]GTPγS binding in $CRIP_{1a}$ WT and KO cerebellum shows no differences in $E_{max}$ or $EC_{50}$ values between genotypes for CP55,940 and NE. Data are mean $E_{max}$ and $EC_{50}$ values ± SEM, derived from the concentration-effect curves shown in Figure 13 (collapsed by sex, n = 8). After two-tailed t-test, data were determined to not be significantly different ($p > 0.05$).

**Table 3b. Basal and SR141716A-inhibited [$^{35}$S]GTPγS Binding in the Cerebellum.**

| Basal (fmol/mg) | | SR141716A (% Stimulation) | |
|---|---|---|---|
| **$CRIP_{1a}$ WT** | **$CRIP_{1a}$ KO** | **$CRIP_{1a}$ WT** | **$CRIP_{1a}$ KO** |
| 101 ± 9 | 99 ± 7 | -17.6 ± 3.3 | -11.0 ± 2.2 |

[$^{35}$S]GTPγS binding in $CRIP_{1a}$ WT and KO cerebellum shows no differences between genotypes for basal or in the presence of the $CB_1$ inverse agonist, SR141716A. Data are represented as mean values ± SEM (collapsed by sex, n = 8). After two-tailed t-test, data were determined to not be significantly different ($p > 0.05$).

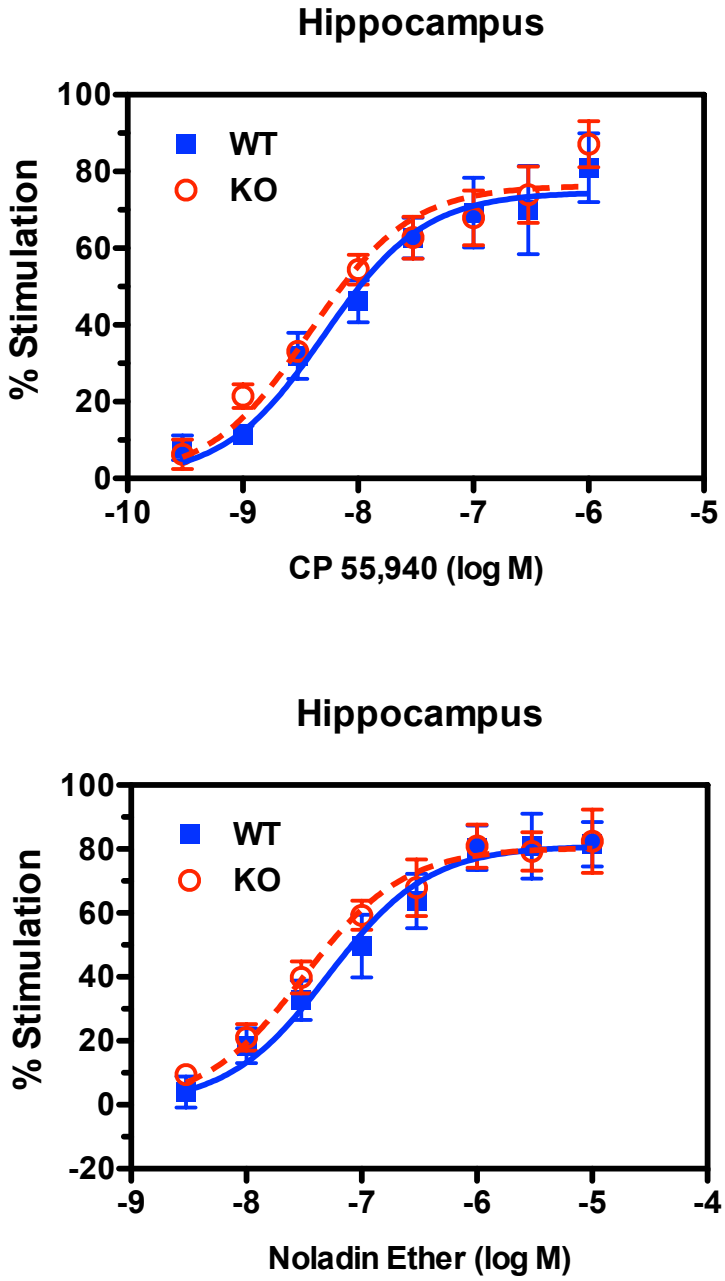


**Figure 14.** Agonist-stimulated [$^{35}$S]GTPγS binding in $CRIP_{1a}$ WT and KO hippocampus. The top panel represents concentration-effect curves for CP55,940, while the bottom represents concentration-effect curves for NE. Data are expressed as mean % stimulation ± SEM (collapsed by sex, n = 8 per genotype). Two-way ANOVA revealed a significant main effect of concentration with CP55,940 ($p < 0.0001$, $F = 39.99$, $df = 7$) and NE ($p < 0.0001$, $F = 34.92$, $df = 7$). No statistically significant interactions or main effect of genotype were observed for CP55,940 or NE.

**Table 4a. $E_{max}$ and $EC_{50}$ Values Derived From Agonist-Stimulated [$^{35}$S]GTPγS Binding in the Hippocampus.**

| | $E_{max}$ (% Stimulation) | | $EC_{50}$ (nM) | |
|---|---|---|---|---|
| | **$CRIP_{1a}$ WT** | **$CRIP_{1a}$ KO** | **$CRIP_{1a}$ WT** | **$CRIP_{1a}$ KO** |
| **CP55,940** | 75 ± 8 | 76 ± 5 | 5.1 ± 0.6 | 3.9 ± 0.2 |
| **NE** | 82 ± 7 | 80 ± 6 | 67.7 ± 21.3 | 32.0 ± 3.2 |

Agonist-stimulated [$^{35}$S]GTPγS binding in $CRIP_{1a}$ WT and KO hippocampus shows no differences in $E_{max}$ or $EC_{50}$ values between genotypes for CP55,940 and NE. Data are mean $E_{max}$ and $EC_{50}$ values ± SEM, derived from the concentration-effect curves shown in Figure 14 (collapsed by sex, n = 8). After two-tailed t-test, data were determined to not be significantly different ($p > 0.05$).

**Table 4b. Basal and SR141716A-inhibited [$^{35}$S]GTPγS Binding in the Hippocampus.**

| Basal (fmol/mg) | | SR141716A (% Stimulation) | |
|---|---|---|---|
| **$CRIP_{1a}$ WT** | **$CRIP_{1a}$ KO** | **$CRIP_{1a}$ WT** | **$CRIP_{1a}$ KO** |
| 163 ± 20 | 159 ± 14 | -9.1 ± 6.7 | -1.3 ± 2.3 |

[$^{35}$S]GTPγS binding in $CRIP_{1a}$ WT and KO hippocampus shows no differences between genotypes for basal or in the presence of the $CB_1$ inverse agonist, SR141716A. Data are represented as mean values ± SEM (collapsed by sex, n = 8). After two-tailed t-test, data were determined to not be significantly different ($p > 0.05$).

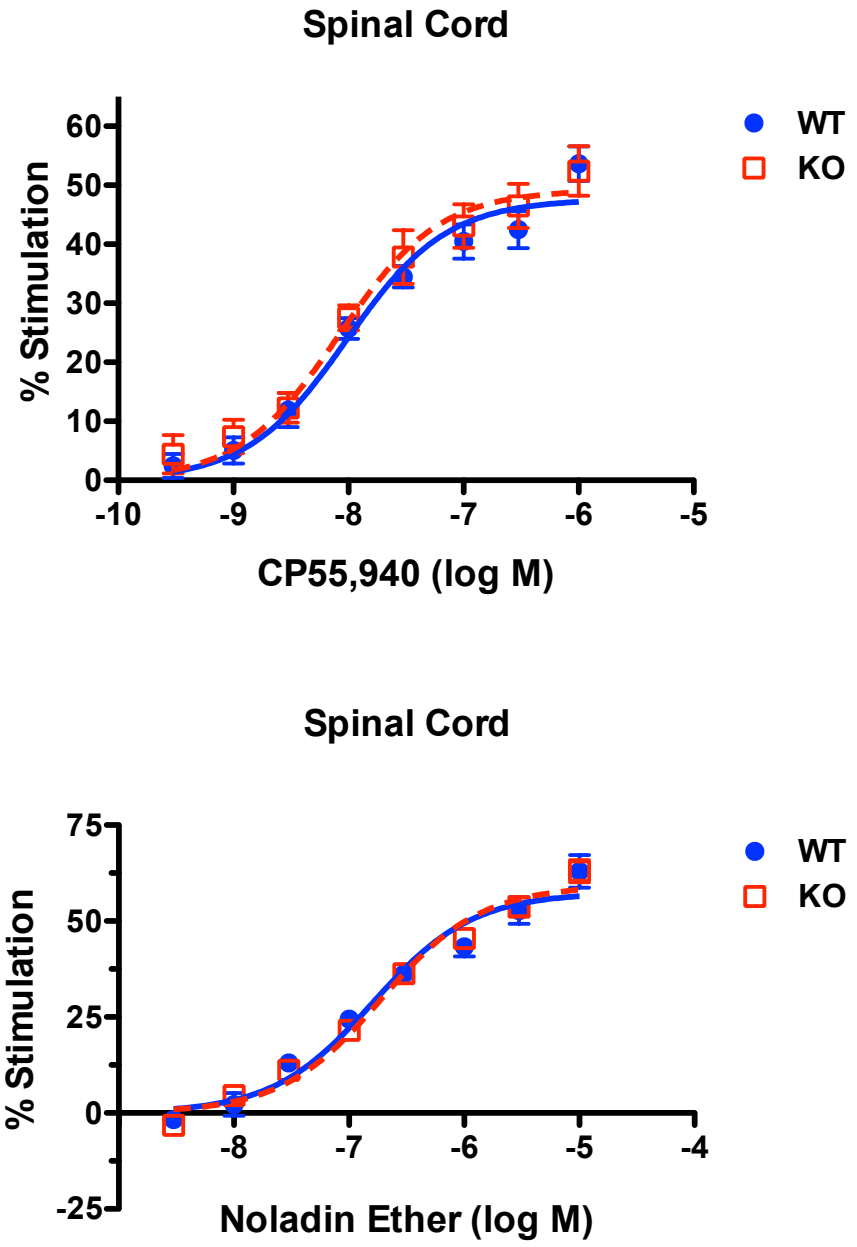


**Figure 15.** Agonist-stimulated [$^{35}$S]GTPγS binding in CRIP$_{1a}$ WT and KO spinal cord. The top panel represents concentration-effect curves for CP55,940, while the bottom represents concentration-effect curves for NE. Data are expressed as mean % stimulation ± SEM (collapsed by sex, n = 8 per genotype). Two-way ANOVA revealed a significant main effect of concentration with CP55,940 ($p < 0.0001$, $F = 82.52$, df = 7) and NE ($p < 0.0001$, $F = 177.5$, df = 7). No significant interactions or main effect of genotype were observed with CP55,940 or NE.

**Table 5a. $E_{max}$ and $EC_{50}$ Values Derived From Agonist-Stimulated [$^{35}$S]GTPγS Binding in the Spinal Cord.**

| | $E_{max}$ (% Stimulation) | | $EC_{50}$ (nM) | |
|---|---|---|---|---|
| | **$CRIP_{1a}$ WT** | **$CRIP_{1a}$ KO** | **$CRIP_{1a}$ WT** | **$CRIP_{1a}$ KO** |
| **CP55,940** | 48 ± 3 | 56 ± 7 | 9.9 ± 0.9 | 8.7 ± 1.6 |
| **NE** | 57 ± 4 | 60 ± 4 | 166 ± 19 | 209 ± 37 |

Agonist-stimulated [$^{35}$S]GTPγS binding in $CRIP_{1a}$ WT and KO spinal cord shows no differences in $E_{max}$ or $EC_{50}$ values between genotypes for NE and CP55,940. Data are mean $E_{max}$ and $EC_{50}$ values ± SEM, derived from the concentration-effect curves shown in Figure 15 (collapsed by sex, n = 8). After two-tailed t-test, data were determined to not be significantly different ($p > 0.05$).

**Table 5b. Basal and SR141716A-inhibited [$^{35}$S]GTPγS Binding in the Spinal Cord.**

| Basal (fmol/mg) | | SR141716A (% Stimulation) | |
|---|---|---|---|
| **$CRIP_{1a}$ WT** | **$CRIP_{1a}$ KO** | **$CRIP_{1a}$ WT** | **$CRIP_{1a}$ KO** |
| 151 ± 14 | 161 ± 17 | -2.9 ± 2 | -1.7 ± 1 |

[$^{35}$S]GTPγS binding in $CRIP_{1a}$ WT and KO spinal cord shows no differences between genotypes for basal or in the presence of the $CB_1$ inverse agonist, SR141716A. Data are represented as mean values ± SEM (collapsed by sex, n = 8). After two-tailed t-test, data were determined to not be significantly different ($p > 0.05$).

### 3.5 Agonist-Stimulated [$^{35}$S]GTPγS Binding Reveals Increased $CB_1$-Mediated G-Protein Activity in the Amygdala of $CRIP_{1a}$ KO Relative to WT Mice.

After no differences were found between genotypes in the cerebellum and hippocampus, we continued surveying $CB_1$ receptor-expressing CNS regions known to be involved in mediating various effects of cannabinoids, and in which $CRIP_{1a}$ expression has been observed. The

amygdala is a brain region involved in regulating anxiety and conditioned fear responses, which are modulated by cannabinoid agonists (Barad *et al*. 2006; Davidson, 2002). Therefore, cannabinoid agonist-stimulated [$^{35}$S]GTPγS binding was examined using identical conditions as described in section 3.4. My hypothesis that the loss of $CRIP_{1a}$ could produce an enhanced response to cannabinoid agonists had not been realized in the regions previously examined, yet interestingly, results in the amygdala revealed enhanced $CB_1$ receptor-mediated G-protein activation in $CRIP_{1a}$ KO relative to WT mice. Concentration-effect curves for CP55,940 and NE each showed greater $CB_1$ receptor-mediated stimulation of [$^{35}$S]GTPγS binding in amygdala of $CRIP_{1a}$ KO mice (Figure 16), and these results were confirmed by two-way ANOVA, which showed a significant main effect of genotype for CP55,940 ($p = 0.0001$, $F = 19.46$, $df = 1$) and NE ($p < 0.0001$, $F = 128.3$, $df = 1$). In addition to a main effect of genotype, Bonferroni post-hoc tests showed enhanced CP55,940-mediated stimulation at 0.03, 0.1, 0.3 and 1 μM, while NE showed enhanced stimulation at 0.1, 0.3 and 1 μM, in $CRIP_{1a}$ KO relative to WT mice (Figure 16). $E_{max}$ values for both agonists were significantly greater in $CRIP_{1a}$ KO compared to WT mice (Table 6a). No difference in potency, however, which is indicated by a leftward or rightward shift of the curve, was observed for either agonist. $EC_{50}$ values for both agonists were found to not be statistically different between WT and KO mice with either agonist (Table 6a). Basal [$^{35}$S]GTPγS binding and the single concentration of 10 nM SR141716A were also not statistically different between genotypes (Table 6b), although SR141716A had minimal effects on [$^{35}$S]GTPγS binding, similar to the other regions examined.

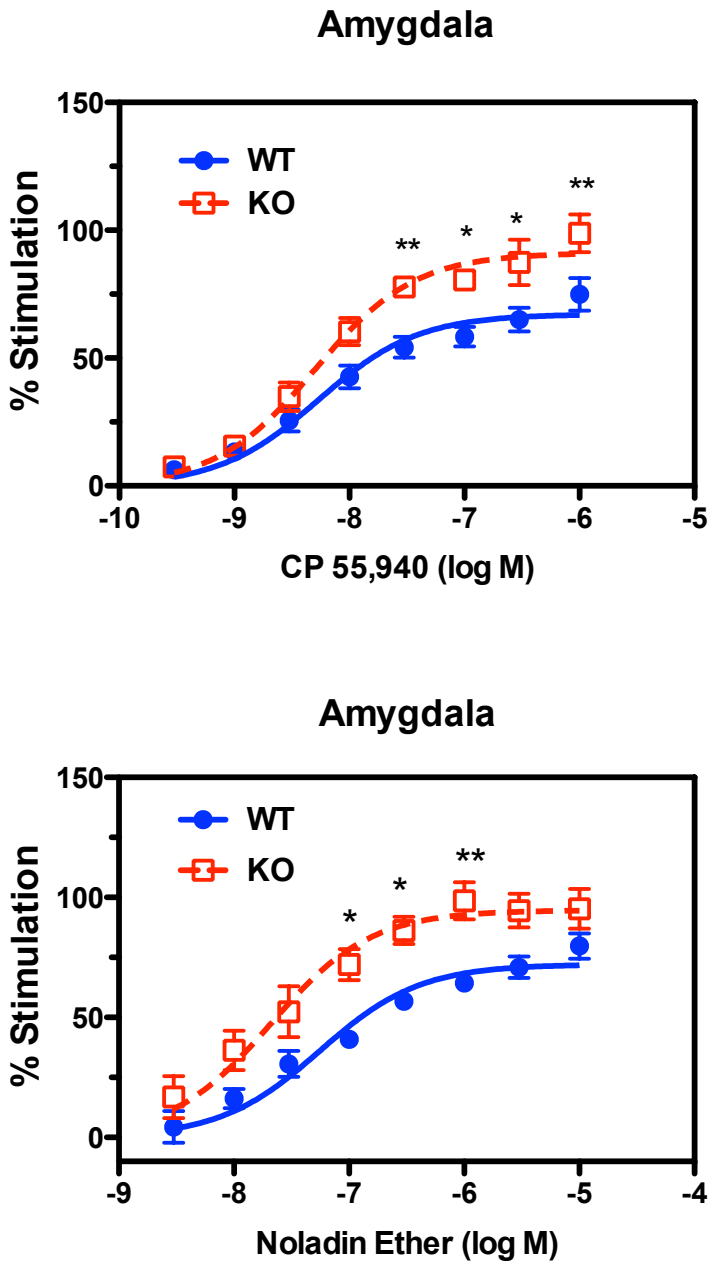


**Figure 16.** Agonist-stimulated [$^{35}$S]GTPγS binding in CRIP$_{1a}$ WT and KO amygdala. The top panel represents concentration-effect curves for CP55,940, while the bottom panel represents concentration-effect curves for NE. Data are expressed as mean % stimulation ± SEM (collapsed by sex, n = 6 per genotype). Two-way ANOVA revealed a significant main effect of concentration with CP55,940 ($p < 0.0001$, $F = 50.39$, $df = 7$) and NE ($p < 0.0001$, $F = 88.79$, $df = 7$). Two-way ANOVA also revealed a significant main effect of genotype with CP55,940 ($p = 0.0001$, $F = 19.46$, $df = 1$) and NE ($p < 0.0001$, $F = 88.79$, $df = 1$). No significant interactions were observed with CP55,940 or NE.

**Table 6a. $E_{max}$ and $EC_{50}$ Values Derived From Agonist-Stimulated [$^{35}$S]GTPγS Binding in the Amygdala.**

| | $E_{max}$ (% Stimulation) | | $EC_{50}$ (nM) | |
|---|---|---|---|---|
| | **$CRIP_{1a}$ WT** | **$CRIP_{1a}$ KO** | **$CRIP_{1a}$ WT** | **$CRIP_{1a}$ KO** |
| **CP55,940** | 72 ± 4 | 95 ± 4** | 6.2 ± 0.9 | 5.1 ± 0.7 |
| **NE** | 72 ± 2 | 99 ± 5* | 50.3 ± 14 | 22.1 ± 8.0 |

**Table 6.** Agonist-stimulated [$^{35}$S]GTPγS binding in $CRIP_{1a}$ WT and KO amygdala revealed statistically significant differences between genotypes in $E_{max}$ values for CP55,940 and NE. Data are mean $E_{max}$ and $EC_{50}$ values derived from the concentration-effect curves shown in Figure 16 ± SEM (collapsed by sex, n = 6). Analysis with two-tailed t-test revealed significant differences between genotypes for CP55,940 $E_{max}$ values (**$p < 0.01$) and NE $E_{max}$ values (*$p < 0.05$), but not for $EC_{50}$ values of either ligand ($p > 0.05$).

**Table 6b. Basal and SR141716A-inhibited [$^{35}$S]GTPγS Binding in the Amygdala.**

| Basal (fmol/mg) | | SR141716A (% Stimulation) | |
|---|---|---|---|
| **$CRIP_{1a}$ WT** | **$CRIP_{1a}$ KO** | **$CRIP_{1a}$ WT** | **$CRIP_{1a}$ KO** |
| 101 ± 22 | 108 ± 12 | -1 ± 4 | 9 ± 5 |

[$^{35}$S]GTPγS binding in $CRIP_{1a}$ WT and KO amygdala shows no differences between genotypes for basal or in the presence of the $CB_1$ inverse agonist, SR141716A. Data are represented as mean values ± SEM (collapsed by sex, n = 6). After two-tailed t-test, data were determined to not be significantly different ($p > 0.05$).

### 3.6 $CRIP_{1a}$ KO Mice Do Not Show a Unique Baseline Phenotype Compared to WT Littermate Controls in Spontaneous Locomotor Activity.

It is well documented that cannabinoid agonists induce acute locomotor suppressive effects (Crawley *et al.* 1993). To determine whether the absence of $CRIP_{1a}$ affects locomotor activity, $CRIP_{1a}$ WT and KO mice were placed in open field test chambers and allowed to explore the area for 30 minutes. Activity was recorded using Fire-i™ digital cameras and ANY-maze™ tracking software. The 30-minute time period was evaluated both as a whole time span and as three separate 10-minute bouts of activity, measured in seconds. Time spent mobile, time spent immobile and time spent freezing were all recorded and compared between genotypes. No significant differences between genotypes were found for any of the measures recorded. Over a total test time of 30 minutes, $CRIP_{1a}$ WT mice were mobile for approximately 83% of the time, while $CRIP_{1a}$ KO mice were mobile for approximately 79% of the time (collapsed by sex, n =8 per genotype; Figure 17a). Time spent immobile was also not different, as $CRIP_{1a}$ WT mice were immobile for approximately 17% of the time, versus $CRIP_{1a}$ KO mice that were immobile for approximately 21% of the time (Figure 17b). Immobility was often due to mice grooming, therefore no movement across the x-y plane occurred, but the mouse was not completely still. There were also no significant differences between genotypes in the time spent freezing, whereby the mice were essentially completely still. $CRIP_{1a}$ WT mice were considered to exhibit freezing behavior for a total of 66 ± 28 seconds whereas $CRIP_{1a}$ KO mice displayed freezing behavior for a total of 136 ± 73 seconds (Figure 17c). Although the total time spent freezing by $CRIP_{1a}$ KO mice was approximately twice that of WT mice, high variability in the results for this measure led to a lack of statistical significance.

When broken down into 10-minute individual periods, there were still no differences between genotypes at each segment, but there were significant differences between the segments themselves. This could be due to habituation, whereby the environmental novelty wears off and the mice stop avidly exploring. In the first 10 minutes, $CRIP_{1a}$ WT mice were mobile for 94.5% of the time, compared to $CRIP_{1a}$ KO mice that were mobile for approximately 92% of the time (Table 7). $CRIP_{1a}$ WT mice spent the remaining 5.5% of the time immobile, which was similar to the $CRIP_{1a}$ KO mice that spent their approximate 8% of remaining time immobile. Freezing behavior was negligible, since both $CRIP_{1a}$ KO and WT mice were "frozen" for only an average of approximately two seconds during the first segment (Table 8).

The second segment of the test saw a marked reduction in the amount of time mice spent mobile, and thus increases in both time spent immobile and freezing. $CRIP_{1a}$ WT mice were mobile for 84%, while $CRIP_{1a}$ KO mice were mobile for 76% of the time (Table 7). No differences between genotypes were observed after two-way ANOVA ($p > 0.05$). $CRIP_{1a}$ WT mice spent significantly more time immobile in segment 2 compared to segment 1, at approximately 16% of the time, as determined by one-way ANOVA followed by Newman-Keuls post-hoc test ($p = 0.0137$, $F = 24.71$, $R^2 = 0.9428$). Alternatively, $CRIP_{1a}$ KO mice did not spend significantly more time immobile in segment 2 (approximately 23%) when compared to segment 1 after analysis with one-way ANOVA ($p = 0.0542$), although they showed a trend toward greater time immobile, but high variability was a factor. There were also no significant differences between genotypes for time spent immobile within segment 2 as determined by one-way ANOVA followed by Newman-Keuls post-hoc test, $p > 0.05$). Time spent freezing increased between segment 1 and 2, although no significant main effects of genotype or test segment were observed (two-way ANOVA, $p > 0.05$) (Table 8).

The time spent mobile in segment 3 was significantly lower for both genotypes compared to the time spent mobile in segment 1 (two-way ANOVA, $p < 0.001$), with robust significance reached in the $CRIP_{1a}$ WT mice (two-way ANOVA followed by Bonferroni post-hoc test, $p < 0.001$) (Table 7). No main effect of genotype was observed however, as total time spent mobile in segment 3 was approximately 71% in the $CRIP_{1a}$ WT mice while $CRIP_{1a}$ KO mice were mobile for a total of about 70% (Table 7). Since time mobile and time immobile are inversely related, it is not surprising that time spent immobile significantly increased across segments for both genotypes. $CRIP_{1a}$ WT mice were immobile for nearly 29% of the time, whereas $CRIP_{1a}$ KO mice were immobile for 30% of the time. Similar to time mobile, statistically significant results were observed after analysis by two-way ANOVA, which revealed a main effect of test segment, but not genotype, between segments 1 and 3 for both $CRIP_{1a}$ WT and KO mice. Time spent freezing however, was determined to not be statistically different between genotypes or across test segments after two-way ANOVA, $p > 0.05$ (Table 8).

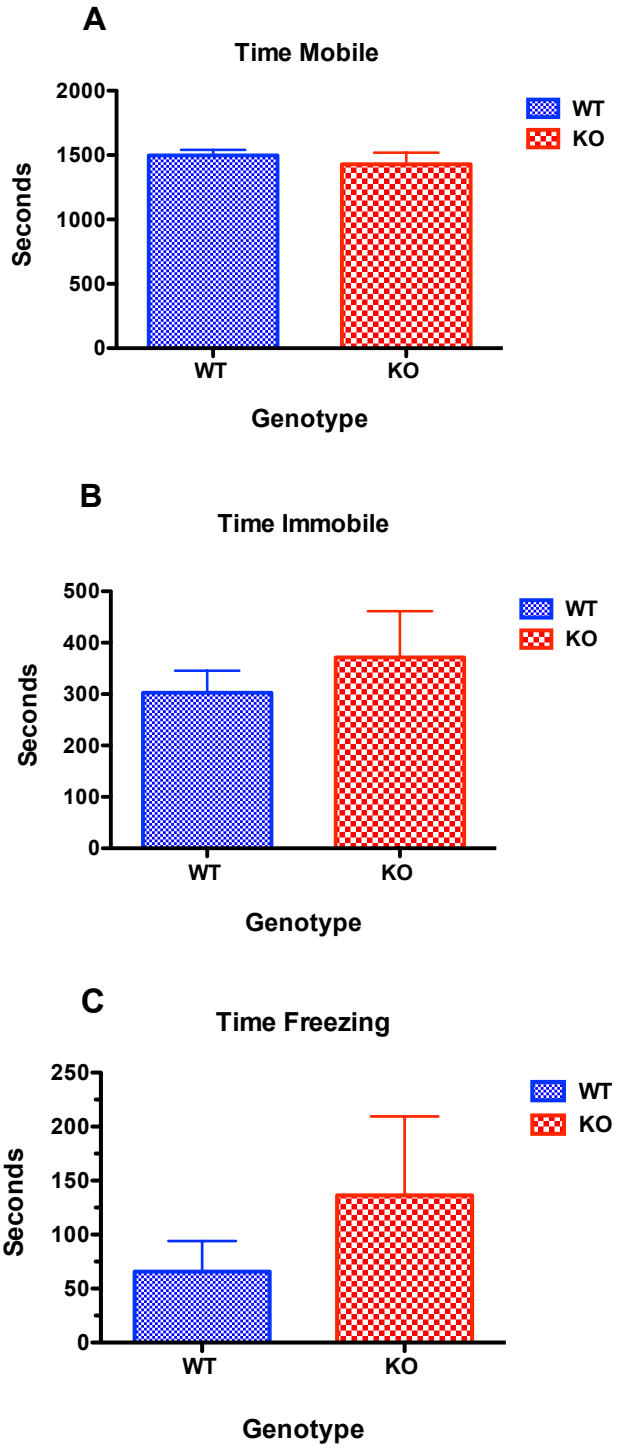


**Figure 17.** Measures of spontaneous locomotor activity in $CRIP_{1a}$ WT and KO mice. Two-tailed t-test revealed no significant differences between genotypes for total time spent mobile (A), time spent immobile (B) or time spent freezing (C) during the 30-minute test ($p > 0.05$). Data are expressed as mean time ± SEM, n = 8 per genotype.

**Table 7. Spontaneous Locomotor Activity: Time Spent Mobile by Segment of Test.**

| | Time Mobile (seconds) | | |
|---|---|---|---|
| | **0-600 sec** | **600-1200 sec** | **1200-1800 sec** |
| **$CRIP_{1a}$ WT** | 567 ± 9 | 503 ± 12 * | 428 ± 30 ** |
| **$CRIP_{1a}$ KO** | 553 ± 6 | 458 ± 42 | 418 ± 49 * |

Spontaneous locomotor activity decreased over time, but no significant genotype effects were observed in $CRIP_{1a}$ KO compared to $CRIP_{1a}$ WT mice. Data are expressed as mean ± SEM for each segment. Results showed a main effect of test segment after two-way ANOVA ($p = 0.0002$, $F = 10.47$, $df = 2$), but no interactions or main effect of genotype ($p > 0.05$) were observed. Bonferroni post-hoc analysis revealed significant differences between the first and second test segment in $CRIP_{1a}$ WT mice (* $p < 0.05$) and significant differences between the first and final test segments for both $CRIP_{1a}$ WT and KO mice (* $p < 0.05$, ** $p < 0.01$).

**Table 8. Spontaneous Locomotor Activity: Average Time Spent Freezing by Segment of Test.**

| | Time Freezing (seconds) | | |
|---|---|---|---|
| | **0-600 sec** | **600-1200 sec** | **1200-1800 sec** |
| **$CRIP_{1a}$ WT** | 2.4 ± 1.6 | 9 ± 4 | 32 ± 13 |
| **$CRIP_{1a}$ KO** | 2.5 ± 1.2 | 21 ± 14 | 17 ± 12 |

Average time spent freezing was not different in $CRIP_{1a}$ KO compared to $CRIP_{1a}$ WT mice. Data are expressed as mean ± SEM for each test segment. Results reveal no significant interactions and no main effects of genotype or test segment after two-way ANOVA ($p > 0.05$).

### 3.7 $CRIP_{1a}$ KO Mice Do Not Show a Unique Phenotype Compared to WT Littermate Controls in Motor Coordination.

Cannabinoid agonists not only disrupt spontaneous locomotor activity, but also locomotor coordination (De Santy and Dar, 2001). To test whether the absence of $CRIP_{1a}$ affects motor coordination, mice were trained to perform on a RotaRod at a moderately low rpm of 10, and later tested at a slightly higher rpm of 16. Data were collected from the time the drum began spinning until the time the mouse fell, jumped, or engaged in a passive rotation. Rotation velocity was held constant at 16 rpm. $CRIP_{1a}$ KO mice performed on average the same as WT mice, with an average time to fall equaling 21.1 ± 3.5 seconds compared to the $CRIP_{1a}$ WT average of 19.6 ± 6.2 seconds (Figure 18a). These latencies did not differ between genotypes, as determined by two-tailed t-test ($p > 0.05$). Distance traveled was also measured, and was found not to differ between genotypes after two-tailed t-test ($p > 0.05$). $CRIP_{1a}$ WT mice traveled an average of 0.54 ± 0.17 meters while $CRIP_{1a}$ KO mice traveled an average of 0.57 ± 0.10 meters (Figure 18b).

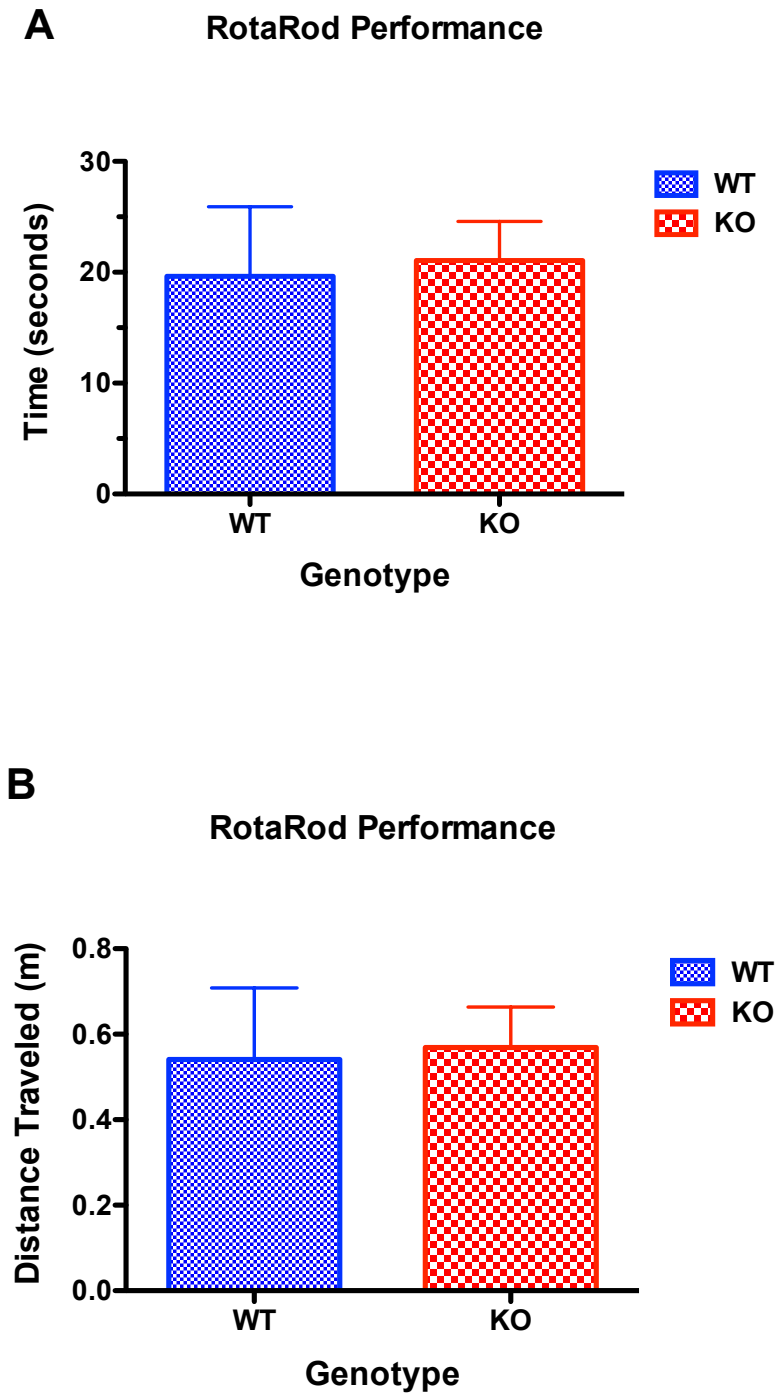


**Figure 18.** $CRIP_{1a}$ WT and KO mice do not differ in RotaRod assessment of motor coordination. Time to fall (A) and distance traveled (B) were not statistically different between $CRIP_{1a}$ WT and KO mice after two-tailed t-test ($p > 0.05$). Data represented are mean time (A) or distance (B) ± SEM, n = 8 per genotype.

### 3.8 $CRIP_{1a}$ KO Mice Do Not Show a Unique Phenotype Compared to WT Littermate Controls in the Hotplate Assessment of Antinociception.

Current proposed medicinal uses of cannabinoids include pain relief, and it is known that cannabinoid agonists can reduce responses to nociceptive stimuli through spinal- and supra-spinally-mediated pathways (Lichtman *et al.* 1991). Therefore, it was of interest to evaluate *in vivo* measures of antinociception in $CRIP_{1a}$ WT and KO mice to determine if loss of $CRIP_{1a}$ affects baseline pain thresholds due to potential changes in $CB_1$ receptor activity. The mice were evaluated for response latencies to a hot plate set at 52º or 56ºC, two temperatures commonly used to assess thermal antinociception in the literature (Zimmer *et al.* 1999). At 52ºC, $CRIP_{1a}$ KO mice responded to the nociceptive stimulus slower than $CRIP_{1a}$ WT mice, but the difference between genotypes was not significant after two-tailed t-test analysis ($p > 0.05$) (Figure 19a).

Average response latencies at 56ºC for $CRIP_{1a}$ WT and KO mice were nearly identical, at $9.04 \pm 1.1$ seconds and $8.96 \pm 1.5$ seconds, respectively (Figure 19b). Two-tailed t-test revealed no significant differences between genotypes or between temperatures ($p > 0.05$).

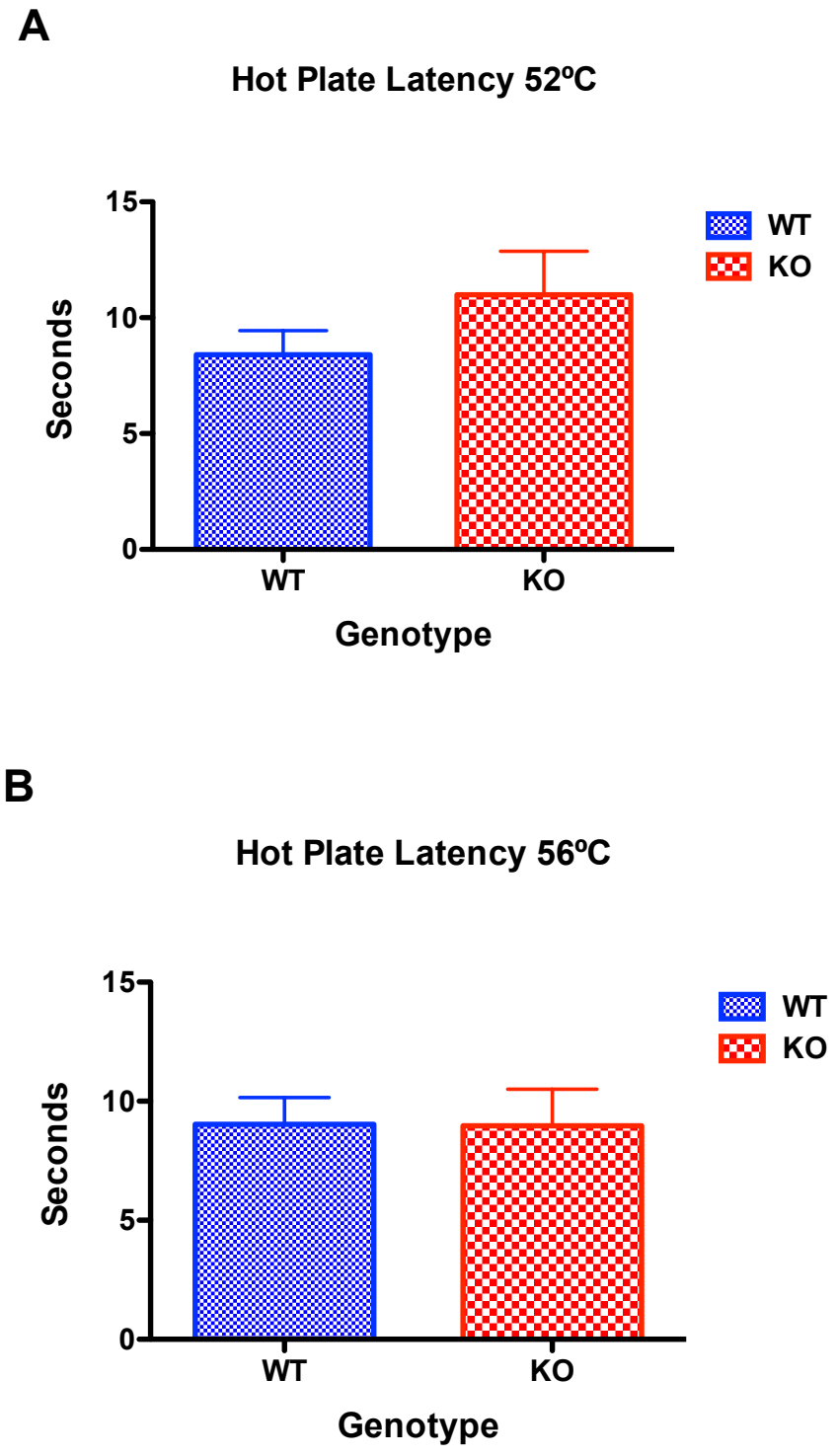


**Figure 19.** $CRIP_{1a}$ WT and KO mice do not differ in the hot plate assessment of antinociception. Mice were tested at 52ºC (A) and 56ºC (B), with response latencies recorded in seconds. Data are mean latencies ± SEM, n = 8 per genotype. Two-tailed t-tests revealed no significant difference between genotypes at either temperature setting ($p > 0.05$).

### 3.9 $CRIP_{1a}$ KO Mice Display an Antinociceptive Phenotype in the Warm Water Tail Withdrawal Assay.

Contrary to the findings in the hot plate assessment of antinociception, a significant difference between genotypes was found in the warm water tail withdrawal assessment of antinociception. A water bath set to 52ºC was used to assess tail withdrawal latency in $CRIP_{1a}$ WT and KO mice. $CRIP_{1a}$ WT mice displayed a tail withdrawal latency of 1.52 ± 0.12 seconds whereas $CRIP_{1a}$ KOs displayed a tail withdrawal latency of 2.14 ± 0.12 seconds (Figure 20a). Even though the average difference between genotypes was just 0.6 seconds, the results were found to be highly significant after two-tailed t-test ($p < 0.01$). Mice were also assessed at slightly higher (56°C; Figure 20b) and lower (48ºC; data not shown) temperatures, however no significant differences were observed between genotypes after two-tailed t-test for either temperature ($p > 0.05$).

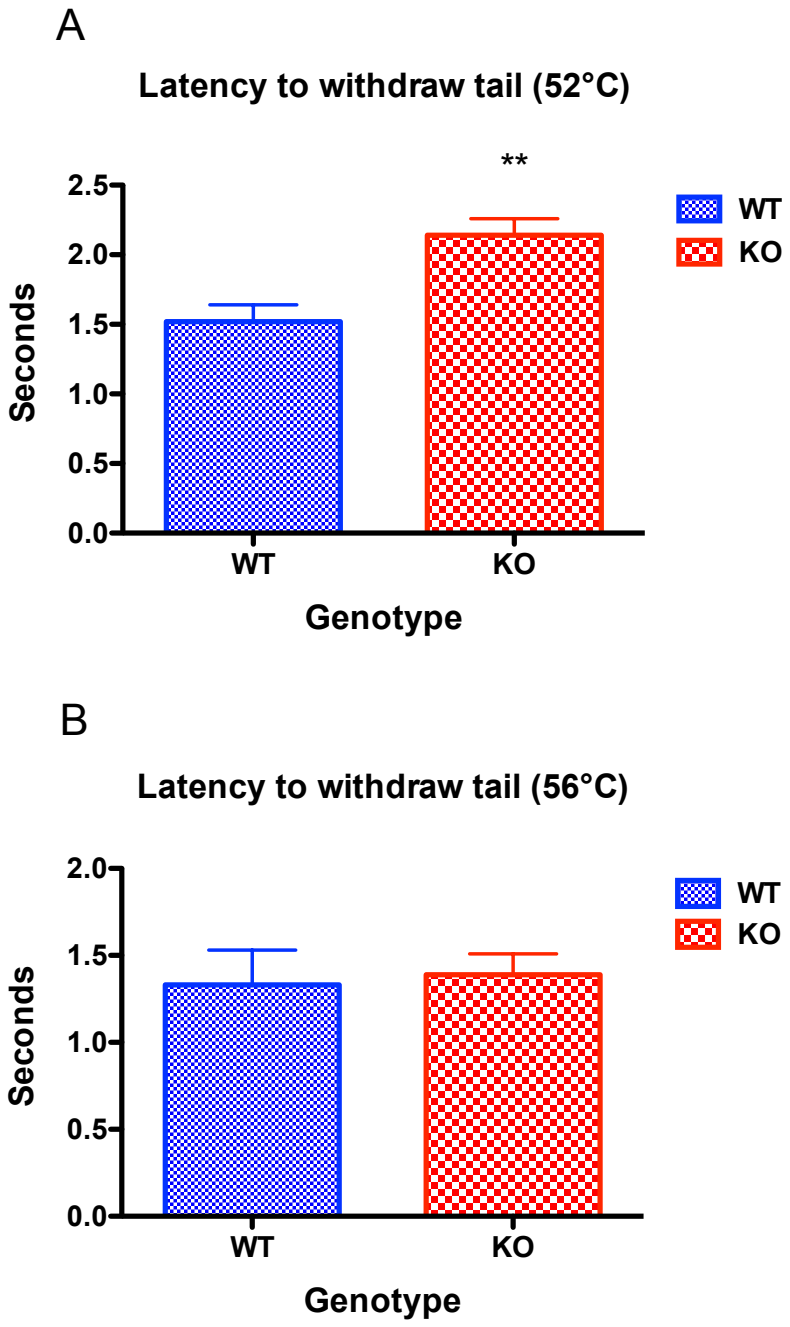


**Figure 20.** Warm water tail withdrawal assessment of antinociception in $CRIP_{1a}$ WT and KO mice. $CRIP_{1a}$ KO mice were found to display significantly longer tail withdrawal latencies in response to the nociceptive stimulus of a warm water bath set to 52ºC (A) (two tailed t-test, $p < 0.01$). Significant differences between genotypes were no longer observed when the temperature was increased to 56ºC (B) (two tailed t-test $p > 0.05$). Data represented are mean latencies ± SEM (n = 8 per genotype).

### 3.10 $CRIP_{1a}$ KO Mice Display an Anxiolytic-like Phenotype in the Light:Dark Box and Marble Burying Assays.

Cannabinoids elicit biphasic effects with regard to anxiety-like behaviors. Current evidence indicates these effects are due to a $CB_1$ receptor-mediated role in the amygdala, hippocampus and prefrontal cortex (Davidson, 2002; Braun *et al.* 2003). In addition, there is evidence that not only can exogenous cannabinoids affect anxiety-like behaviors, but also the endocannabinoids may play a role. For example, FAAH KO mice were shown to display an anxiolytic-like phenotype (Cravatt and Lichtman, 2003), likely a result of elevated anandamide levels. This effect was shown to be $CB_1$ receptor-mediated, as it was reversible by SR141716A. Moreover, the results of [$^{35}$S]GTPγS binding assays revealed significantly greater G-protein activation by $CB_1$ receptors in the amygdala of $CRIP_{1a}$ KO relative to WT mice (see Section 3.5). Therefore, naïve $CRIP_{1a}$ WT and KO mice were evaluated for possible anxiety-related phenotypes. A robust and repeatable anxiolytic-like phenotype was observed in $CRIP_{1a}$ KO compared to WT mice (Figure 21) in the light:dark box assay. Within the five-minute time period of this test, $CRIP_{1a}$ KO mice spent an average of 178 ± 20 seconds in the light side, which was significantly greater than $CRIP_{1a}$ WT mice, which spent an average of 111 ± 11 seconds in the light side (two-tailed t-test, $p < 0.01$). Video tracking ensured that no deficits in locomotor activity contributed to the findings (Figure 22), confirming previous results that indicated no differences between genotypes in open field locomotor activity (see section 3.6).

Based on the finding of an anxiolytic-like phenotype in $CRIP_{1a}$ KO mice in the light:dark box test, it was important to determine whether other measures of anxiety-related behaviors would yield similar results. This was particularly important because animals tested in the light:dark box assay could not be reexamined in the same conditions due to habituation, thus repeating the test

would have required a new cohort of test-naïve mice. Another common behavioral assay used to measure anxiety-related behaviors is marble burying. Typical murine digging behavior leads to many of the marbles being buried in loose pine bedding, however under the influence of anxiolytic drugs such as benzodiazepines, mice bury significantly fewer marbles (Njung'e and Handley, 1991). After assessing naïve $CRIP_{1a}$ WT and KO mice in the marble-burying test, a significant anxiolytic-like phenotype was observed in the KO relative to WT mice (two-tailed t-test, $p < 0.05$). $CRIP_{1a}$ WT mice buried over twice as many marbles on average compared to $CRIP_{1a}$ KO mice (Figure 23). Together with the light:dark box results, these results indicate that the absence of $CRIP_{1a}$ produces an anxiolytic-like phenotype in mice.

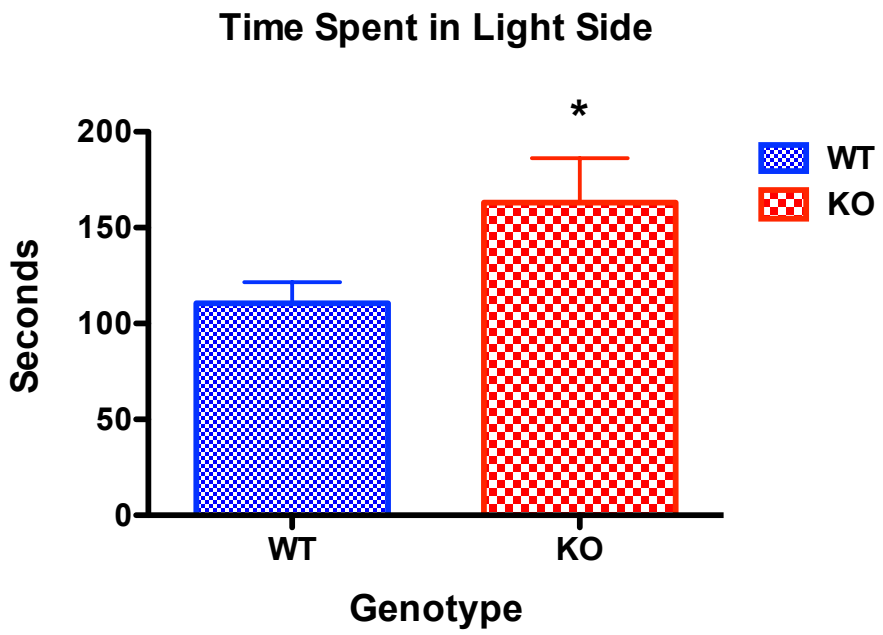


**Figure 21.** $CRIP_{1a}$ KO mice spend more time in the light side compared to $CRIP_{1a}$ WT mice. $CRIP_{1a}$ WT and KO mice (n = 8 per genotype, collapsed by sex) were placed in a light:dark box chamber and allowed to freely explore both compartments for five minutes. Time spent in either side was recorded using the video-tracking software, ANY-maze™, and total time in each compartment was measured in seconds. Data represented are mean time spent in the light side ± SEM. $CRIP_{1a}$ KO mice spent significantly more time (two-tailed student's t-test, $p < 0.05$) in the light side compared to WT mice, suggesting an anxiolytic-like phenotype.

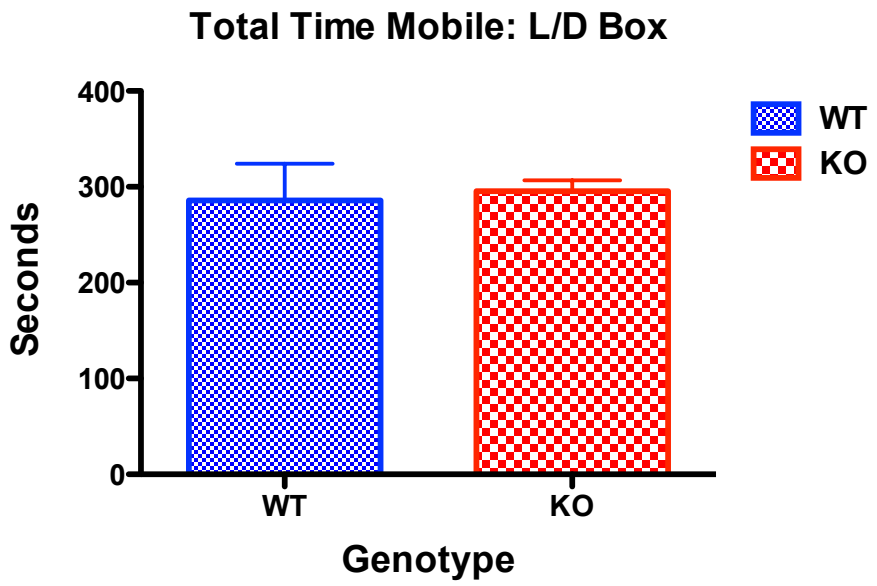


**Figure 22.** $CRIP_{1a}$ WT and KO mice do not differ in time spent mobile during light:dark box assay. $CRIP_{1a}$ WT and KO mice (n = 8 per genotype, collapsed by sex) were placed in a light:dark box chamber and allowed to freely explore both compartments for five minutes. Time spent in either side was recorded using the video-tracking software, ANY-maze™, and total time in each compartment was measured in seconds and summed. Data represented are mean time mobile ± SEM. No significant differences were observed after two-tailed student's t-test, $p > 0.05$.

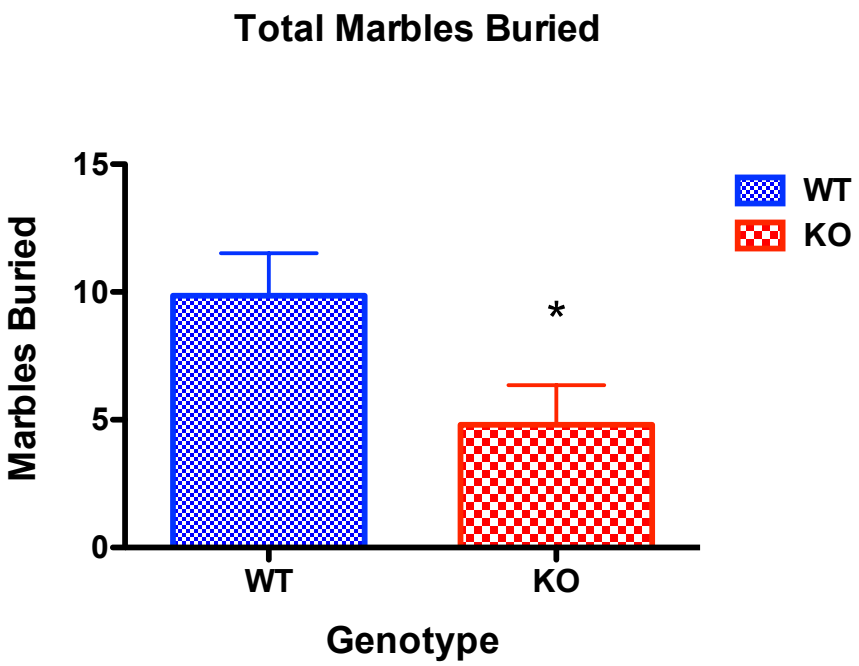


**Figure 23.** $CRIP_{1a}$ KO mice bury less marbles compared to $CRIP_{1a}$ WT mice. $CRIP_{1a}$ WT and KO mice (n = 16 KO and 13 WT mice, collapsed by sex) were placed in a cage containing 20 evenly spaced marbles on fluffed bedding. After twenty minutes, total marbles buried was assessed. Data represented are mean number of marbles buried ± SEM. $CRIP_{1a}$ KO mice buried significantly less marbles (two-tailed student's t-test, $p < 0.05$) compared to WT mice, suggesting an anxiolytic-like phenotype.

### 3.11 $CRIP_{1a}$ KO Mice Do Not Show a Unique Phenotype Compared to WT Littermate Controls in the Tetrad Assay After Cumulative Doses of CP55,940.

$CRIP_{1a}$ WT and KO mice have thus far been assessed solely in a naïve state. With the exception of anxiolytic-like behavior, the findings have yielded either small effects (see section 3.7) or no significant differences between genotypes. It is possible that further phenotypic differences related to loss of $CRIP_{1a}$ could be unmasked by activating $CB_1$ receptors with an agonist. Based on our laboratory's results using $CRIP_{1a}$ over-expression in cell culture models,

which showed $CRIP_{1a}$ reduced agonist-stimulated $CB_1$ receptor-mediated G-protein activity, a lack of $CRIP_{1a}$ could affect *in vivo* results by producing exaggerated agonist effects due to the absence of $CRIP_{1a}$-mediated negative regulation of $CB_1$ receptor activation. Of the CNS regions examined so far, however, only the amygdala revealed an enhancement of $CB_1$ receptor-mediated G-protein activation in $CRIP_{1a}$ KO relative to WT mice. However, it is possible that a life-long absence of $CRIP_{1a}$ might have caused adaptation in $CB_1$ receptor-mediated G-protein activation, which could have masked the expected effect of $CRIP_{1a}$ deletion. Because such compensatory adaptation is less likely in mice that are heterozygous for the KO allele, $CRIP_{1a}$ HET mice could potentially exhibit an enhanced sensitivity to cannabinoid agonists. Therefore, $CRIP_{1a}$ WT, HET and KO male mice were evaluated in a cumulative dosing tetrad paradigm using the potent synthetic cannabinoid agonist, CP55,940 (n = 8 per genotype). Mice were examined for baseline responses in the following measures: catalepsy, warm water tail withdrawal, hot plate, RotaRod performance and body temperature. These measures were repeatedly evaluated after each increasing dose of CP55,940 was administered, to assess dose-response effects in our mice. The actual doses that were administered to mice were designed such that together, they cumulatively equaled the test doses shown below.

Catalepsy was first observed in $CRIP_{1a}$ WT and HET males after receiving a total of 0.03mg/kg CP 55,940. The $CRIP_{1a}$ KO mice did not exhibit catalepsy until the 0.1mg/kg dose. All genotypes were equally affected at the 0.3 mg/kg dose and final dose of 1mg/kg, whereby many mice remained motionless for the full 60 seconds. Therefore, catalepsy was not exaggerated in the $CRIP_{1a}$ KO mice; in fact, they displayed a slightly reduced sensitivity to CP55,940 in this measure (Figure 24), although this apparent difference did not reach the level of statistical significance, as indicated by the findings of no significant main effect of genotype nor

an interaction between dose and genotype after analysis by two-way ANOVA. Data were then transformed to a percentage of the maximum possible effect (%MPE), with a cut-off time of 60 seconds. However, no differences were seen among genotypes using this normalization of the data. Only a main effect of CP55,940 dose was determined to be significant by two-way ANOVA ($p < 0.0001$, $F = 108.1$, $df = 3$), while no interactions between dose and genotype were observed.

Baseline tail withdrawal latencies at 52ºC were not significantly different among genotypes as determined by two-way ANOVA ($p > 0.05$), differing from previously observed results (see section 3.7). Significant effects among genotypes were also not observed for tail withdrawal latency upon cumulative dosing with CP55,940. No main effect of genotype was found in either the raw latency data or the data transformed to % MPE (Figure 25), when analyzed by two-way ANOVA ($p > 0.05$). No interactions were observed either, however a main effect of CP55,940 dose was found ($p < 0.0001$, $F = 65.33$, $df = 5$).

A second measure of antinociception was evaluated using a hot plate set to 52ºC. Baseline latencies were slightly higher in $CRIP_{1a}$ KOs, but not significantly different (one-way ANOVA with Newman-Keuls post hoc, $p > 0.05$), similar to previous results (see section 3.8). By the final CP55,940 dose of 1 mg/kg, a ceiling effect prevented any potential genotype differences from being observed, as each mouse reached the maximum cut-off time of 20 seconds without responding to the nociceptive stimulus. No significant differences among genotypes were observed, as indicated by the finding of no significant main effect of genotype after analysis by two-way ANOVA ($p > 0.05$). Transforming data to %MPE also revealed no differences among genotypes (Figure 26). Similar to the previously reported behaviors, no interactions were

observed, however a main effect of CP55,940 dose was determined by two-way ANOVA ($p < 0.0001$, $F = 32.88$, $df = 5$).

Motor coordination was assessed using an accelerating RotaRod protocol starting at 6 RPM and increasing to 25 RPM over a period of 60 seconds. Both maximum RPM and time to stay on the RotaRod drum (in seconds) were recorded for baseline and at each dose of CP55,940 (Figure 27). Surprisingly, $CRIP_{1a}$ KO mice exhibited longer average times on the RotaRod than either WT or HET mice throughout the course of the experiment, though no significant main effect was obtained among genotypes after two-way ANOVA ($p > 0.05$). Not until the maximum assessed dose of 1 mg/kg CP55,940 were there apparent deficits in motor coordination. Two-way ANOVA revealed a significant main effect of CP55,940 dose ($p = 0.0002$, $F = 5.26$, $df = 5$), but no interactions.

The final output measure was change in core body temperature. As expected, temperatures declined with increasing doses of CP55,940, however no significant main effect was obtained between genotypes after two-way ANOVA ($p > 0.05$) (Figure 28). A main effect of CP55,940 dose was observed ($p < 0.0001$, $F = 128.4$, $df = 5$), though no interactions were revealed. Thus, these results indicate no significant effects of $CRIP_{1a}$ deletion on several prototypical pharmacological actions of cannabinoid agonists, including catalepsy, thermal antinociception, hypothermia or motor incoordination.

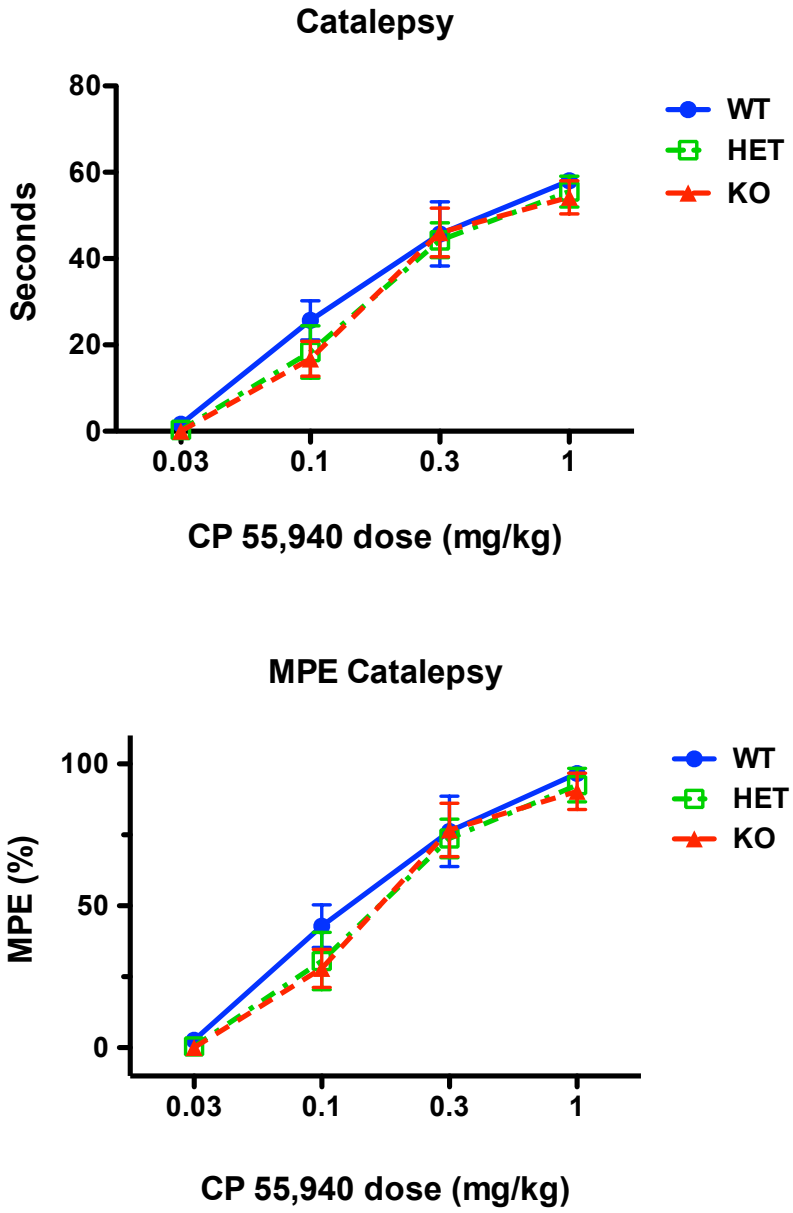


**Figure 24.** Change in cataleptic behavior during cumulative dosing with CP55,940 in $CRIP_{1a}$ WT, HET and KO male mice (n = 8 per genotype). After baseline latencies were measured, intraperitoneal (i.p.) injections of increasing CP55,940 doses were administered and a 30 minute incubation period elapsed prior to assessing catalepsy at each dose. Data represented are mean values ± SEM. Two-way ANOVA revealed a significant main effect of dose ($p < 0.0001$, $F = 108.1$, $df = 5$). No significant interactions or main effect of genotype were observed ($p > 0.05$).

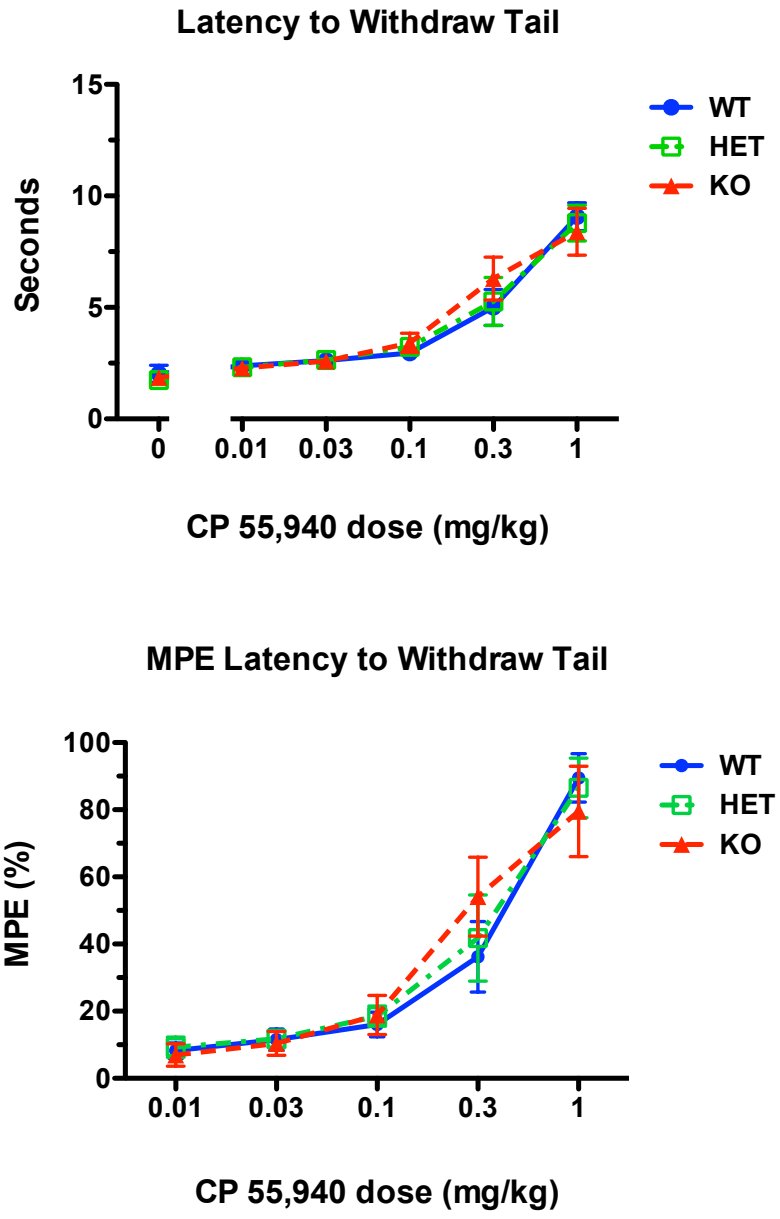


**Figure 25.** Change in latency to withdraw tail from a 52°C warm water bath during cumulative dosing with CP55,940 in $CRIP_{1a}$ WT, HET and KO male mice (n = 8 per genotype). Mice were evaluated for antinociception. After baseline latencies were measured, intraperitoneal (i.p.) injections of increasing CP55,940 doses were administered and a 30 minute incubation period elapsed prior to assessing antinociception at each dose. Data represented are mean values ± SEM. Two-way ANOVA revealed a significant main effect of dose ($p < 0.0001$, $F = 65.33$, $df = 5$). No significant interactions or main effect of genotype were observed ($p > 0.05$).

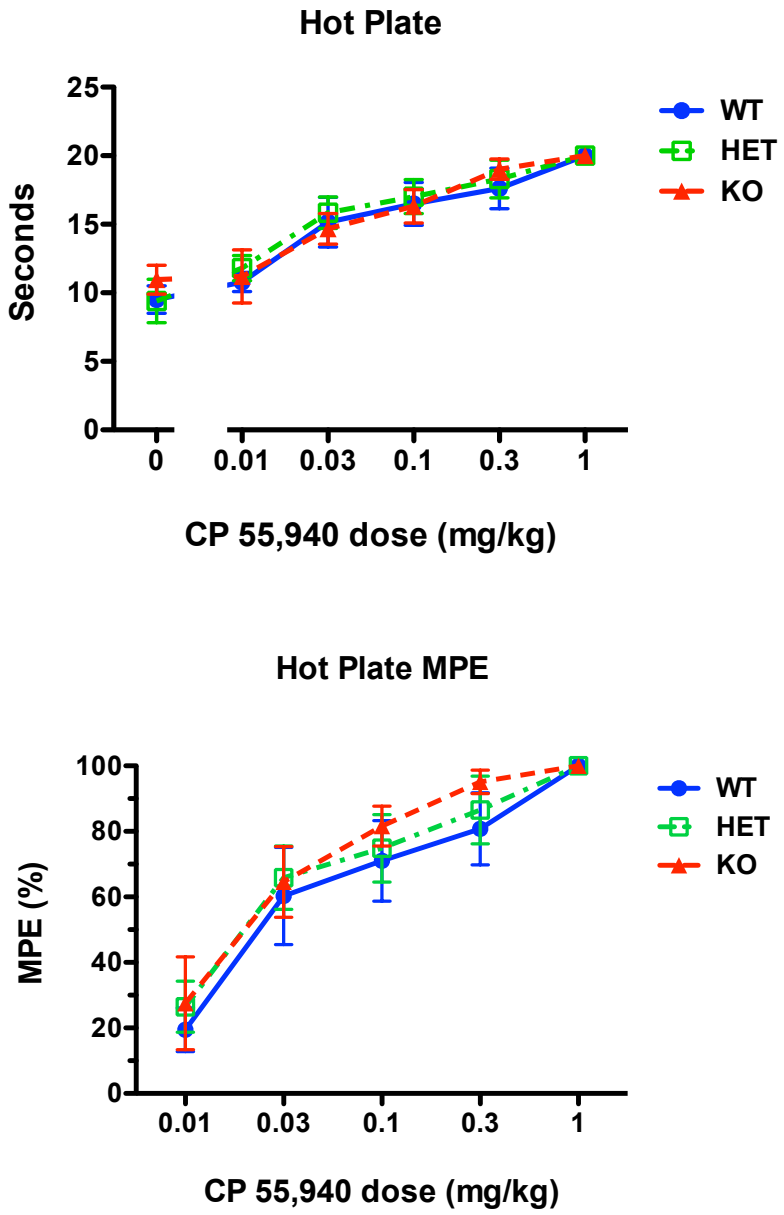


**Figure 26.** Change in response times to a 52°C hot plate during cumulative dosing with CP55,940 in $CRIP_{1a}$ WT, HET and KO male mice (n = 8 per genotype). Mice were evaluated for antinociception. After baseline latencies were measured, intraperitoneal (i.p.) injections of increasing CP55,940 doses were administered and a 30 minute incubation period elapsed prior to assessing antinociception at each dose. Data represented are mean values ± SEM. Two-way ANOVA revealed a significant main effect of dose ($p < 0.0001$, $F = 32.88$, $df = 5$). No significant interactions or main effect of genotype were observed ($p > 0.05$).

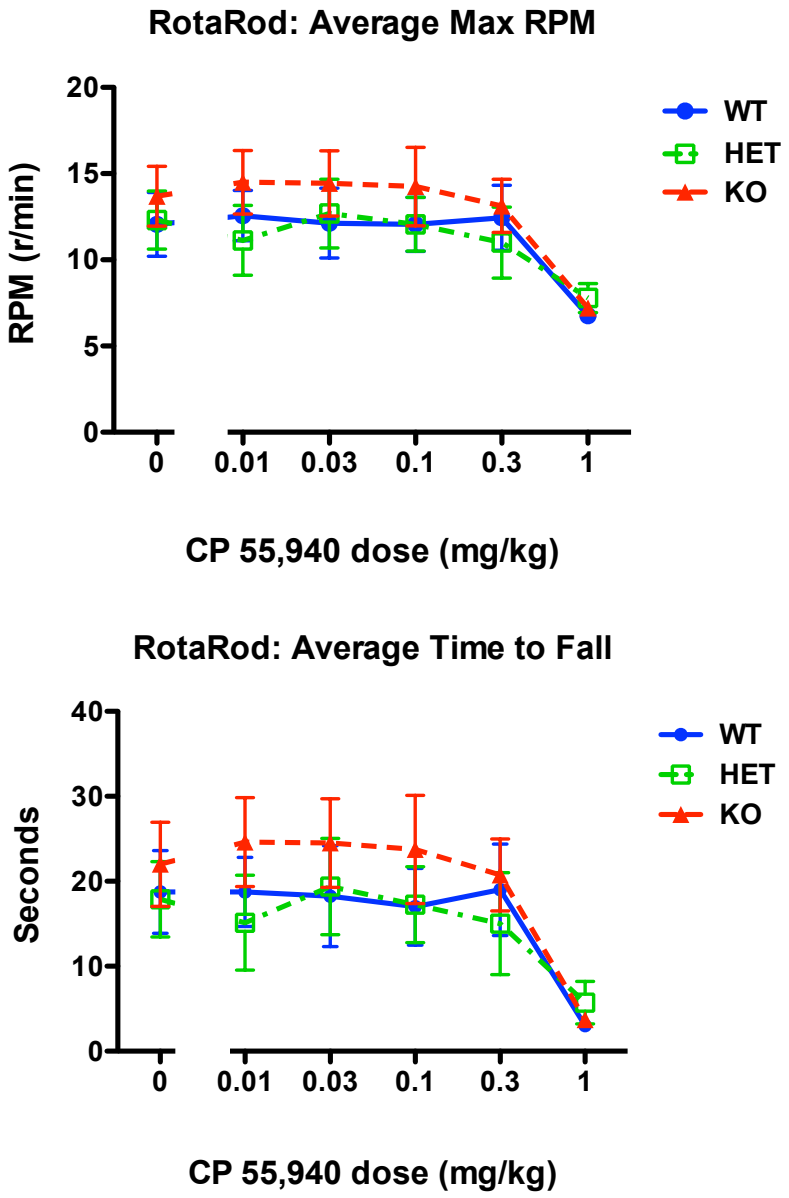


**Figure 27.** Change in motor coordination during cumulative dosing with CP55,940 in $CRIP_{1a}$ WT, HET and KO male mice (n = 8 per genotype). After baseline measures were recorded, intraperitoneal (i.p.) injections of increasing CP55,940 doses were administered and a 30 minute incubation period elapsed prior to assessing motor coordination at each dose via accelerating RotaRod. Data represented are mean values ± SEM. Two-way ANOVA revealed a significant main effect of dose ($p = 0.0002$, $F = 5.26$, $df = 5$). No significant interactions or main effect of genotype were observed ($p > 0.05$).

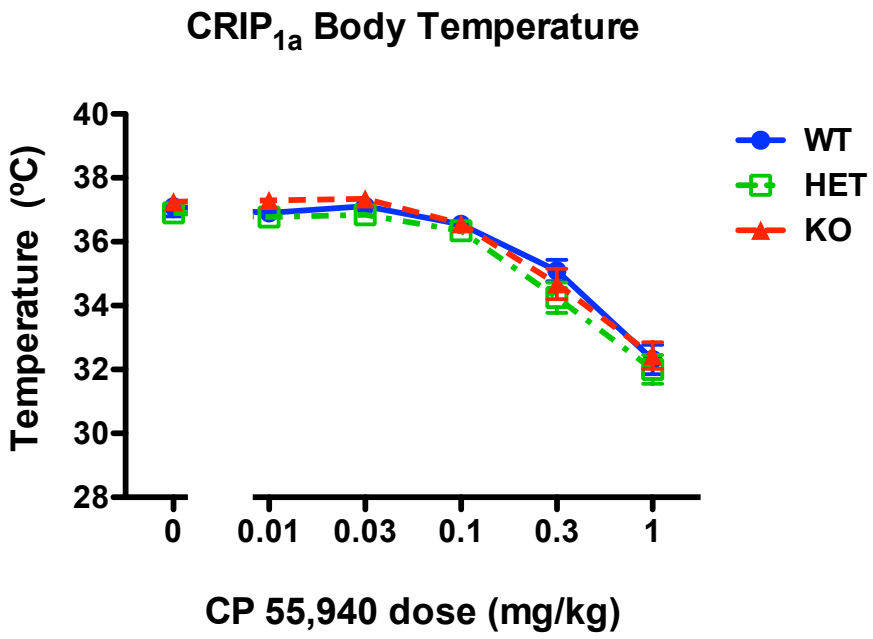


**Figure 28.** Change in core body temperature during cumulative dosing with CP55,940 in $CRIP_{1a}$ WT, HET and KO male mice (n = 8 per genotype). Mice were evaluated for core body temperature using a digital rectal probe. After baseline body temperature was measured, intraperitoneal (i.p.) injections of increasing CP55,940 doses were administered and a 30 minute incubation period elapsed prior to assessing body temperature at each dose. Data represented are mean values ± SEM. Two-way ANOVA revealed a significant main effect of dose ($p < 0.0001$, $F = 128.4$, $df = 5$). No significant interactions or main effect of genotype were observed ($p > 0.05$).

### 3.12 $CRIP_{1a}$ Expression is Not Affected by Repeated THC Treatment or by Genetic Knockout of $CB_1$ Receptors in Mice.

I previously showed that $CRIP_{1a}$ is present in the cerebellum, hippocampus and the spinal cord, but other regions of the brain have not been specifically investigated. Moreover, the effect of prolonged activation or genetic deletion of $CB_1$ receptors on the expression of $CRIP_{1a}$ in $CB_1$ receptor-expressing regions of the CNS has not been investigated. Therefore, $CB_1$ WT and KO male mice were treated chronically with either vehicle (VEH) or 10 mg/kg THC twice a day for 13.5 days – a standard dosing treatment used to activate $CB_1$ receptors and potentially induce adaptation in expression or activity of $CB_1$ receptors – after which $CRIP_{1a}$ expression was analyzed for differences between treatment groups and genotypes in the amygdala, cerebellum and prefrontal cortex. Each of these regions expresses moderate-to-high levels of $CB_1$ receptors and plays various roles in mediating behavioral effects of cannabinoids (Herkenham *et al*. 1991; Rubino *et al.* 2008; Bambico *et al.* 2007). It is important to determine whether $CRIP_{1a}$ expression is altered when $CB_1$ receptors are not present by examining VEH-treated $CB_1$ receptor KO and WT mice, and additionally if it is affected by prolonged activation of $CB_1$ receptors, as determined in THC-treated mice. These two factors provide an initial indication of the extent to which $CRIP_{1a}$ levels are affected by alterations of $CB_1$ receptor expression or activity in a subset of brain regions, and therefore whether $CRIP_{1a}$ expression could be regulated by the status of the endocannabinoid system.

Western immunoblots were performed under [my] supervision by a rotation student, Cassandra Slater, and showed $CRIP_{1a}$ presence does not statistically differ in the cerebellum, prefrontal cortex or amygdala of $CB_1$ WT and KO mice or between VEH and THC treatments (Figure 29, 30 and 31). A slight trend toward increased $CRIP_{1a}$ expression was observed in the

cerebellum of both VEH- and THC-treated $CB_1$ KO mice (main effect of genotype by two-way ANOVA, $p = 0.133$), however no interaction or main effect of treatment was observed ($p > 0.05$) (Figure 29). In both the prefrontal cortex (Figure 30) and amygdala (Figure 31), expression was nearly identical across treatment conditions and genotypes. After two-way ANOVA, no interaction or main effects of genotype or treatment were found with regard to either region ($p > 0.05$). These results indicate that $CRIP_{1a}$ expression is not dependent on the expression of $CB_1$ receptors and is not altered by repeated administration of 10 mg/kg THC, at least in these particular brain regions.

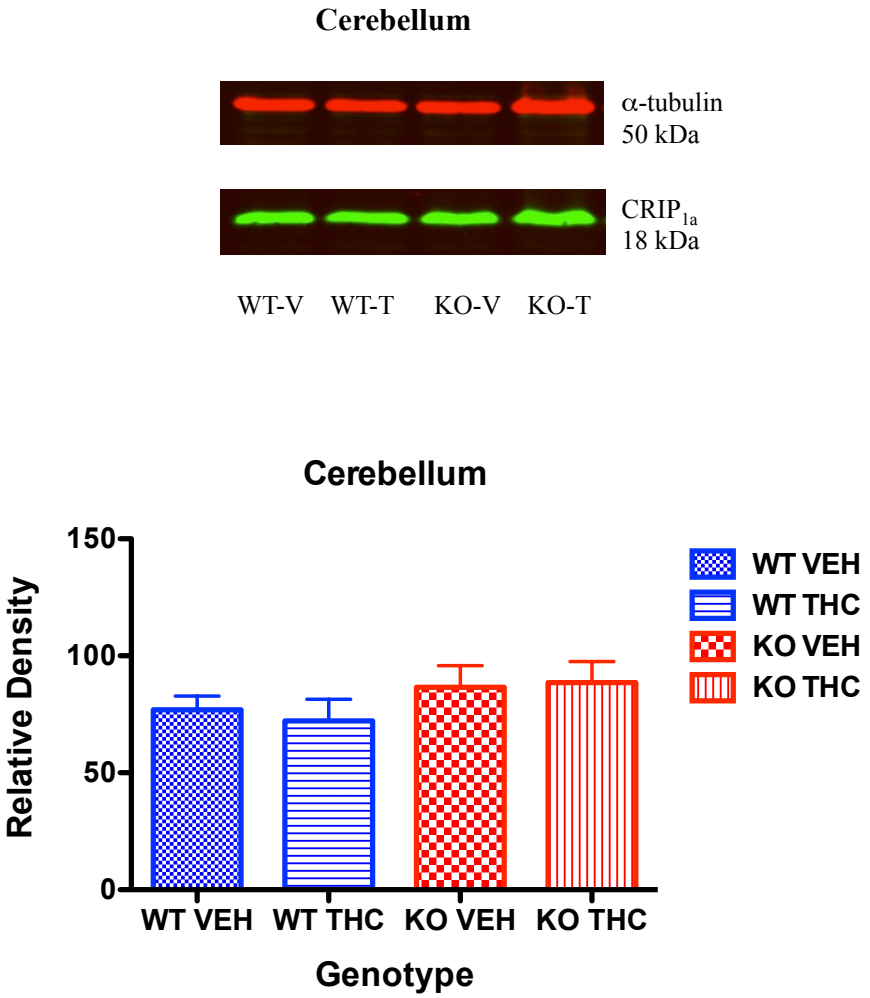


**Figure 29.** Expression of $CRIP_{1a}$ in the cerebellum is not affected by $CB_1$ receptor KO or repeated THC treatment. Representative immunoblots of $CRIP_{1a}$ protein in cerebellum (top panel) shows expression in $CB_1$ WT and KO vehicle-treated and THC-treated mice (n=8 per genotype, per treatment). WT-V and WT-T represent WT vehicle-treated and THC-treated mice, respectively. KO-V and KO-T represent KO vehicle-treated and THC-treated mice, respectively. Relative densities (bottom panel) were measured from blots and analyzed by two-way ANOVA. No significant main effects of treatment or genotype were observed, nor was there an interaction ($p > 0.05$).

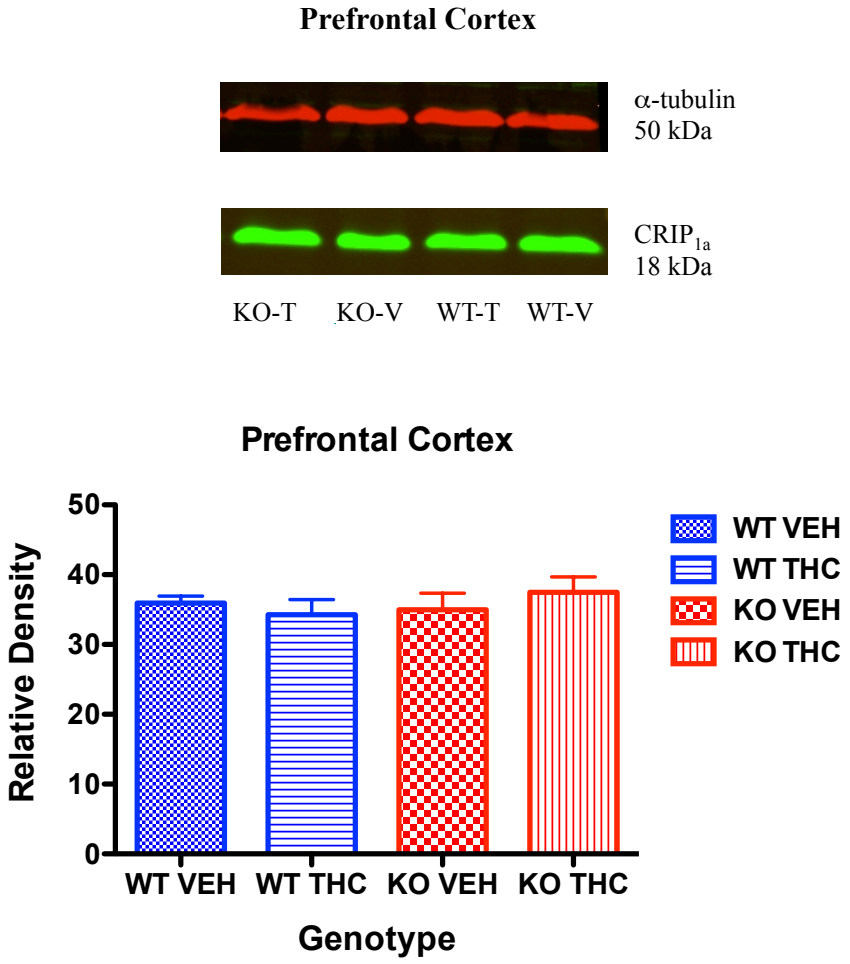


**Figure 30.** Expression of $CRIP_{1a}$ in the prefrontal cortex is not affected by $CB_1$ receptor KO or repeated THC treatment. Representative immunoblots of $CRIP_{1a}$ protein in prefrontal cortex (top panel) shows expression in $CB_1$ WT and KO vehicle-treated and THC-treated mice (n=8 per genotype, per treatment). WT-V and WT-T represent WT vehicle-treated and THC-treated mice, respectively. KO-V and KO-T represent KO vehicle-treated and THC-treated mice, respectively. Relative densities (bottom panel) were measured from blots and analyzed by two-way ANOVA. No significant main effects of treatment or genotype were observed, nor was there an interaction ($p > 0.05$).

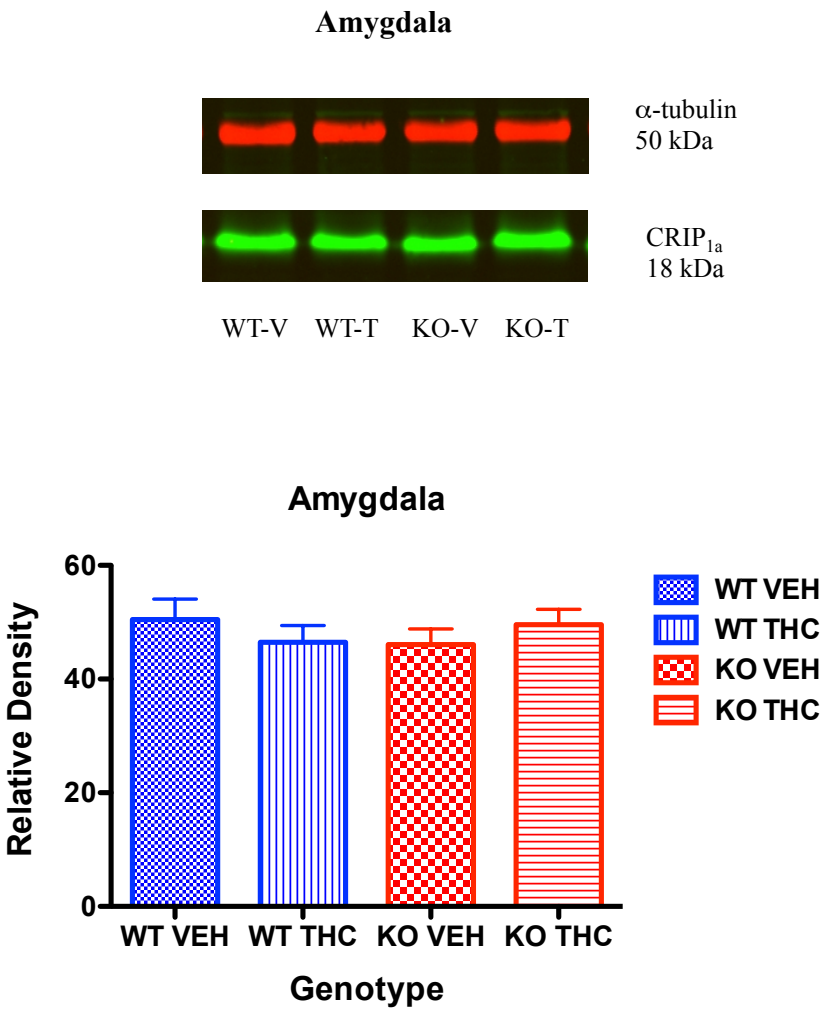


**Figure 31.** Expression of $CRIP_{1a}$ in the amygdala is not affected by $CB_1$ receptor KO or repeated THC treatment. Representative immunoblots of $CRIP_{1a}$ protein in amygdala (top panel) shows expression in $CB_1$ WT and KO vehicle-treated and THC-treated mice (n=8 per genotype, per treatment). WT-V and WT-T represent WT vehicle-treated and THC-treated mice, respectively. KO-V and KO-T represent KO vehicle-treated and THC-treated mice, respectively. Relative densities (bottom panel) were measured from blots and analyzed by two-way ANOVA. No significant main effects of treatment or genotype were observed, nor was there an interaction ($p > 0.05$).

## Chapter 4. Discussion and Conclusions

### 4.1 Overview.

The purpose of this thesis project was to investigate the physiological role(s) of $CRIP_{1a}$ in the whole animal by using the first ever $CRIP_{1a}$ knockout mouse line. To generate the first $CRIP_{1a}$ KO mice, $CRIP_{1a}$ HET mice (generated by the initial chimeric mice) were placed in breeding pairs. Our first litter contained $CRIP_{1a}$ WT, HET and KO mice, determined by genotyping with PCR and specific primers. In order to demonstrate that *Cnrip1* gene-targeted mice were in fact null for $CRIP_{1a}$ expression, several experiments were preformed. First, Western immunoblot analysis of cerebellar homogenates probed with $CRIP_{1a}$ antiserum showed robust expression in the $CRIP_{1a}$ WT mouse, whereas a complete absence of $CRIP_{1a}$ was observed in the $CRIP_{1a}$ KO mouse, even up to 100 μg of protein. We also evaluated immunoblots of the hippocampus and spinal cord of $CRIP_{1a}$ KO mice, and again, found no evidence of $CRIP_{1a}$ expression. Because immunoblots represent protein expression, it was important to show that the null status was a result of the lack of transcription and not a truncated protein. qPCR analysis showed that $CRIP_{1a}$ KO mice produced a maximum of 0.4% transcript relative to $CRIP_{1a}$ WT mice, further verifying that we have a true null *Cnrip1* status in these mice.

Despite the confirmation of $CRIP_{1a}$ null status, *Cnrip1* KO mice appeared to be normal and viable, as determined by the expected Mendelian ratio of genotypic yield in HET x HET crossing. In addition, these mice were determined to be fertile, as assessed by KO x KO crossing, and exhibited a normal rate of growth and development, as assessed by bodyweight gain over a 14 week period, from weaning at the age of 3 weeks, to adulthood at the age of 16 weeks.

A standard battery of in vivo assessments was then chosen to evaluate how the absence of $CRIP_{1a}$ affects baseline physiological and behavioral status, as well as common pharmacological responses after the administration of a cannabinoid agonist. It is well reported in the literature that cannabinoids affect general locomotor activity (Varvel *et al.* 2006), anxiety-like behaviors (Viveros *et al.* 2005), motor coordination (Desanty and Dar, 2001), and can mediate both spinal and supra-spinal components of antinociception (Lichtman *et al.* 1991, Varvel *et al.* 2005). Each of these behaviors have also been linked to specific brain regions that appear to play a role in these effects. For example, the cerebellum and striatum are involved in locomotor activity and motor coordination (Day *et al.* 1991; Thach *et al.* 1992), while the amygdala, hippocampus and prefrontal cortex contribute to stress responses and anxiety-like behaviors (Davis, 1992; Davidson, 2002; Braun *et al.* 2003). Nociception has been linked to regions of the brain such as the periaqueductal gray area (PAG) and lateral posterior thalamus, while others have also reported a role of the spinal cord (Lichtman *et al.* 1996; Martin *et al.* 1999; Welch and Stevens, 1992). We chose to evaluate a subset of these behaviors in $CRIP_{1a}$ KO mice, both in drug-free and cannabinoid agonist-induced states. Additionally, we evaluated many of these specific regions *ex vivo* through [$^3$H]CP55,940 saturation binding and agonist-stimulated [$^{35}$S]GTPγS binding assays to determine potential genotype-related differences in $CB_1$ receptor levels and $CB_1$ receptor-mediated G-protein activity, respectively.

My major findings were that $CRIP_{1a}$ KO mice exhibit: 1) an anxiolytic-like phenotype, with few differences from WT mice in other baseline measures of behavior or physiological status, 2) enhanced $CB_1$ receptor-mediated G-protein activation in the amygdala, with only minor or no differences from WT mice in other CNS regions examined, 3) no differences in $CB_1$ receptor expression levels versus WT mice in any CNS region examined, and 4) no difference from WT

mice in pharmacological sensitivity to a cannabinoid agonist in several in vivo measures examined. Furthermore, from the finding that $CRIP_{1a}$ KO mice exhibited either no significant differences or enhancement of cannabimimetic effects relative to WT mice in all measures examined, we can conclude that $CRIP_{1a}$ does not appear to mediate these effects of $CB_1$ receptor activation (i.e. is not required for these actions of cannabinoids). Finally, neither $CB_1$ receptor null status nor repeated administration of THC significantly altered $CRIP_{1a}$ expression in any CNS region examined. Thus, the effects of $CRIP_{1a}$ deletion on $CB_1$ receptor function in the CNS appear to be quite specific in nature. Details of these findings and related interpretations are discussed in the following sections.

**4.2 The Role of the Amygdala and $CRIP_{1a}$ in Anxiolytic-like Behavior.**

By employing a loss-of-function approach, we have discovered a novel role of $CRIP_{1a}$ in anxiety-like behaviors. Two different models were used to independently investigate anxiety-like behavior in naïve $CRIP_{1a}$ WT and KO mice. The first was the light:dark box assay, which is a one-time assessment (due to habituation) that tracks the animal's movements between an open, brightly lit area and a dark, enclosed area, and sums the time spent in each compartment (for review, see Bourin and Hascoët, 2003). Rodents, including mice, are expected to spend more time in the dark side due to their natural tendencies as prey animals to hide from predators out in the open. Therefore, any manipulation, whether it be biological or pharmacological, that leads to increased times in the light suggests an anxiolytic-like effect. Studies have previously shown that this model can predict anxiolytic-like actions of drugs such as benzodiazepines and serotonergic ($5HT_{1A}$) agonists (Crawley and Goodwin, 1980; Sanchez, 1995). In our studies, naïve $CRIP_{1a}$ KO mice displayed an anxiolytic-like phenotype by spending more time in the light

side compared to their WT littermates. $CRIP_{1a}$ WT behavior in the light:dark box was consistent with typical murine tendencies to remain in the dark, as reported in the literature (Crawley and Goodwin, 1980; Crawley and Davis, 1982). It is important to note that this anxiolytic-like effect was not due to differences in locomotor activity or freezing behavior, as determined by video tracking software. This finding is congruent with studies that pharmacologically targeted the endocannabinoid system with specific enzyme and uptake inhibitors, leading to reduced anxiety-like behavior without alterations in motor activity or coordination (Patel and Hillard, 2006). Furthermore, our results are not likely due to strain influences, as the 129sv line and its substrains are particularly found to be anxiogenic when compared to other strains, including C57BL6/J. This fact is important to consider given that our mice are on a hybrid background of C57BL6/J and 129sv lines, a result of the technique used to create this KO line. The behavior observed in $CRIP_{1a}$ KO mice not only provides further insight into one functional role of $CRIP_{1a}$, but also provides an additional line of support that altering the endocannabinoid system, particularly by increasing its activation, can lead to anxiolytic-like phenotypes. This effect has been previously demonstrated genetically and pharmacologically, as FAAH KO mice or C57BL/6N WT mice treated with the FAAH inhibitor, URB597, have reportedly displayed anxiolytic-like behaviors in the elevated plus maze and light:dark box assays (Moeira *et al.* 2008). These relative increases in anandamide specifically, that lead to a reduced anxiety-like state, conveniently offer physiological support for its name, which was derived from the Sanskrit word for "bliss".

Since the mice can only be tested once in the light:dark box assay, we wanted to confirm this phenotype by testing mice in a second model capable of predicting anxiety-like behaviors: the marble burying assay. Again, a robust anxiolytic-like phenotype was observed in $CRIP_{1a}$ KO

compared to WT mice. Previous studies have investigated the role of the endogenous cannabinoid system in anxiety-like behaviors using the marble-burying assay and found that burying behavior was reduced after treatment with low doses (1 to 3 mg/kg) of cannabinoid agonists such as WIN or the FAAH inhibitors, URB597 and PF-3845 (Gomes *et al.* 2011; Kinsey *et al.* 2011). The *in vivo* results observed in our $CRIP_{1a}$ KO mice could be explained by a possible increase in endocannabinoid signaling due to the lack of negative regulation of $CB_1$ receptors by $CRIP_{1a}$. Our findings, combined with current reports in the literature, further support an anxiolytic role for endogenous cannabinoid signaling. Though it might seem unlikely that endocannabinoid ligands would be significantly altered by the loss of $CRIP_{1a}$, 2-AG and anandamide levels have yet to be measured in $CRIP_{1a}$ KO mice. It makes sense however, that without this negative regulatory protein present, endocannabinoids might be more effective at activating the $CB_1$ receptor and thus eliciting behaviors such as this anxiolytic-like phenotype. Particular interest for future studies would include treating $CRIP_{1a}$ KO mice acutely with specific catabolic enzyme inhibitors for FAAH and MAGL using compounds such as URB597 and JZL-184, respectively, as well as the new dual FAAH/MAGL enzyme inhibitor, JZL-185 (Long *et al*. 2009). Not only could these studies provide further insight into the role of, and alterations in endocannabinoid signaling in the absence of $CRIP_{1a}$ *in vivo*, but they might also pinpoint which, if either, ligand is primarily responsible for mediating the anxiolytic-like behaviors in $CRIP_{1a}$ KO mice.

The *ex vivo* findings of significantly increased $CB_1$ receptor-mediated G-protein activity within the amygdala of $CRIP_{1a}$ KO mice might also be playing a role in the observed anxiolytic-like phenotype (Results 3.5). These results showed that maximal activation of G-proteins by the synthetic cannabinoid agonist CP55,940 or the putative endocannabinoid NE was significantly

elevated in $CRIP_{1a}$ KO relative to WT mice. Moreover, $CB_1$ receptor expression was not altered in $CRIP_{1a}$ KO compared to WT mice in any of the regions examined, including the amygdala (Results 3.3). Together, these data suggest that the increases in G-protein activity are not due to a greater density in $CB_1$ receptors, but a greater signaling capacity of the available receptors. These data agree with our hypothesis that $CB_1$ receptor levels would remain unaltered and agonist-stimulated G-protein activity would increase, based on previous studies in our laboratory where overexpression of $CRIP_{1a}$ did not affect $CB_1$ receptor levels and attenuated agonist-stimulated activity. However, it is not completely certain whether enhanced $CB_1$ receptor-mediated G-protein activity in the amygdala is responsible for the anxiolytic-like phenotype seen in $CRIP_{1a}$ KO mice. Future studies will need to determine involvement of $CB_1$ receptors in this effect, for example, by administration of a $CB_1$ antagonist such as SR141716A or by breeding of dual $CB_1$ receptor/ $CRIP_{1a}$ null mice. Moreover, local infusion of $CB_1$ antagonist or siRNA-mediated $CB_1$ receptor knockdown in the amygdala could more selectively implicate altered $CB_1$ receptor signaling in this region as the mechanism of the anxiolytic-like phenotype.

Most reports suggest that the amygdala does play a role in stress and anxiety-like behaviors, though it is largely thought to be involved in anxiogenic behaviors (Onaivi *et al*. 1995; Patel *et al.* 2004). Observed in both animal models and humans, cannabinoid agonists produce bi-phasic effects with regard to anxiety in a dose-dependent manner, such that low doses are often anxiolytic, whereas higher doses are anxiogenic (Giuliani *et al*. 2000; Ashton, 1999). Rubino *et al.* (2008) attempted to determine which brain regions were responsible for the anxiogenic- and anxiolytic-like behaviors elicited by centrally injecting varying doses of cannabinoids. After administering low and high doses of THC directly into the basolateral amygdala of rats, results indicated that only one low dose (1 μg) elicited anxiogenic-like behaviors, while all other doses

produced no response. Assuming our agonist-stimulated [$^{35}$S]GTPγS binding results in the amygdala relate to and/or play a part in our findings in the marble burying and light:dark box assays, our data collectively suggest the opposite function of the amygdala with regard to cannabinoids and anxiety. There is however, a notable species difference between rats and mice in regard to dose-sensitivity to cannabinoid agonists, as one study showed that the $ED_{50}$ value of THC to induce anxiogenic-like behavior was three-fold lower in rats (Onaivi *et al.* 1990).

It is also important to note that the amygdala can be distinctly separated into subregions, each of which provides specific projection pathways to other brain regions (Figure 33) and is comprised of different neuronal populations. The basolateral amygdala (BLA) is primarily comprised of glutamatergic neurons, with estimates as high as 90%, whereas the central amygdala is reportedly comprised of 95% GABAergic medium spiny neurons (Tye *et al.* 2011; McDonald, 1982). The central amygdala (CeA) is also the primary output region, projecting to the brainstem and thought to be responsible for mediating behavioral responses associated with anxiety and fear (Davis, 2000; Krettek and Price, 1978). $CB_1$ receptors are expressed on a subset of cholecystokinin-positive (CCK) GABAergic neurons as well as glutamatergic pyramidal neurons within the BLA (McDonald and Mascagni, 2001). Activation of $CB_1$ receptors within this region attenuates GABAergic and glutamatergic neurotransmission via presynaptic inhibition (Azad *et al.* 2003). However, within the CeA, GABAergic transmission is not affected by $CB_1$ receptor activation (Katona *et al.* 2001). $CB_1$ KO mice have been shown to exhibit anxiogenic behaviors in the elevated plus maze test by spending less time in the open arms of the apparatus (Haller *et al.* 2002). Interestingly, this same study found that administration of SR141716A not only led to increases in anxiety-like behavior in WT mice, but also led to further increases in anxiety in $CB_1$ KO mice, suggesting the presence of a possible novel receptor for

SR141716A that plays a role in anxiogenic-like behaviors. Furthermore, $CB_1$ KO mice did not exhibit any anxiolytic-like behaviors, which supports the argument that activation of the $CB_1$ receptor by endocannabinoids leads to anxiolytic-like behaviors and agrees with our findings in $CRIP_{1a}$ KO mice. The role of $CRIP_{1a}$ in anxiolytic-like phenotypes is far from being completely understood, but offers a valuable new area of research regarding cannabinoids and anxiety-like behaviors.

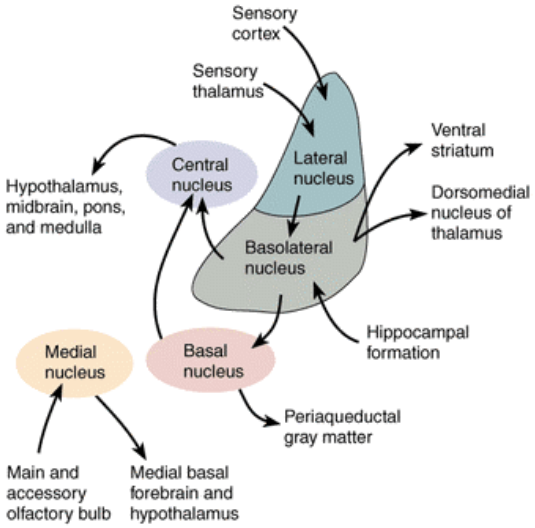


**Figure 32.** A schematic adapted from Tye *et al.* (2011) displaying the subnuclei of the amygdala and their respective projections within the amygdala, as well as to other brain regions. Primary input is received by the lateral amygdala from the cortex and thalamus, while primary output is mediated by the central amygdala to the hypothalamus and hindbrain. $CB_1$ receptors are highly expressed in the lateral and basal nuclei, while little-to-no expression is observed in the central and medial nuclei (Katona *et al*. 2001).

### 4.3 $CRIP_{1a}$ and Nociception.

Naïve $CRIP_{1a}$ KO mice displayed significantly longer latencies in the warm water tail withdrawal test at 52ºC, however similar differences in nociceptive sensitivity were not observed at other temperatures (48ºC and 56ºC) or in other measures such as the hot plate assay at 52ºC

and 56ºC. This restricted temperature range is not uncommon in mouse models of altered cannabinoid signaling, as Cravatt *et al.* (2001) found FAAH KO mice exhibited longer latencies in the hot plate assay at 56ºC only, but not at 54ºC or 58ºC. The same study also showed FAAH KO mice exhibited longer latencies compared to WT mice in the warm water tail withdrawal assay at 56ºC. These findings, along with our own results of antinociception in the $CRIP_{1a}$ KO mice, suggest that the endocannabinoid system plays a role in pain signaling pathways and thus pain thresholds. However, it is important to note that although the warm water tail withdrawal assay is considered a spinal measure of antinociception (Franklin *et al.* 1989; Lichtman *et al.* 1991), our [$^{35}$S]GTPγS binding data revealed no significant differences in $CB_1$ agonist-stimulated G-protein activity within the spinal cord of $CRIP_{1a}$ WT and KO mice. Thus, future studies using the antagonist, SR141716A, should be performed to determine whether the loss of $CRIP_{1a}$ affects spinally mediated nociception in a $CB_1$ receptor-dependent manner.

Stress-induced analgesia is a common caveat in behavioral tests requiring the mice to be handled and/or restrained, and has been shown to have an endocannabinoid-mediated mechanism (Connell *et al*. 2006; Kurrikoff *et al.* 2008). Additionally, stress-induced analgesia may be a result of signaling pathways originating from the BLA (Connell *et al*. 2006). As discussed earlier, this portion of the amygdala expresses high levels of $CB_1$ receptors, and our [$^{35}$S]GTPγS binding data showed increased $CB_1$ agonist-stimulated G-protein activity in the amygdala of $CRIP_{1a}$ KO mice. Therefore, the antinociception observed in $CRIP_{1a}$ KO mice could have been a result of a genotype-related difference in stress-induced analgesia and not due to the loss of $CRIP_{1a}$ in the spinal cord. While this is a possible interpretation, it is important to recognize that the projections from the BLA primarily terminate in the PAG, though some reports suggested projections could terminate in the dorsal horn of the spinal cord (Kurrikoff *et al*. 2008; Walker

and Hohmann, 2005). However, central administration of CP55,940 into the PAG has been shown to elicit antinociceptive effects in the tail-flick test in rats (Lichtman *et al.* 1996). We did not find a main effect of genotype in either baseline latencies (see Results 3.8) or latencies after CP55,940 administration (see Figure 26) in the hot plate assay, in which the PAG is also thought to play a role. Perhaps there are species differences regarding dose-sensitivity between rats and mice within the PAG, as there are in the amygdala, which could explain the lack of effects observed in $CRIP_{1a}$ KO mice. Furthermore, the PAG has yet to be investigated in $CRIP_{1a}$ KO mice, and assessments of both $CB_1$ receptor saturation binding and agonist-stimulated [$^{35}$S]GTPγS binding should be performed in the future to determine whether loss of $CRIP_{1a}$ affects $CB_1$ receptor expression or G-protein activation within the PAG.

**4.4 Implications That Expression of $CB_1$ Receptors Is Independent of $CRIP_{1a}$ Expression and Vice Versa.**

We examined the cerebellum, hippocampus and amygdala of $CRIP_{1a}$ KO mice for alterations in $CB_1$ receptor expression by performing [$^3$H]CP55,940 saturation binding assays. $CB_1$ receptor expression, as determined by [$^3$H]CP55,940 $B_{max}$ values, was found to not differ from that of $CRIP_{1a}$ WT mice in all regions examined (see Results 3.3). Our findings confirm that alterations in $CRIP_{1a}$ expression do not affect $CB_1$ receptor levels, as previous reports showed that over-expression of $CRIP_{1a}$ also did not affect $CB_1$ receptor expression (Niehaus *et al*. 2007). It should be noted that these studies reflect total receptor levels, since the assays are performed in total membrane fractions that were isolated by high-force centrifugation (at 50,000 x *g*) from tissue homogenates, and do not reflect changes in subcellular localization of receptors. Therefore, even though no differences have been detected in our receptor saturation binding assays thus far, there

could still be differences in $CB_1$ receptor densities at the plasma membrane *in vivo* and/or possible alterations in receptor internalization patterns within these regions that could result in altered $CB_1$ receptor signaling.

We also investigated $CRIP_{1a}$ expression in the cerebellum, prefrontal cortex and amygdala of $CB_1$ WT and KO mice after repeated vehicle and THC treatments. Since we had established that $CB_1$ receptor expression was not altered after either the loss or over-expression of $CRIP_{1a}$, this study was important to show the relationship between the loss of $CB_1$ receptors and $CRIP_{1a}$ expression, as well as the effects of prolonged THC treatment on $CRIP_{1a}$ expression, both in the presence and absence of $CB_1$ receptors. After Western immunoblots were analyzed, we found that neither the loss of $CB_1$ receptors, nor the prolonged activation of $CB_1$ receptors affects $CRIP_{1a}$ expression (see results 3.12). This study provided a first examination of whether chronic THC administration could directly affect $CRIP_{1a}$ expression, by analyzing THC-treated *Cnr1* WT and KO mice. In each of these cases, the results showed no significant differences in $CRIP_{1a}$ expression among treatments and genotypes. The fact that $CRIP_{1a}$ expression was not affected by any of these perturbations in $CB_1$ receptor expression or function could suggest an interpretation that $CRIP_{1a}$ has important roles in addition to negatively regulating the $CB_1$ receptor. Other receptor systems were not examined in these studies, but future studies should investigate alterations in receptors such as dopamine $D_2$ receptors. Previous reports suggested that alterations in $CB_1$ and $D_2$ receptor expression within the striatum inversely affected $CRIP_{1a}$ expression, such that when the expression of these receptors was reduced, $CRIP_{1a}$ expression increased, and vice versa (Blume *et al.* 2013). Since the striatum was not investigated in our studies, we do not yet know whether genetic disruption of $CB_1$ receptors or $CRIP_{1a}$ can alter each other's expression in this brain region. However, future experiments could be performed to

determine whether alterations in $CB_1$ receptor expression or activation can affect $CRIP_{1a}$ expression, or if $CRIP_{1a}$ deletion affects $CB_1$ receptor expression or activity, in the striatum and other CNS regions not examined in the present studies.

### 4.5 Interpretations for the Lack of Effects in the Cerebellum and Hippocampus After Global, Life-Long Absence of $CRIP_{1a}$.

Our [$^{35}$S]GTPγS binding results indicated no differences between $CRIP_{1a}$ WT and KO mice in the cerebellum, hippocampus or spinal cord. This result was supported by *in vivo* evidence gathered by testing $CRIP_{1a}$ WT, HET and KO mice in a cumulative dosing tetrad assessment with CP55,940, where no significant differences were observed. The results obtained were not expected, as our hypothesis was that $CRIP_{1a}$ KO mice might exhibit exaggerated responses to cannabinoid agonists in CNS regions where $CB_1$ receptors and $CRIP_{1a}$ are co-distributed. Though we did not evaluate behaviors known to involve the hippocampus, such as learning and memory, we were somewhat surprised that loss of $CRIP_{1a}$ did not affect agonist-stimulated G-protein activity given previous results obtained in autaptic hippocampal neurons, which showed that over-expression of $CRIP_{1a}$ attenuated 2-AG-mediated DSE and decreased inhibition of excitatory post-synaptic currents. However, if $CB_1$ receptors and $CRIP_{1a}$ are not normally expressed in the same cells or subcellular elements in the hippocampus, this could potentially explain the lack of effect of $CRIP_{1a}$ KO on $CB_1$ receptor-mediated G-protein activation.

The fact that $CB_1$ agonist-stimulated G-protein activity did not differ between $CRIP_{1a}$ WT and KO mice within the cerebellum could offer some explanation for the lack of effects of genotype on motor activity and RotaRod performance, but [$^{35}$S]GTPγS binding experiments need to be performed in the striatum of all genotypes in order to gain a better understanding of how

these particular motor behaviors might be affected by deletion of $CRIP_{1a}$. An analysis of the fitted curves in Figure 13 showed that the KO mice display slightly less G-protein activity in the cerebellum in response to CP55,940, which was significant by two-way ANOVA. One interpretation could be that a greater fraction of $CB_1$ receptors were uncoupled from G-proteins due to prolonged over-activation of $CB_1$ receptors in $CRIP_{1a}$ KO mice, which might account for the results we observed. Studying the $CRIP_{1a}$ HET mice in more detail will be a valuable tool in determining how a reduction in $CRIP_{1a}$ expression affects the system compared to a complete abolishment as seen in the KO mice. Different results could be obtained in HET mice because less compensation might be expected to occur relative to KO mice. If $CRIP_{1a}$ KO mice experience a global, life-long abolishment of $CRIP_{1a}$, it is possible that $CB_1$ receptors are continuously dysregulated and over-active in some brain regions. Often times, the cell compensates for this over-activation by increasing receptor internalization and desensitization. We know that $CRIP_{1a}$ KO mice are not exhibiting $CB_1$ receptor downregulation, as shown by our [$^3$H]CP55,940 saturation binding results. However, what we do not know is the subcellular localization of these receptors *in vivo*. There is evidence to suggest that knock-down of $CRIP_{1a}$ in the N18TG2 cell line increases $CB_1$ receptor densities at the plasma membrane, while over-expression of $CRIP_{1a}$ leads to increased $CB_1$ receptor internalization, as determined by co-immunoprecipitation studies (Blume *et al.* 2013a). It is possible that $CRIP_{1a}$ KO mice may initially exhibit greater $CB_1$ receptor densities at the plasma membrane, and thus potentially be subjected to increased activation via endocannabinoids, and eventually, desensitization and internalization. The same study also found that exposure to WIN led to $CB_1$ receptor internalization in both control and $CRIP_{1a}$ knock-down cells, while receptor externalization was observed in the $CRIP_{1a}$ over-expressing cells. This effect could explain why under agonist-

stimulated conditions, both *in vivo* and *ex vivo*, we did not see any genotype-related differences in regions such as the cerebellum. Since these studies were performed in a cell line, which does not exactly replicate *in vivo* conditions, similar studies should be repeated in various brain regions of $CRIP_{1a}$ WT and KO mice to reveal effects on $CB_1$ receptor trafficking patterns that result from the loss of $CRIP_{1a}$. However, such experiments would be difficult to perform because $CB_1$ receptors are largely localized on axonal projections and terminals, so $CB_1$ receptor subcellular localization would have to be studied using electron microscopy. Furthermore, temporally controlled conditional $CRIP_{1a}$ KO mice could be developed to reduce the potential for compensation in specific brain regions. In addition, *in vivo* tools such as central injections of siRNA could aid in determining the effects of $CRIP_{1a}$ knockdown, but not deletion, in specific brain regions, thus providing a complementary approach to investigating $CRIP_{1a}$ functions when compared to observing the $CRIP_{1a}$ HET mice we possess currently.

Though there is some evidence of $CRIP_{1a}$ and $CB_1$ receptor co-localization within the cerebellum on granule cell terminals (K. Sayers and D.E. Selley, unpublished results), other regions have not yet been investigated. It should be noted that while some regions have been shown to express both $CRIP_{1a}$ and $CB_1$ receptors, such as the prefrontal cortex and the hippocampus, perhaps these two do not co-localize in the same cells. Cellular trafficking of $CRIP_{1a}$ has not been well established and it is possible that $CB_1$ receptors and $CRIP_{1a}$ are not distributed the same area of the cell, even where they are co-expressed by the same cells. Future studies should examine various brain regions for evidence of $CRIP_{1a}$:$CB_1$ receptor co-localization. In particular, the amygdala (where we did observe genotype-related differences) and hippocampus (where we did not observe any differences between genotypes) should be investigated to unmask possible explanations for the opposite results observed in our studies.

Lastly, the possibility of redundancy should not be dismissed. The existence of $CRIP_{1a,}$ and one of its known functions, was discovered somewhat indirectly by earlier studies conducted by Nie and Lewis (2001) that focused on mutational analysis of the $CB_1$ receptor. When an alteration in $CB_1$ receptor function was observed after deleting a portion of the C-terminus, the search for a regulatory protein was initiated. It is possible that an as yet undiscovered protein exists in mice that is capable of producing similar functions to $CRIP_{1a}$. If this is the case, perhaps it is only expressed in specific brain regions or co-localized with $CB_1$ receptors in particular regions, accounting for a subset of our results where we did not observe significant differences between genotypes. Although the initial yeast two-hybrid screening results did not reveal additional proteins that bound to distal C-terminus of the $CB_1$ receptor (Niehaus *et al.* 2007), it does not eliminate the possibility that another protein could bind to another intracellular portion of the $CB_1$ receptor and elicit effects that mimic $CRIP_{1a}$ function.

### 4.6 Interpretation of the Lack of Effects of $CRIP_{1a}$ KO on SR141716A-Mediated Inhibition of [$^{35}$S]GTPγS Binding in the CNS.

We did not observe substantial constitutive $CB_1$ receptor activity in either $CRIP_{1a}$ WT or KO mice using a single concentration of SR141716A that was found to be maximally effective to inhibit constitutive $CB_1$ receptor activity in cell lines. Because $CRIP_{1a}$ inhibits constitutive $CB_1$ receptor activity in cell models, we predicted enhanced constitutive activity of $CB_1$ receptors in multiple brain region of CRIP1a KO mice, which would be observed by greater SR141716A-mediated inhibition of [$^{35}$S]GTPγS binding. In the cerebellum, modest SR141716A-mediated inhibition was seen, but did not differ WT and KO mice. These results are consistent with the lack of effect of $CRIP_{1a}$ deletion on agonist-stimulated G-protein activity in this region.

However, inhibition of basal [$^{35}$S]GTPγS binding by this inverse agonist was minimal or not observed in other CNS regions, including amygdala, hippocampus and spinal cord. These results were essentially consistent with previous studies, as constitutive activity of cannabinoid receptors has traditionally been difficult to measure in the brain. Cerebellar homogenates from rat brain have been investigated in search of constitutively active $CB_1$ receptors, but the results indicated that the inhibitory actions of SR141716A were maximal at μM concentrations, and were therefore either not $CB_1$ receptor-mediated or were mediated by allosteric site on $CB_1$ receptors (Sim-Selley *et al.* 2001). The finding that significant inhibition of basal [$^{35}$S]GTPγS binding was not seen at inverse agonist concentrations that antagonized $CB_1$ agonist-induced activity suggest that $CB_1$ receptor constitutive activity in these membranes was not detectable under the conditions of the [$^{35}$S]GTPγS binding assay. In fact, μM concentrations of SR141716A have also been shown to exhibit inhibitory effects on basal [$^{35}$S]GTPγS binding even in $CB_1$ receptor KO mice (Breivogel *et al*. 2001), further suggesting that these concentrations are not relevant for measuring inhibition of $CB_1$ receptor-mediated activity. Thus, our results further indicate that constitutive $CB_1$ receptor activity is minimal or that the [$^{35}$S]GTPγS approach is not optimal for evaluating constitutive activity of $CB_1$ receptors in the brain.

**4.7 Conclusions.**

The results gathered in this thesis have revealed important and novel information regarding $CRIP_{1a}$ by employing a loss of function model through a new knockout mouse line. Our data provide new lines of evidence that $CRIP_{1a}$, a putative new member of the endogenous cannabinoid system, plays an essential role in anxiety-like phenotypes. The data also revealed that the previously determined role of $CRIP_{1a,}$ to negatively regulate $CB_1$ receptor-mediated G-

protein signaling was upheld by our [$^{35}$S]GTPγS binding results in the amygdala of $CRIP_{1a}$ KO mice, which revealed increased agonist-stimulated G-protein activity. Whether this enhancement of $CB_1$ receptor signaling in the amygdala is responsible for the anxiolytic-like phenotype that was observed in $CRIP_{1a}$ KO mice in vivo is a matter to be resolved by future research. In addition, we have shown that the expression of $CRIP_{1a}$ and $CB_1$ receptors is independent of one another in brain regions investigated thus far. We now have a greater appreciation for the potential roles of $CRIP_{1a}$ *in vivo*, as our studies were the first investigation of $CRIP_{1a}$ function to be performed in live animals. Our exciting findings suggest that $CRIP_{1a}$ could be a key player in the endocannabinoid system and could serve as a promising future pharmacological target for studying and treating anxiety disorders.

## List of References


Ango F., L. Prezeau, T. Muller, J. C. Tu, B. Xiao, P. F. Worley, J. P. Pin, J. Bockaert, and L. Fagni (2001). "Agonist-independent activation of metabotropic glutamate receptors by the intracellular protein Homer." Nature **411**:962–65**.**

Ashton, C. H. (1999). "Adverse effects of cannabis and cannabinoids." Br J Anaesth **83**: 637–49.

Atwood, B.K., J. Huffman, A. Straiker and K. Mackie (2010). "JWH018, a common constituent of 'Spice' herbal blends, is a potent and efficacious CB1 receptor agonist." Br J Pharmacol **160:**585-93.

Azad, S.C., M. Eder, G. Marsicano, B. Lutz, W. Zieglgansberger and G. Rammes (2003). "Activation of the cannabinoid receptor type 1 de- creases glutamatergic and GABAergic synaptic transmission in the lateral amygdala of the mouse." Learn Mem **10**:116-28.

Bambico, F. R., N. Katz, G. Debonnel and G. Gobbi (2007). "Cannabinoids elicit antidepressant-like behavior and activate serotonergic neurons through the medial prefrontal cortex." J Neurosci **27:**11700-11.

Barad, M., P. Gean and B. Lutz (2006). "The Role of the Amygdala in the Extinction of Conditioned Fear." Biological Psychiatry 60: 322–28.

Bayewitch, M., M. H. Rhee, T. Avidor-Reiss, A. Breuer, R. Mechoulam and Z. Vogel (1996). "(−)-Delta9-tetrahydrocannabinol antagonizes the peripheral cannabinoid receptor-mediated inhibition of adenylyl cyclase." J Biol Chem, **271**:9902–5.

Blume L. C., C. E. Bass, G. D. Dalton, D. E. Selley and A. C. Howlett (2010). "Cannabinoid Receptor Interacting Protein (CRIP) 1a: Signal Transduction and Epigenetic Phenomena." Symposium on the Cannabinoids **20:**3-30.

Blume, L. C., C. E. Bass, S. R. Childers, G. D. Dalton, D. C. S. Roberts, J. M. Richardson, R. Xiao, D. E. Selley and A. C. Howlett (2013). "Striatal $CB_1$ and $D_2$ receptors regulate expression of each other, CRIP1A and delta opioid systems." J Neurochem, **124**:808-20.

Blume, L. C., G. D. Dalton, D. E. Selley and A. C. Howlett (2013a). "Cannabinoid receptor interacting protein 1a (CRIP1a) regulates CB1 receptor trafficking." FASEB J **27**: 1173.11

Bohn, L. M. (2009). "Selectivity for G protein or arrestin-mediated signaling. Functional Selectivity of G Protein-Coupled Receptor Ligands (K. Neve, ed.) Humana Press: 71-85.

Bouaboula M., Poinot-Chazel, B. Bourrie, X. Canat, B. Calandra, M. Rinaldi-Carmona, G. LeFur and P. Casellas (1995). "Activation of mitogen-activated protein kinases by stimulation of the central cannabinoid receptor CB1." Biochem J **312**: 637–41.

Bouaboula, M., S. Perrachon, L. Milligan, X. Canat, M. Rinaldi-Carmona, M. Portier, F. Barth, B. Calandra, F. Pecceu, J. Lupker, J. P. Maffrand, G. Le Fur and P. Casellas (1997). "A selective inverse agonist for central cannabinoid receptor inhibits mitogen-activated protein kinase activation stimulated by insulin or insulin-like growth factor 1. Evidence for a new model of receptor/ligand interactions." J Biol Chem **272**(35): 22330-9.

Bourin, M. and M. Hascoët (2003). "The mouse light/dark box test." Eur J Pharmacol **463**: 55–65.

Bradford, M. M. (1976). "A rapid and sensitive method for the quantitation of microgram quantities of protein utilizing the principle of protein-dye binding." Anal Biochem **72:** 248-54.

Braestrup, C., M. Nielsen, T. Honore, L. H. Jensen and E. N. Petersen (1983). "Benzodiazepine receptor ligands with positive and negative efficacy." Neuropharmacology 22: 1451-57.

Braun, K., Ziabreva, I., Poeggel, G., and R. Schnabel (2003). "Separation-Induced Receptor Changes in the Hippocampus and Amygdala of Octodon degus: Influence of Maternal Vocalizations." J Neurosci **23**: 5329–36.

Breivogel, C.S., D.E. Selley and S.R. Childers (1998). "Cannabinoid receptor agonist efficacy for stimulating [$^{35}$S]GTPgS binding to rat cerebellar membranes correlates with agonist-induced decreases in GDP affinity." J Biol Chem, **273:** 16865–73.

Breivogel, C. S., S. R. Childers, S. A. Deadwyler, R. E. Hampson, L. J. Vogt and L. J. Sim-Selley (1999). "Chronic $\Delta^9$-Tetrahydrocannabinol Treatment Produces a Time-Dependent Loss of Cannabinoid Receptors and Cannabinoid Receptor-Activated G Proteins in Rat Brain." J Neurochem **73**: 2447–59.

Buczynski, M. W. and L. H. Parsons (2010). "Quantification of brain endocannabinoid levels: methods, interpretations and pitfalls." Br J Pharmacol. **160**(3): 423-42.

Cabral G.A. and F. Marciano-Cabral (2005). "Cannabinoid receptors in microglia of the central nervous system: Immune functional relevance." J Leukoc Biol, **78:**1192-97.

Carlisle S.J., F. Marciano-Cabral, A. Staab, C. Ludwick, G.A. Cabral (2002). "Differential expression of the CB2 cannabinoid receptor by rodent macrophages and macrophage-like cells in relation to cell activation." Int Immunopharmacol, **2:**69-82.

Colombo, G., R. Agabio, G. Diaz, C. Lobina, R. Reali and G. L. Gessa (1998). "Appetite suppression and weight loss after the cannabinoid antagonist SR 141716." Life Sci **63**:113-7.

Compton D., M. Aceto, J. Lowe and B. Martin (1996). "In vivo characterization of a specific cannabinoid receptor antagonist (SR141716A): Inhibition of $\Delta^9$-tetrahdrocannabinol-induced responses and apparent agonist activity." J. Pharmacol Exp Ther, **277**:586-94.

Connell, K., N. Bolton, D. Olsen, D. Piomelli and A. G. Hohmann (2006). "Role of the basolateral nucleus of the amygdala in endocannabinoid-mediated stress-induced analgesia." Neuroscience letters **397**: 180-4.

Costa T. and A. Hertz (1989). "Antagonists with negative intrinsic activity at **δ** opioid receptors coupled to GTP-binding proteins." Proc Natl Acad Sci **86**:7321–25.

Cravatt B. F., D. K. Giang, S. P. Mayfield, D. L. Boger, R. A. Lerner and N. B. Gilula (1996). "Molecular characterization of an enzyme that degrades neuromodulatory fatty-acid amides." Nature **384**:83-7.

Cravatt, B. F., K. Demarest, M. P. Patricelli, M. H. Bracey, D. K. Giang, B. R. Martin and A. H. Lichtman (2001). "Supersensitivity to anandamide and enhanced endogenous cannabinoid signaling in mice lacking fatty acid amide hydrolase." Proc Natl Acad Sci **98**: 9371-76.

Cravatt, B.F. and A. H. Lichtman (2003). "Fatty acid amide hydrolase: an emerging therapeutic target in the endocannabinoid system." Curr Opin Chem Biol **7**:469–75.

Crawley, J. N. and F. K. Goodwin (1980). "Preliminary report of a simple animal behaviour for the anxiolytic effects of benzodiazepines." Pharmacol Biochem Behav **13**: 167–70.

Crawley, J.N. and L.G. Davis (1982). "Base line exploratory activity predicts anxiolytics responsiveness to diazepam in five mouse strains." Brain Res Bull **8**: 609–12.

Crawley, J.N., R. L. Corwin, J. K. Robinson, C. C. Felder, W. A. Devane and J. Axelrod (1993). "Anandamide, an endogenous ligand of the cannabinoid receptor, induces hypomotility and hypothermia in vivo in rodents." Pharmacol Biochem and Behav **46:** 967–72.

Davidson, R. J. (2002). "Anxiety and affective style: role of prefrontal cortex and amygdala." Biological Psychiatry **51**:68–80.

Davis W. M., J. E. Moreton, W. T. King and H. B. Pace (1972). "Marihuana on locomotor activity: biphasic effect and tolerance development." Res Commun Chem Pathol Pharmacol **3**:29–35.

Davis, M (2000). "The Amygdala: A Functional Analysis." (Aggleton, J.P., ed.) Oxford Univ. Press: 213–288

Day, J., G. Damsma and H.C. Fibiger (1991). "Cholinergic activity in the rat hippocampus, cortex and striatum correlates with locomotor activity: An in vivo microdialysis study." Pharmacol Biochem and Behav **38**: 723–29.

Deacon, R. M. J. (2013). “Measuring motor coordination in mice.” J Vis Exp **75**: e2609-e2609.

de Ligt R.A., A.P. Kourounakis and A. P. IJzerman (2000). “Inverse agonism at G protein-coupled receptors: (patho)physiological relevance and implications for drug discovery.” Br J Pharmacol **130**:1–12.

DeLong, G. T, C. E. Wolf, A. Poklis and A. H. Lichtman (2010). “Pharmacological evaluation of the natural constituent of Cannabis sativa, cannabichromene and its modulation by $\Delta^9$-tetrahydrocannabinol.” Drug and Alcohol Dependence **112**:126–33.

DeSanty, K. P. and M. Saeed Dar (2001). “Cannabinoid-induced motor incoordination through the cerebellar $CB_1$ receptor in mice.” Pharmacol Biochem and Behav **69**: 251–59.

Devane, W. A., F. A. Dysarz, 3rd, M. R. Johnson, L. S. Melvin and A. C. Howlett (1988). "Determination and characterization of a cannabinoid receptor in rat brain." Mol Pharmacol, **34**(5): 605-13.

Devane, W. A., L. Hanus, A. Breuer, R. G. Pertwee, L. A. Stevenson, G. Griffin, D. Gibson, A. Mandelbaum, A. Etinger and R. Mechoulam (1992). "Isolation and structure of a brain constituent that binds to the cannabinoid receptor." Science, **258**(5090): 1946-9.

Dewey, W.L. (1986). “Cannabinoid pharmacology.” Pharmacol Rev, **38**:151–78

Dinh T. P., D. Carpenter, F. M. Leslie, T. F. Freund, I. Katona, S. L. Sensi, S. Kathuria and D. Piomelli (2002). "Brain monoglyceride lipase participating in endocannabinoid inactivation". Proc Natl Acad Sci, **99** (16): 10819–24.

El-Alfy, A. T., K. Ivey, K. Robinson, S. Ahmed, M. Radwan, D. Slade, I. Khan, M. ElSohly and S. Ross (2010). “Antidepressant-like effect of $\Delta^9$-tetrahydrocannabinol and other cannabinoids isolated from cannabis sativa L.” Pharmacol Biochem and Behav, 95(4): 434–42.

ElSohly, M. A. and D. Slade (2005). “Chemical constituents of marijuana: the complex mixture of natural cannabinoids.” Life sciences **78**:539-48.

Elphick, M. R. and M. Egertova (2001). "The neurobiology and evolution of cannabinoid signaling." Philos Trans R Soc Lond B Biol Sci **356**: 381–408.

Felder, C. C., K. E. Joyce, E. M. Briley, J. Mansouri, K. Mackie, O. Blond, Y. Lai, A. L. Ma and R. L. Mitchell (1995). "Comparison of the pharmacology and signal transduction of the human cannabinoid CB1 and CB2 receptors." Mol Pharmacol, **48**(3): 443-50.

File, S. E. (2001). “Factors controlling measures of anxiety and responses to novelty in the mouse.” Behav Brain Res, **125**:151–57.

Franklin, K. B. J. and F. V. Abbott (1990). "Techniques for assessing the effects of drugs on nociceptive responses." Psychopharmacology, Humana Press: 145-216.

Fride, E. (2002). “Endocannabinoids in the central nervous system – an overview.” Prostaglandins, Leukotrienes and Essential FattyAcids, **66**: 221-33.

Fride, E. and R. Mechoulam (2003). “New advances in the identification and physiological role of the different components of the endogenous cannabinoid system.” Molecular Biology of Drug Addiction (Maldonado, R., ed.) Humana Press: 173-198.

Gaoni, Y. and R. Mechoulam (1964). “Isolation, structure, and partial synthesis of an active constituent of hashish.” J. Am. Chem. Soc. **86**:1646–47.

Gatley, S. J., R. Lan, B. Pyatt, A. N. Gifford, N. D. Volkow and A. Makriyannis (1997). "Binding of the non-classical cannabinoid CP 55,940, and the diarylpyrazole AM251 to rodent brain cannabinoid receptors." Life Sci **61**(14): 191-7.

Gérard, C.M., C. Mollereau, G. Vassart and M. Parmentier (1991). “Molecular cloning of a human cannabinoid receptor which is also expressed in testis.” J Biochem **279**:129-34.

Gilman, A.G. (1987). “G Proteins: Transducers of receptor-generated signals.” Ann. Rev. Biochem. **56**:615-49.

Gomes, F. V., P. C. Casarotto, L. B. M. Resstel and F. S. Guimarães (2011). “Facilitation of CB1 receptor-mediated neurotransmission decreases marble burying behavior in mice.” Prog Neuropsychopharmacol Biol Psychiatry **35:** 434–38.

Gomez, R., M. Navarro, B. Ferrer, J. M. Trigo, A. Bilbao, I. Del Arco, A. Cippitelli, F. Nava, D. Piomeli and F. Rodriguez (2002). “A peripheral mechanism for CB1 cannabinoid receptor-dependent modulation of feeding.” J Neurosci **21**: 9612-17.

Griffin, G., P. J. Atkinson, V. M. Showalter, B. R. Martin and M. E. Abood (1998). "Evaluation of cannabinoid receptor agonists and antagonists using the guanosine-5′-O-(3-[35S] thio)-triphosphate binding assay in rat cerebellar membranes." J Pharmacol Exp Ther **285**: 553-60.

Giuliani, D., F. Ferrari and A. Ottani (2000). “The cannabinoid agonist HU 210 modifies rat behavioural responses to novelty and stress.” Pharmacol Res **41**: 47–53.

Haller, J., N. Bakos, M. Szirmay, C. Ledent and T. F. Freund (2002). “The effects of genetic and pharmacological blockade of the CB1 cannabinoid receptor on anxiety.” Eur J of Neurosci **16**: 1395–98.

Hammond, D. L. (1986). “Control systems for nociceptive afferent processing.” Spinal Afferent Processing (Yaksh, T. L., ed.) Springer US: 363-90.

Hampson, R.E. and S. A. Deadwyler (2000). “Cannabinoids reveal the necessity of hippocampal neural encoding for short-term memory in rats.” J Neurosci **20**: 8932–42.

Hanuš, L., S. Abu-Lafi, E. Fride, A. Breuer, Z. Vogel, D. E. Shalev, I. Kustanovich and R. Mechoulam (2001). "2-Arachidonyl glyceryl ether, an endogenous agonist of the cannabinoid CB1 receptor." Proc Natl Acad Sci **98**: 3662-65.

Herkenham, M., A. B. Lynn, M. R. Johnson, L. S. Melvin, B. R. de Costa and K. C. Rice (1991). "Characterization and localization of cannabinoid receptors in rat brain: a quantitative in vitro autoradiographic study." J Neurosci **11**(2): 563-83.

Hollister, L.E. (1986). "Health aspects of cannabis." Pharmacol. Rev. **38**: 1–20

Howlett, A.C. (1985). "Cannabinoid inhibition of adenylate cyclase. Biochemistry of the response in neuroblastoma cell membranes." Mol Pharmacol **27**: 429-36.

Howlett, A. C., J. M. Qualy and L. L. Khachatrian (1986). "Involvement of Gi in the inhibition of adenylate cyclase by cannabimimetic drugs." Mol Pharmacol **29(3):**307-13.

Howlett, A.C., T.M. Champion, G.H. Wilken, and R. Mechoulam (1990). "Stereochemical effects of 11-OH-delta 8-tetrahydrocannabinol-dimethylheptyl to inhibit adenylate cyclase and bind to the cannabinoid receptor." Neuropharmacology **29**:161-65.

Howlett, A. C. (1995). "Pharmacology of cannabinoid receptors." Annu Rev Pharmacol Toxicol **35**:607–34.

Howlett, A. C. (2002). "The cannabinoid receptors." Prostaglandins Other Lipid Mediat **68-69**:619- 31.

Hsieh, C., S. Brown, C. Derleth and K. Mackie (1999). "Internalization and recycling of the CB1 cannabinoid receptor." J Neurochem **73:** 493-501.

Hu S., A. Arnold, J. M. Hutchens, J. Radicke, B. F. Cravatt, J. Wager-Miller, K. Mackie and A. Straiker (2010). "Architecture of cannabinoid signaling in mouse retina." J Comp Neurol **518**:3848–66.

Jin, W., S. Brown, J. P. Roche, C. Hsieh, J. P. Celver, A. Kovoor, C. Chavkin and K. Mackie (1999). "Distinct domains of the CB1 cannabinoid receptor mediate desensitization and internalization." J Neurosci **19**: 3773-3780.

Katona, I., E. A. Rancz, L. Acsady, C. Ledent, K. Mackie, N. Hajos et al (2001). "Distribution of CB1 cannabinoid receptors in the amygdala and their role in the control of GABAergic transmission." J Neurosci **21**: 9506–18.

Katona, I. and T. F. Freund (2008). "Endocannabinoid signaling as a synaptic circuit breaker in neurological disease." Nat Med **14**: 923–30.

Kearn, C. S., M. J. Greenberg, R. DiCamelli, K. Kurzawa and C. J. Hillard (1999). "Relationships Between Ligand Affinities for the Cerebellar Cannabinoid Receptor CB1 and the Induction of GDP/GTP Exchange." J Neurochem **72**: 2379–87.

King, L., C. Carpentier, and P. Griffiths (2005). “Cannabis potency in Europe.” Addiction **100:** 884–86.

Kinsey, S. G., S. T. O'Neal, J. Z. Long, B. F. Cravatt and A. H. Lichtman (2011). “Inhibition of endocannabinoid catabolic enzymes elicits anxiolytic-like effects in the marble burying assay.” Pharmacol Biochem and Behav **98**: 21–7.

Kodirov, S. A., J. Jasiewicz, P. Amirmahani, D. Psyrakis, K. Bonni, M. Wehrmeister and B. Lutz (2010). "Endogenous cannabinoids trigger the depolarization-induced suppression of excitation in the lateral amygdala." Learn Mem **17**: 43-9.

Korzekwa, A. J., M. M. Bah, A. Kurzynowski, K. Lukasik, A. Groblewska and D. J. Skarzynski (2010). "Leukotrienes modulate secretion of progesterone and prostaglandins during the estrous cycle and early pregnancy in cattle: an in vivo study." Reproduction **140**: 767-76.

Krettek, J. E. and J. L. Price (1978). “A description of the amygdaloid complex in the rat and cat with observations on intra-amygdaloid axonal connections.” J Comp Neurol **178**: 255–79.

Kurrikoff, K., J. Inno, T. Matsui and E. Vasar (2008). “Stress-induced analgesia in mice: evidence for interaction between endocannabinoids and cholecystokinin.” Eur J of Neurosci **27**: 2147–55.

Kuster, J. E., J. I. Stevenson, S. J. Ward, T. E. D'Ambra and D. A. Haycock (1993). "Aminoalkylindole binding in rat cerebellum: selective displacement by natural and synthetic cannabinoids." J Pharmacol Exp Ther **264**(3): 1352-63.

Landsman R.S., T. H. Burkey, P. Consroe, W. R. Roeske and H. I. Yamamura (1997). “SR141716A is an inverse agonist at the human cannabinoid CB1 receptor.” Eur J Pharmacol **334**: R1–R2.

Lefkowitz, R. J., S. Cotecchia, P. Samama and T. Costa (1993). “Constitutive activity of receptors coupled to guanine nucleotide regulatory proteins.” Trends in Pharmacological Sciences **14:** 303-7.

Leggett, T. and T. Pietschmann (2008). "Global cannabis cultivation and trafficking." EMCDDA MONOGRAPHS 189.

Lévénès, C., H. Daniel, P. Soubrié and F. Crépel. "Cannabinoids decrease excitatory synaptic transmission and impair long-term depression in rat cerebellar Purkinje cells." J physiol **510**: 867-79.

Litchman, A. H. and B. R. Martin (1991). “Spinal and supraspinal components of cannabinoid-induced antinociception.” J Pharmacol Exp Ther **258:**517–23.

Lichtman, A. H., S. A. Cook and B. R. Martin. (1996). "Investigation of brain sites mediating cannabinoid-induced antinociception in rats: evidence supporting periaqueductal gray involvement." J Pharmacol Exp Ther **276**: 585-93.

Little, P. J., D. R. Compton, M. R. Johnson, L. S. Melvin and B. R. Martin (1988). "Pharmacology and stereoselectivity of structurally novel cannabinoids in mice." J Pharrnacol Exp Ther **247**:1046-51.

Long, J. Z., D. K. Nomura, R. E. Vann, D. M. Walentiny, L. Booker, X. Jin, J. J. Burston, L. J. Sim-Selley, A. H. Lichtman, J. L. Wiley and B. F. Cravatt (2009). "Dual blockade of FAAH and MAGL identifies behavioral processes regulated by endocannabinoid crosstalk in vivo." Proc Natl Acad Sci **106:** 20270-75.

Lopez-Rubalcava, C., A. Saldivar and A. Fernandez-Guasti (1992). "Interaction of GABA and serotonin in the anxiolytic action of diazepam and serotonergic anxiolytics." Pharmacol Biochem Behav **43**: 433–440.

Mackie, K. and B. Hille (1992). "Cannabinoids inhibit N-type calcium channels in neuroblastoma-glioma cells." Proc Natl Acad Sci **89**: 3825-29.

MacLennan, S. J., P. H. Reynen, J. Kwan and D. W. Bonhaus (1998). "Evidence for inverse agonism of SR141716A at human recombinant cannabinoid CB1 and CB2 receptors." Br J Pharmacol **124**: 619–22.

Marr, D. (1969). "A theory of cerebellar cortex". J Physiol **202**: 437–70.

Martin, B. R., R. L. Balster, R. K. Razdan, L. S. Harris and W. L. Dewey (1981). "Behavioral comparisons of the stereoisomers of tetrahydrocannabinols." Life Sci **29**: 565-74.

Martin, W. J., P. O. Coffin, E. Attias, M. Balinsky, K. Tsou and J. M. Walker (1999). "Anatomical basis for cannabinoid-induced antinociception as revealed by intracerebral microinjections." Brain Research **822**: 237–42.

Martini, L, D. Thompson, V. Kharazia and J. L. Whistler (2010). "Differential regulation of behavioral tolerance to WIN55, 212-2 by GASP1." Neuropsychopharmacology **35**: 1363-73.

Matsuda, L. A., S. J. Lolait, M. J. Brownstein, A. C. Young and T. I. Bonner (1990). "Structure of a cannabinoid receptor and functional expression of the cloned cDNA." Nature **346**(6284): 561-4.

McDonald, A.J. (1982). "Cytoarchitecture of the central amygdaloid nucleus of the rat." J Comp Neurol **208**: 401–18.

McDonald, A. J. (1982). "Neurons of the lateral and basolateral amygdaloid nuclei: a Golgi study in the rat." J Comp Neurol **212**:293–312.

McDonald, A. J. and F. Mascagni (2004). "Parvalbumin-containing interneurons in the basolateral amygdala express high levels of the α1 subunit of the GABAA receptor." J Comp Neurol **473**: 137-46.

Mechoulam, R., S. Ben-Shabat, L. Hanus, M. Ligumsky, N. E. Kaminski, A. R. Schatz, A. Gopher, S. Almog, B. R. Martin, D. R. Compton and et al. (1995). "Identification of an endogenous 2-monoglyceride, present in canine gut, that binds to cannabinoid receptors." Biochem Pharmacol **50**(1): 83-90.

Milvae, R. A. and W. Hansel (1983). "Prostacyclin, prostaglandin F2 alpha and progesterone production by bovine luteal cells during the estrous cycle." Biol Reprod **29**: 1063-68.

Mir, A, A. Obafemi, A. Young and C. Kane (2011). "Myocardial infarction associated with use of the synthetic cannabinoid k2." Pediatrics **128**: 1622–27.

Moreira, F. A., N. Kaiser, K. Monory and B. Lutz (2008). "Reduced anxiety-like behaviour induced by genetic and pharmacological inhibition of the endocannabinoid-degrading enzyme fatty acid amide hydrolase (FAAH) is mediated by CB1 receptors." Neuropharmacology **54**:141–50.

Montero, C., Campillo, N.E., Goya, P., and J. A. Páez (2005). "Homology models of the cannabinoid CB1 and CB2 receptors. A docking analysis study." Eur. J. Med. Chem. **40**: 75–83.

Moore, R. J., R. Xiao, L. J. Sim-Selley and S. R. Childers (2000). "Agonist-stimulated [$^{35}$S] GTPγS binding in brain: Modulation by endogenous adenosine." Neuropharmacology **39**: 282-89.

Mukhopadhyay, S. and A. C. Howlett (2001). "$CB_1$ receptor-G protein association. Subtype selectivity is determined by distinct intracellular domains." Eur J Biochem **268**(3): 499-505.

Müller, H., W. Sperling, M. Köhrmann, H. Huttner, J. Kornhuber, J. Maler (2010). "The synthetic cannabinoid Spice as a trigger for an acute exacerbation of cannabis induced recurrent psychotic episodes." Schizophrenia research **118**: 309–10.

Munro, S., K. L. Thomas and M. Abu-Shaar (1993). "Molecular characterization of a peripheral receptor for cannabinoids." Nature **365**(6441): 61-5.

Nie, J. and D. L. Lewis (2001). "The proximal and distal C-terminal tail domains of the CB1 cannabinoid receptor mediate G-protein coupling." Neuroscience **107**(1): 161-7.

Niehaus, J. L., Y. Liu, K. T. Wallis, M. Egertová, S. G. Bhartur, S. Mukhopadhyay, S. Shi, H. He, D. E. Selley, A. C. Howlett, M. R. Elphick and D. L. Lewis (2007). "CB1 cannabinoid receptor activity is modulated by the cannabinoid receptor interacting protein CRIP 1a." Mol pharm **72**: 1557-66.

Njung'e, K. and S.L. Handley (1991). "Evaluation of marble-burying behavior as a model of anxiety." Pharmacol Biochem Behav, **38**:63–7.

Ohno-Shosaku, T., H. Tsubokawa, I. Mizushima, N. Yoneda, A. Zimmer and M. Kano (2002).

"Presynaptic cannabinoid sensitivity is a major determinant of depolarization-induced retrograde suppression at hippocampal synapses." J Neurosci **22**(10): 3864-72.

Onaivi, E.S., M. R. Green and B. R. Martin (1990). "Pharmacological characterization of cannabinoids in the elevated plus maze." J Pharmacol Exp Ther **253**: 1002-9.

Onaivi, E. S., A. Chakrabarti, E. T. Gwebu, and G. Chaudhuri (1995). "Neurobehavioral effects of $\Delta^9$-THC and cannabinoid (CB1) receptor gene expression in mice." Behav Brain Res **72**: 115-25.

Onaivi, E. S., C. M. Leonard, H. Ishiguro, P. W. Zhang, Z. Lin, B. E. Akinshola and G. R. Uhl (2002). "Endocannabinoids and cannabinoid receptor genetics." Prog Neurobiol **66** (5): 307–44

Pacher, P., S. Batkai and G. Kunos (2006). "The endocannabinoid system as an emerging target of pharmacotherapy." Pharmacol Rev **58**(3): 389-462.

Pan, X., S. R. Ikeda and D. L. Lewis (1998). "SR 141716A acts as an inverse agonist to increase neuronal voltage-dependent $Ca^{2+}$ currents by reversal of tonic $CB_1$ cannabinoid receptor activity." Mol Pharmacol **54**(6): 1064-72.

Patel, S., B. F. Cravatt and C. J. Hillard (2004). "Synergistic interactions between cannabinoids and environmental stress in the activation of the central amygdala." Neuropsychopharm **30**: 497-507.

Patel, S. and C. J. Hillard (2006). "Pharmacological evaluation of cannabinoid receptor ligands in a mouse model of anxiety: further evidence for an anxiolytic role for endogenous cannabinoid signaling." J Pharmacol Exp Ther **318**: 304–11.

Pertwee, R. G., S. R. Fernando, J. E. Nash, A. A. Coutts (1996). "Further evidence for the presence of cannabinoid CB1 receptors in guinea pig small intestine." Br J Pharmacol. **118**: 2199–205.

Pertwee, R. G. (2008). "The diverse CB1 and CB2 receptor pharmacology of three plant cannabinoids: **Δ**9-tetrahydrocannabinol, cannabidiol and **Δ**9-tetrahydrocannabivarin". Br J Pharmacol **153**:199–215.

Rinaldi-Carmona, M., F. Barth, M. Heaulme, D. Shire, B. Calandra, C. Congy, S. Martinez, J. Maruani, G. Neliat and D. Caput (1994). "SR141716A, a potent and selective antagonist of the brain cannabinoid receptor." FEBS letters **350**:240-4.

Rockhold, R. W. (2002). "The Chemical Basis for Neuronal Communication." Fundamental Neuroscience. D. E. Haines. New York, Churchill Livingstone: 57- 70.

Rubino, T., C. Guidali, D. Vigano, N. Realini, M. Valenti, P. Massi, and D. Parolaro (2008). "CB1 receptor stimulation in specific brain areas differently modulate anxiety-related behaviour." Neuropharmacology **54**: 151-60.

Russo, E.B. (2007). "History of cannabis and its preparations in saga, science, and sobriquet." Chemistry & biodiversity **4**(8): 1614-48.

Sanchez, C. (1995). "Serotonergic mechanisms involved in the exploratory behaviour of mice in a fully automated two-compartment black and white test box." Pharmacol Toxicol **77**: 71–8.

Savinainen, J. R., T. Järvinen, K. Laine and J. T. Laitinen (2001). "Despite substantial degradation, 2-arachidonoylglycerol is a potent full efficacy agonist mediating CB(1) receptor-dependent G-protein activation in rat cerebellar membranes". British Journal of Pharmacology **134** (3): 664–72.

Sim, L. J., R. E. Hampson, S. A. Deadwyler and S. R. Childers (1996). "Effects of chronic treatment with Δ9-tetrahydrocannabinol on cannabinoid-stimulated [35S] GTPγS autoradiography in rat brain." J Neurosci **16**:8057-66.

Sim-Selley, L. J., L. K. Brunk and D. E. Selley (2001). "Inhibitory effects of SR141716A on G-protein activation in rat brain." Eur J Pharmacol **414:** 135-43.

Smith, P. B., D. R. Compton, S. P. Welch, R. K. Razdan, R. Mechoulam and B. R. Martin (1994). "The pharmacological activity of anandamide, a putative endogenous cannabinoid, in mice." J Pharmacol Exp Ther **270**: 219-27.

Smith, T. H., L. J. Sim-Selley and D. E. Selley (2010). "Cannabinoid CB1 receptor-interacting proteins: novel targets for central nervous system drug discovery?" Br J Pharmacol **160**:454–66.

Sprang, S. R. (1997). "G protein mechanisms: insights from structural analysis." Annu Rev Biochem **66**: 639-78.

Straiker, A., S. Shu-Jung Hu, J. Z. Long, A. Arnold, J. Wager-Miller, B. F. Cravatt and K. Mackie (2009). "Monoacylglycerol lipase limits the duration of endocannabinoid-mediated depolarization-induced suppression of excitation in autaptic hippocampal neurons." Mol Pharmacol **76**: 1220-27.

Sugiura, T., S. Kondo, A. Sukagawa, S. Nakane, A. Shinoda, K. Itoh, A. Yamashita and K. Waku (1995). "2-Arachidonoylglycerol: a possible endogenous cannabinoid receptor ligand in brain." Biochem Biophys Res Commun **215**(1): 89-97.

Sugiura, T., T. Kodaka, S. Nakane, T. Miyashita, S. Kondo, Y. Suhara, H. Takayama, K. Waku, C. Seki, N. Baba and Y. Ishima (1999). "Evidence that the cannabinoid CB1 receptor is a 2-arachidonoylglycerol receptor. Structure–activity relationship of 2-arachidonoylglycerol, ether-linked analogues, and related compounds." J Biol Chem **274**: 2794–2801.

Thach, W. T., H. P. Goodkin and J. G. Keating (1992). "The cerebellum and the adaptive coordination of movement." Annu Rev Neurosci **15**: 403-442.

Thomas, A., L. A. Stevenson, K. N. Wease, M. R. Price, G. Baillie, R. A. Ross and R. G. Pertwee (2005). "Evidence that the plant cannabinoid $\Delta^9$-tetrahydrocannabivarin is a cannabinoid $CB_1$ and $CB_2$ receptor antagonist." Br J Pharmacol **146**: 917–26.

Truett, G. E., P. Heeger, R. L. Mynatt, A. A. Truett, J. A. Walker JA and M. L. Warman (2000). "Preparation of PCR-quality mouse genomic DNA with hot sodium hydroxide and tris (HotSHOT)." Biotechniques **29:** 52, 54.

Tsou, K., S. Brown, M. C. Sanudo-Pena, K. Mackie and J. M. Walker (1998). "Immunohistochemical distribution of cannabinoid CB1 receptors in the rat central nervous system." Neuroscience **83**(2)**:** 393-411.

Tuccinardi, T., P. L. Ferrarini, C. Manera, G. Ortore, G. Saccomanni and A. Martinelli (2006). "Cannabinoid CB2/CB1 Selectivity. Receptor Modeling and Automated Docking Analysis." J. Med. Chem. **49**(3):984-94.

Twitchell, W., S. Brown and K. Mackie (1997). "Cannabinoids inhibit N- and P/Q-type calcium channels in cultured rat hippocampal neurons." J Neurophysiol **78**: 43–50

Tye, K. M., R. Prakash, S. Kim, L. E. Fenno, L. Grosenick, H. Zarabi, K. R. Thompson, V. Gradinaru, C. Ramakrishnan and K. Deisseroth (2011). "Amygdala circuitry mediating reversible and bidirectional control of anxiety." Nature **471**: 358-62.

Van Sickle M.D., M. Duncan, P. J. Kingsley, A. Mouihate, P. Urbani, K. Mackie, N. Stella, A. Makriyannis, D. Piomelli, J. S. Davison, L. J. Marnett, V. Di Marzo, Q. J. Pittman, K. D. Patel and K. A. Sharkey (2005). "Identification and functional characterization of brainstem cannabinoid $CB_2$ receptors." Science 310: 329–32.

Varvel, S.A., D. T. Bridgen, Q. Tao, B. F. Thomas, B. R. Martin and A.H. Lichtman (2005). "$\Delta^9$-Tetrahydrocannbinol accounts for the antinociceptive, hypothermic, and cataleptic effects of marijuana in mice." J Pharmacol Exp Ther **314**:329–37.

Varvel, S. A., J. L. Wiley, R. Yang, D. T. Bridgen, K. Long, A. H. Lichtman and B. R. Martin (2006). "Interactions between THC and cannabidiol in mouse models of cannabinoid activity." Psychopharmacology (Berl) **186**:226–34.

Viveros M.P., E. M. Marco and S. E. File (2005). "Endocannabinoid system and stress and anxiety responses." Pharmacol Biochem Behav **81**: 331–42.

Walker, J. M. and A. G. Hohmann (2005). "Cannabinoid mechanisms of pain suppression." Cannabinoids. Handbook of Experimental Pharmacology. (Pertwee, R.G., ed.) Heidelburg: Springer-Verlag **168**: 509-54.

Wang, H., Y. Guo, D. Wang, P. J. Kingsley, L. J. Marnett, S. K. Das, R. N. DuBois, and S. K. Dey (2004). "Aberrant cannabinoid signaling impairs oviductal transport of embryos." Nature medicine **10**: 1074-80.

Wang, J. and N. Ueda (2009). "Biology of endocannabinoid synthesis system." Prostaglandins & Other Lipid Mediat **89**: 112–19.

Welch, S.P. and D. L. Stevens (1992). "Antinociceptive activity of intrathecally administered cannabinoids alone and in combination with morphine in mice." J Pharmacol Exp Ther **262**:10–18.

Wiley, J. L., R. L. Barrett, J. Lowe, R. L. Balster and B. R. Martin (1995). "Discriminative stimulus effects of CP 55,940 and structurally dissimilar cannabinoids in rats." Neuropharmacology **34**(6): 669-76.

Williams, C. M., P. J. Rogers and T. C. Kirkham (1998). "Hyperphagia in pre-fed rats following oral $\Delta^9$-THC." Physiol Behav **65**: 123-42.

Wlodawer, P., H. Kindahl and M. Hamberg (1976). "Biosynthesis of prostaglandin $F_{2\alpha}$ from arachidonic acid and prostaglandin endoperoxides in the uterus." Biochim Biophysica Acta **431**: 603-14.

Zimmer, A., A. M. Zimmer, A. G. Hohmann, M. Herkenham and T. I. Bonner (1999). "Increased mortality, hypoactivity, and hypoalgesia in cannabinoid CB1 receptor knockout mice". Proc Natl Acad Sci **96**: 5780-85.

Zimmermann, U. S., P. R. Winkelmann, M. Pilhatsch, J. A. Nees, R. Spanagel and K. Schulz (2009). "Withdrawal phenomena and dependence syndrome after the consumption of "spice gold"." Deutsches Arzteblatt International **106**:464.

## Vita

Joanna C. “Jacy” Jacob was born on February 5, 1987 in Richmond, Virginia, and is an American citizen. She graduated Cum Laude from Virginia Polytechnic Institute and State University (Virginia Tech) in Blacksburg, Virginia, with a Bachelor of Science in Animal and Poultry Science in 2009.